MELTING OF POLYMERS.

by

Cefn Blundell

A thesis submitted for the
degree of
Doctor of Philosophy.

October 1974.

CONTENTS PAGE

SUMMARY

The project set out to investigate the relative effectiveness of thermal conductive heating (from external resistance heaters) and viscous heating in the heating (and melting) of low density polyethylene.

A model system was used in order to simplify the mathematical analysis. A theory was developed to describe both processes in the model apparatus.

The results showed large differences between the experimental and predicted results at low melt temperatures (the predicted results were much greater than the experimental).

Analysis of the results indicated that the apparatus was probably not producing the required shear rates in the sample.

The theory appeared to be satisfactory, in that it did not over estimate the viscous heating to any significant extent. The theoretical results could therefore be considered to be a reasonable estimate of the viscous heating.

ACKNOWLEDGEMENTS

I wish to express my gratitude to Mr. A.J. Lovett, Dr. M.C. Jones and Dr. G.S. Learmonth for their advice and help throughout the course of this work.

I also wish to thank Mr. J. Kemp and the staff of the plastics laboratory at Aston for their assistance.

Special thanks are due to Mr. J. Ludlow and Mr. P. McGuire for their patience in building and modifying the apparatus and for the use of their facilities on numerous occasions.

Finally, I would like to thank the Rubber and Plastics Research Association of Great Britain for making this project possible.

1.0 INTRODUCTION

1.1 STATEMENT OF THE PROBLEM

This project is concerned with some of the heat transfer processes which contribute to the melting and heating of polymers during extrusion.

Figure (1) shows a schematic diagram of an extruder showing how the physical state of the material changes as it progresses along the barrel. Sometimes, with certain polymers, the melt does not become homogeneous in the metering zone (Figure (1)) and poor quality extrudates are obtained. The problem is particularly serious with rigid polyvinyl chloride compounds and ultra high molecular weight polyolefins.

1.1.1. Rigid or Unplasticised Polyvinyl Chloride (PVC)

Good heat transfer is important with this polymer for three reasons. Firstly, extrusion is a particularly important process with this polymer. Secondly, because of the high intermolecular forces between the PVC chains and the temperature restrictions imposed by its thermal stability, it has a high melt viscosity. In fact, there is evidence of partial retention of the structure of the solid particles in the extrudate. Finally, for economic reasons the polymer may be fed to the extruder in unchanged powder form (it is obtained as powder from the polymerisation process), having been compounded with stabiliser and lubricant without melting in a high speed

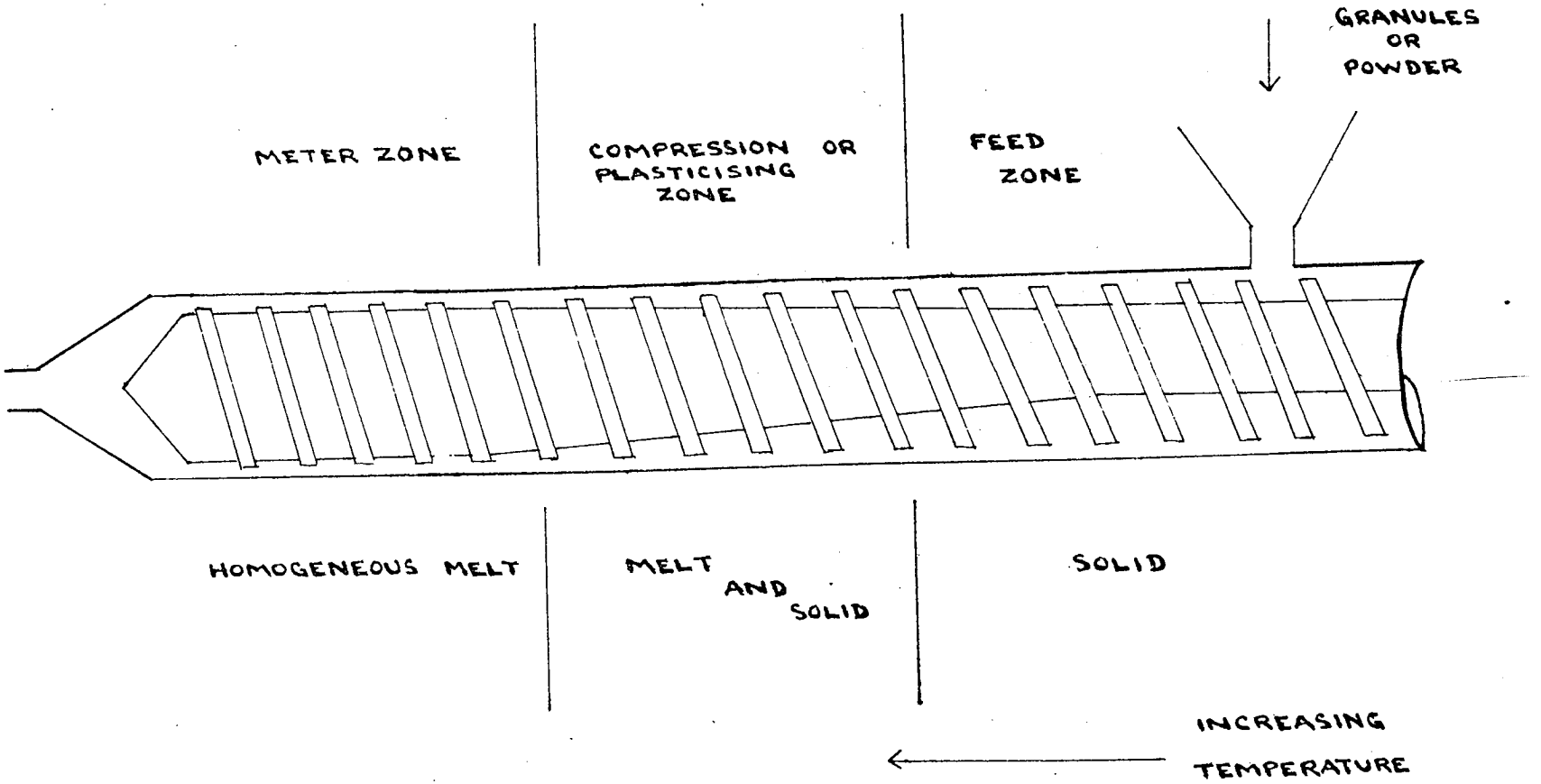
GRANULES
OR
POWDER
METER ZONE
COMPRESSION OR
PLASTICISING
ZONE
FEED
ZONE
HOMOGENEOUS MELT
MELT
AND
SOLID
SOLID
INCREASING
TEMPERATURE

FIG. 1.

mixer. This powder compounded PVC is called 'dry blend' and extrusion of material in this form tends to accentuate the problems discussed above.

1.1.2. Ultra High Molecular Weight Polyolefins

These polymers have weight average molecular weights of the order of 1,000,000 compared to 50,000 - 300,000 for "normal" polyethylene. This means that their melt viscosities are extremely high, for example at 190°C the melt flow index for such materials would be zero. They can be processed on twin screw extruders but this tends to restrict their usage since single screw machines are more common in the United Kingdom. The use of these polymers has therefore been somewhat restricted and the advantages they offer, such as excellent mechanical strength, cannot be utilised.

1.1.3. The Heat Transfer Process

The heat transfer process in the extruder can be broken down into several components.

(a) Conduction in the solid polymer due to temperature gradients in the screw channel.

(b) Frictional heating in the solid polymer due to contact with moving surfaces.

(c) Conduction in molten polymer.

(d) Convection in molten polymer due to movement of melt with the screw channel.

(e) Viscous heating in the melt due to conversion of mechanical work into heat.

While the overall process is well understood and operated empirically, there is lack of fundamental information about the physical changes and processes involved and therefore little knowledge of how to control them.

It was not possible to consider all the aspects of heat transfer mentioned above (a - e), therefore to reduce the problem to a convenient size, two areas of study were chosen, namely (c) and (e). Literature searches showed these to be areas where little work had been done.

It was not considered practical especially for a first study, to measure thermal conduction and viscous heating using an extruder because the geometry of the screw would be too complex for practical mathematical analysis. It appeared to be more practical to devise a mathematically analysable model apparatus capable of measurement of these properties. The decision was also made to use low density polyethylene as the polymeric material, since at this stage the type of polymer was not really important to the development of the technique. Now, because the project was to be based on the use of a model apparatus, the study of convection processes mentioned previously would have been of no use

because they are very geometry dependent. Any study of convection processes in an extruder should therefore only be undertaken using the extruder.

1.1.4 The Development of the Apparatus

For convenience it was desirable to have one piece of equipment for measurement of both thermal conduction and viscous heating. The apparatus geometry had to be chosen such that a moveable surface was in good contact with the polymer. The following types of apparatus were considered :-

(a) Flat discs.

(b) Cone and Plate.

(c) Concentric Cylinders.

Table (1) shows some advantages and disadvantages of the three constructions with respect to heat transfer, viscous heating (a function of shear rate) and some practical aspects of design. No geometry had outstanding advantages,but the decisive factors which led to the selection of concentric cylinders (c) were :-

(a) The similarity between concentric cylinder geometry and that of the extruder. An extruder has a helical channel; a concentric cylinder apparatus has an annular channel which could be considered to be a section of the extruder channel.

TABLE 1.

Apparatus Geometry	Heat Transfer	Shear Rate	Thermal Contact	Samples	Apparatus Size Etc.
Flat discs	Easiest geometry to analyse	Varies across face of disc: zero at centre, maximum at edge	Easily minimised by application of pressure	Easily produced in the laboratory	Bulky, complex large diameter to thickness required to avoid guard heaters
Cone and plate	More complex due to varying gap	Uniform throughout specimen	As Above	Produce in laboratory or in apparatus	As Above
Concentric Cylinders	Complicated only by cylindrical co-ordinates	Varies radially across gap	Not easily minimised must rely on expansion of sample with increasing temperature	Need to use premoulded samples	Comparatively simple if length to diameter ratio large enough no guard heaters required. Extruder-like in geometry.

(b) The apparatus construction was potentially simpler and the mathematical description was slightly simpler. For example, no compensation for heat losses from the apparatus extremities need be made provided the apparatus was long enough, i.e. a length to diameter ratio of at least 10:1 was required.

1.2. SUMMARY OF PROPOSED WORK

(1) Determination of the thermal conduction through the polymer by measurement of the thermal conductivity (λ) and/or the thermal diffusivity (α) over a wide temperature range.

(2) Development of a mathematical model to describe the conduction process.

(3) Determination of the viscous heating effect in the polymer resulting from a known shear stress or shear rate. Measurements to be made over a wide temperature and shear rate/stress range.

(4) Development of a mathematical model to describe the viscous heating process.

(5) Comparison of the energy input from thermal conduction and by viscous heating.

(6) Estimation of the importance of viscous heating in the processing of polymers (especially extrusion).

2.0 LITERATURE SURVEY

2.1. THEORIES OF HEAT TRANSFER IN POLYMERS

In a solid, energy can be transferred by either of two mechanisms(1).

(a) Coupling of vibrations resulting from thermal excitation of the constituent atoms.

(b) Electronic movement.

With polymers and other non-metallic solids electrons are not normally free to move and therefore (b) may be neglected in this case.

The main difference between polymers and non-polymers is of course molecular weight and a consequence of the long chain molecules is that orientation also becomes important under certain circumstances.

These effects are considered in the theory of Hansen and Ho (2) for amorphous polymers. They considered the polymer chain to be made up of segments and considered the interaction with neighbouring segments both in the same molecule and in adjacent molecules. The heat transfer was considered to be dependent upon the type of bond between adjacent segments. In addition, it also depended on the energy difference between the segments. This was a function of the individual arrangement of polymer molecules in the imposed temperature field across the sample.

RELATIONSHIP BETWEEN THERMAL CONDUCTIVITY AND WEIGHT AVERAGE MOLECULAR WEIGHT

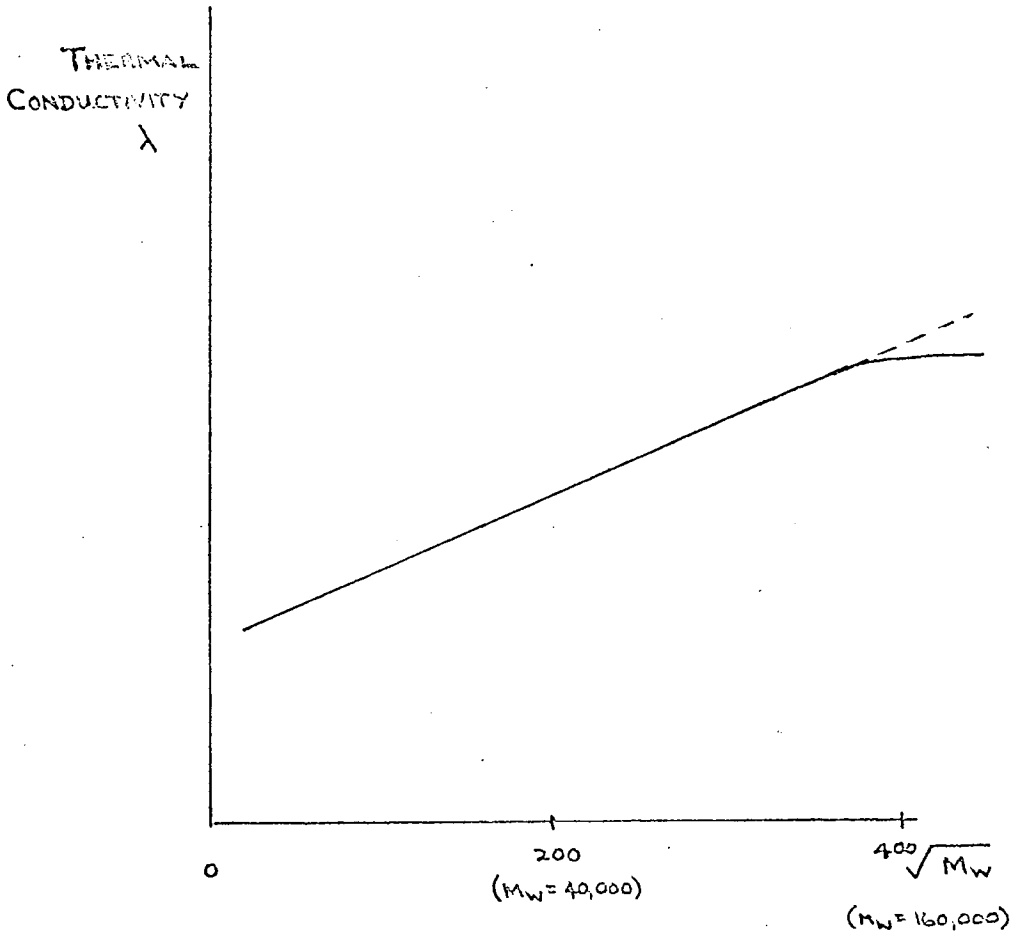

FIG. 2

Thermal conductivity was found to be proportional to the weight average molecular weight (Mw) for polymers of Mw values up to approximately 100,000, as illustrated in Figure (2). Hansen and Ho also found a relationship between conductivity and anisotropy.

$$\frac{\lambda_o}{\lambda_\perp} = \left(\frac{\lambda_{11}}{\lambda_o}\right)^{1/2}$$

Where : λ_o = thermal conductivity of non-orientated polymer

$\lambda_\perp$ = perpendicular to the orientation

λ_{11} = parallel to the orientation

The theory was extended to consider partially crystalline polymers and in particular polyethylene. A relationship was given which related the conductivity of the polymer to the conductivities of the component crystalline and amorphous phases and the degree of crystallinity.

i.e. $$\lambda = \gamma(\lambda_c) + (1-\gamma)\lambda_a$$

Where : λ_c = thermal conductivity of the crystalline phase

λ_a = thermal conductivity of the amorphous phase

γ = degree of crystallinity of the polymer sample.

This separation of the polymer into crystalline and amorphous phases suggests that the authors have assumed the "fringed micelle theory" of polymer morphology, although this was not specifically stated. (See Appendix (1)for brief description

TEMPERATURE DEPENDENCE OF 'λ' FOR THE CRYSTALLINE PHASE OF POLYETHYLENE

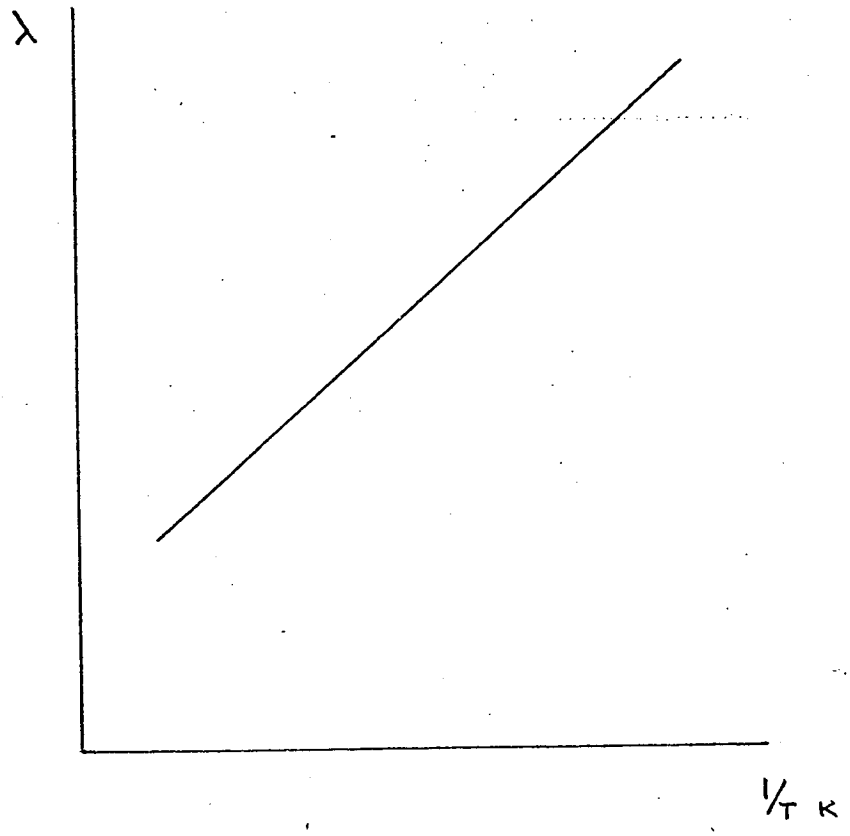

FIG. 3

on fringed micelle theory.)

Figure (3) shows a plot of 'λ' of the crystalline phase against the reciprocal of absolute temperature. The linear nature of the graph indicates agreement with the classical phonon theory for the conductivity of dielectric solids. This seems to lend support to the theory of Hansen and Ho for the behaviour of polymer phases.

Eiermann (3) also developed a theory for amorphous polymers. Each bond between adjacent atoms was considered equivalent to a thermal resistance (the elementary thermal resistance - R_e). The thermal resistance of a macroscopic amorphous specimen was the integral result of all the elementary thermal resistances due to the molecular bonds and the Van der Waal bonds. The quantity R_e was proportional to the bond force between atoms, decreasing with increasing bond strength. Therefore, a primary valence bond was equivalent to a small thermal resistance and a Van der Waal bond equivalent to a large thermal resistance. It should be noted that Van der Waal bonds vary in length and therefore presumably the thermal resistances will too.

The following relationship was found connecting the elementary thermal resistance to the bond force :

$$R_e = \frac{M_{a.k}}{C.C_b} \cdot \lambda_e$$

Where : M_a = Arithmetic mean of the masses of the atoms bonded.

k = Heat capacity per atom.

C_b = Interatomic bond force.

λ_e = Elementary thermal conductivity.

Amorphous polymers were said to consist of a mass of coiled molecules, the arrangement being such that heat cannot travel through a specimen merely along the valence bonds. Eiermann showed that the conductivity of the entire mass of molecules and thus of the specimen, was proportional to the elementary conductivity of the Van der Waal bonds in the specimen. Instead of assuming a statistical arrangement of chain segments in an isotropic test piece, one third were considered to be orientated in each of three cartesian co-ordinate directions. The overall conductivity was a series connection of the thermal resistances of the three cubes (see Figure (4)) which make up the unit volume in each cartesian direction. The prediction was tested using conductivity values for inorganic glasses (considered to transmit heat via primary valence bonds only) and the value for non-polar liquids (considered to transmit heat via Van der Waal bonds only).

The conductivity for inorganic glasses $\lambda_{gl} = 3 \times 10^{-3}$ cal/cm.s.°C

" " " non-polar liquids $\lambda_{fl} = 2.8 \times 10^{-4}$ cal/cm.s.°C

Then using the derived equation :

$$\frac{3}{\lambda_{hp}} = \frac{1}{\lambda_{gl}} + \frac{2}{\lambda_{fl}}$$

ARRANGEMENT OF MOLECULES
ASSUMED BY EIERMANN

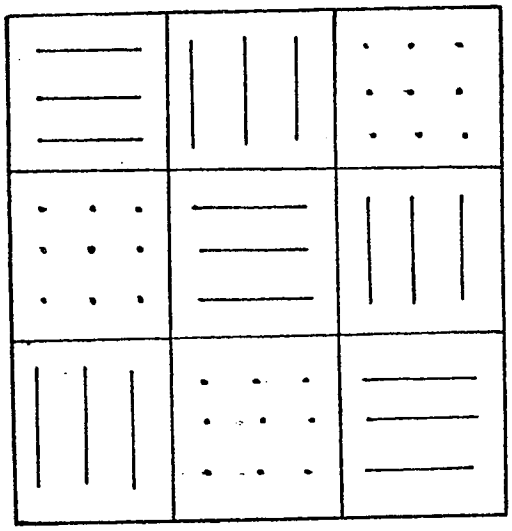

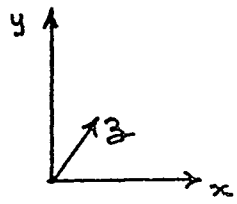

'y' DIRECTION = |||

'x' DIRECTION = ≡

'z' DIRECTION = ···

FIG. 4

Where : λ_{hp} = thermal conductivity of polymer.

From the above values :

$$\frac{\lambda_{fl}}{\lambda_{gl}} = \sim \frac{1}{10}$$

$$\lambda_{hp} = 1.4\, \lambda_{fl}$$

therefore : $\lambda_{hp} = 4 \times 10^{-4}$ cal/s.cm.^{o}C

$= 0.17$ W/m C

This was in reasonable agreement with Eiermann's experimental results and those of other workers, indicating that the model was an adequate description in spite of the approximations made.

According to classical theory of heat conduction (Peierls (4)), below the glass transition temperature (Tg) of the sample the thermal conductivity of amorphous materials should remain constant, or increase, with increasing temperature. On the other hand, the conductivity of crystalline materials should decrease, or remain constant, with increasing temperature up to the melt temperature (Tm). After the Tm the behaviour should resemble that of amorphous polymers.

The increase in conductivity for amorphous polymers has been explained (1) by an increase in segmental motion of the polymer chains. Sometimes an increase in conductivity is not observed. This is explained by taking into account

the density reduction resulting from the volume increase (which on Eiermann's theory would increase the length of the Van der Waal bond therefore reducing conductivity) which occurs with increasing temperature. With crystalline polymers, conductivity was said to decrease, because of the destruction of the ordered regions as the temperature increases. This assumes that the polymer crystals are imperfect and melt over a wide temperature range. Eventually, when the polymer becomes amorphous (on reaching its Tm) it should behave as previously described. Some workers (5), (6) and (7) have found a decrease in conductivity with increasing temperature for amorphous polymers. These measurement have been made above the Tg of the polymers where volume and density changes are large. In this region the volume increase which leads to the increase in length of Van der Waal bonds, must decrease the conductivity faster than the segmental motion increases it.

Cherkosova (8) predicted an increase in conductivity with increasing temperature for amorphous polymers, and after reaching the glass transition temperature (Tg) the rate of increase was said to increase. Published results in general, do not agree with this latter prediction, possibly because the volume increase of the polymer (with increasing temperature) more than compensates for the increased molecular mobility.

Crystalline polymers were predicted to behave as previously described.

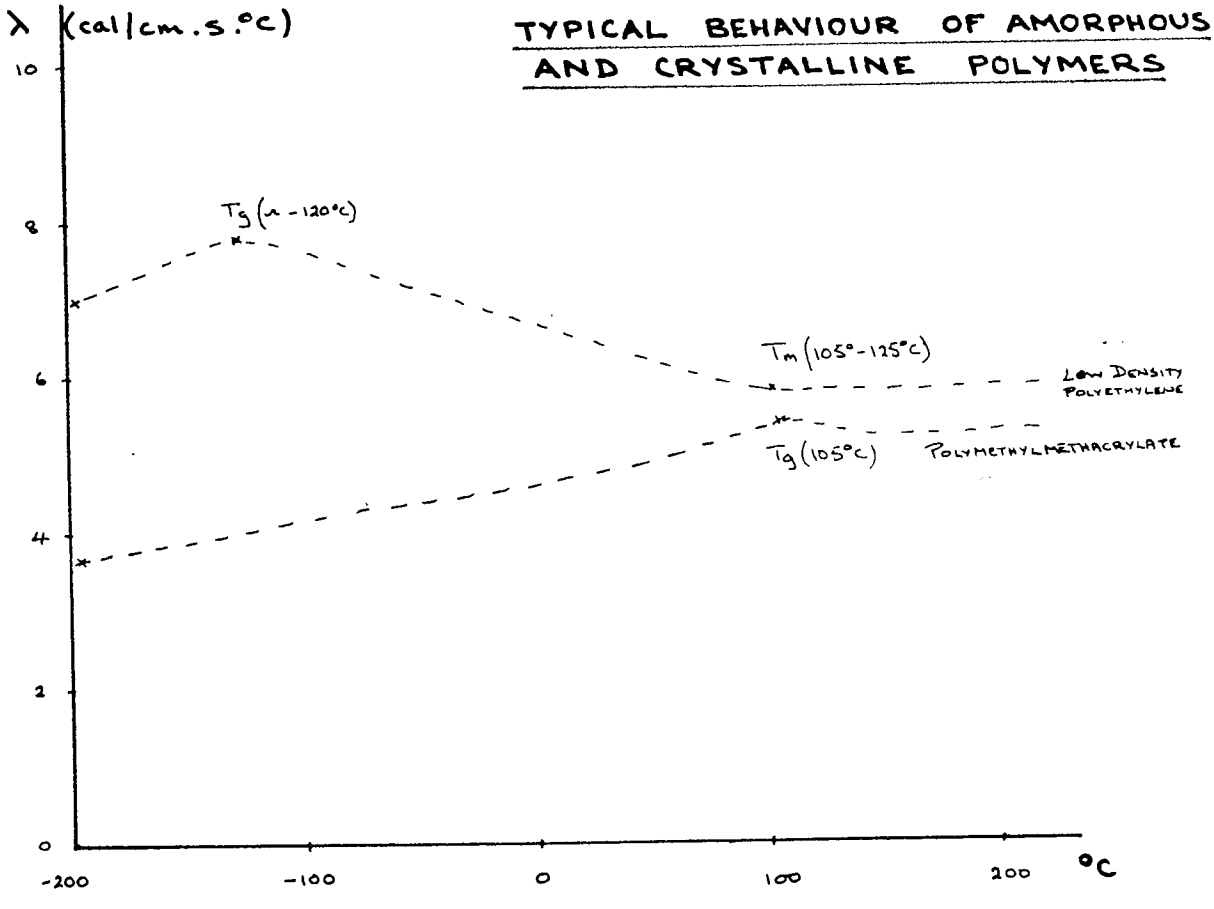
λ (cal/cm.s.°C)
TYPICAL BEHAVIOUR OF AMORPHOUS AND CRYSTALLINE POLYMERS
10
8
6
4
2
0
Tg (≈ -120°C)
Tm (105°-125°C)
LOW DENSITY POLYETHYLENE
Tg (105°C)
POLYMETHYLMETHACRYLATE
-200
-100
0
100
200
°C

FIG. 5.

The general, experimentally observed, behaviour for amorphous and crystalline polymers is illustrated in Figure (5).

2.2. THE MEASUREMENT OF THERMAL CONDUCTIVITY

The significance of thermal conductivity can be understood by considering Figure (6) which represents an elemental volume of substance. The heat flux vector 'q' is perpendicular to the face of area 'A' and $\Delta\theta$ is the temperature difference over the distance Δx. Thermal conductivity is then the quantity of heat Q which flow per unit time through the area 'A' under the influence of the temperature gradient given by :

$$\lambda = \frac{Q}{A} \cdot \frac{\theta_1 - \theta_2}{\Delta x}$$

The units for thermal conductivity are :

C.G.S.		cal/cm s. ^{o}C
S.I.		W/m K
1 W/mK	=	0.00239 cal/cm s ^{o}C

Mathematically, thermal conductivity can be defined in one direction by :

$$q_x = -\lambda \left(\frac{d\theta}{dx}\right)$$

Where : λ = thermal conductivity

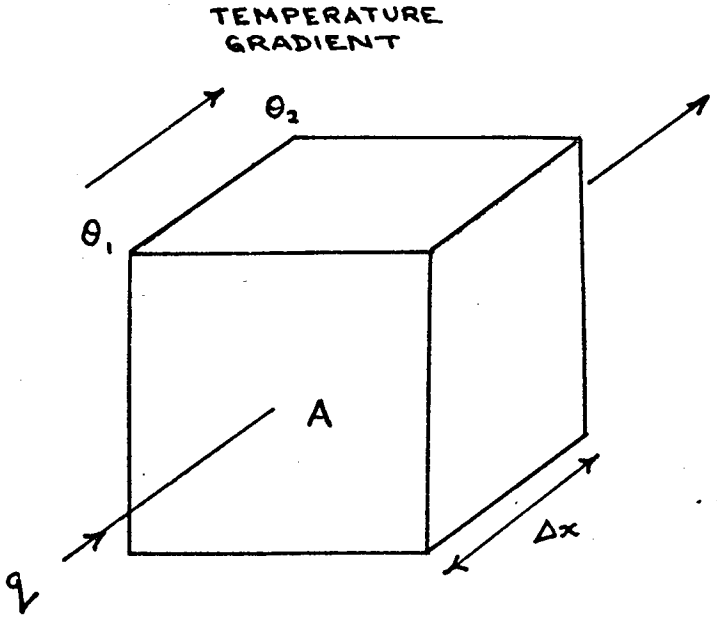
TEMPERATURE
GRADIENT
θ_2
θ_1
A
Δx
q
AN ELEMENTAL
VOLUME

FIG. 6.

ASTM GUARDED HOT PLATE APPARATUS

A = HEAT SOURCE
B = HEAT SINK
C = SAMPLE
D = GUARD HEATER
E = HEAT SINK THERMOCOUPLES
F = HEATER THERMOCOUPLES
G = DIFFERENTIAL THERMOCOUPLES FOR GUARD HEATER AND HEAT SOURCE

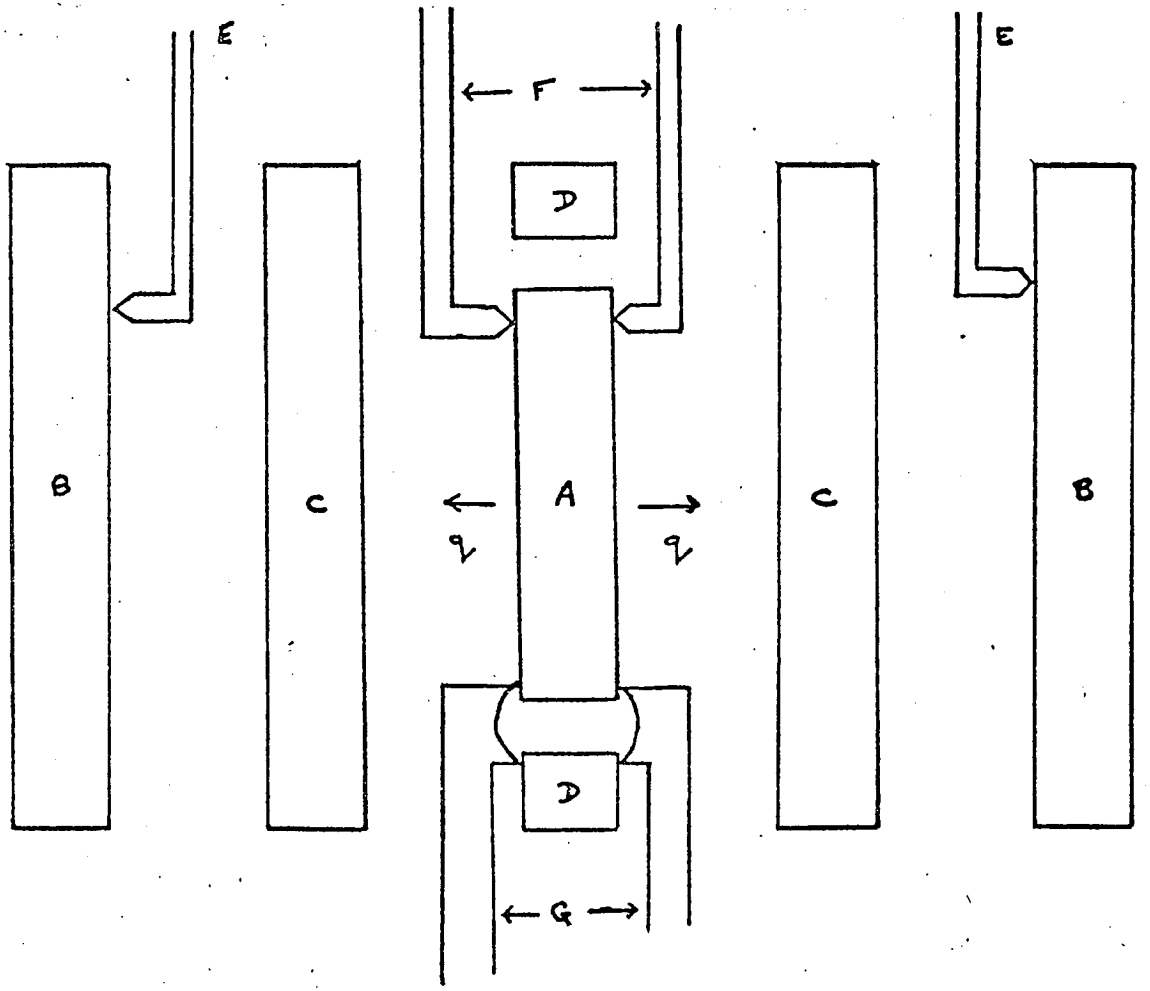

FIG. 7.

2.2.1. Steady State Methods of Measurement

A good method to discuss first is the standard ASTM guarded hot plate technique (9). The apparatus is illustrated in Figure (7); the plates may be circular or rectangular and should be precisely machined. The test procedure should take at least $1\frac{1}{2}$ hours, once the steady state has been attained, during this time a number of readings are taken and if the temperature drop across the sample does not differ by more than 1% for all the readings taken, then the calculated values of conductivity should also not differ by more than 1%.

A concentric cylinder apparatus was developed by Kline (10) for the measurement of thermal conductivity over the temperature range 0° - $100^{\circ}C$. Figure (8) shows the basic construction of the apparatus. The heat sink was a water jacket which was connected to a constant temperature bath. The length to diameter (L:D) ratio was made so large that the heat losses from the ends could be ignored. It was found by experiment that the minimum L:D ratio necessary to avoid end losses was of the order of 12:1. This was determined by performing experiments with apparatus of 4", 6" and 12" lengths, with a sample diameter of 0.5".

The L:D ratios were therefore 8:1, 12:1, and 24:1 respectively. The results with the 6" and 12" samples were found to be identical but those of the 4" cell were low, of the order of 10%.

Eiermann and Knappe (11) used a flat plate apparatus similar to the

KLINE'S APPARATUS

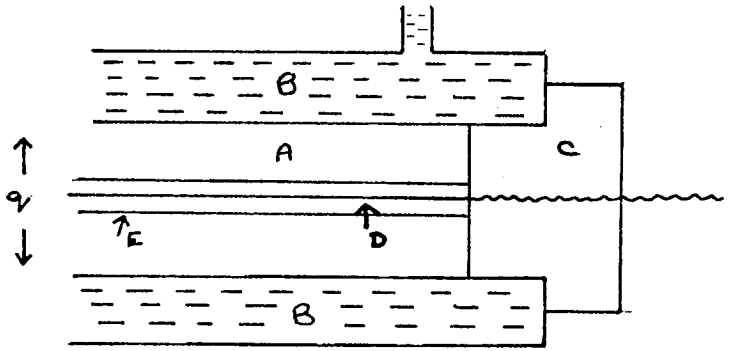

A = SAMPLE
B = COOLING FLUID
C = END PLUG
D = EPOXY (ALUMINIUM FILLED) ADHESIVE TO HOLD THE HEATING WIRE IN TUBE 'E'

q = HEAT FLOW

FIG. 8.

ASTM design. Measurements were made in the region of the polymers glass transition or melting point. They also attempted to determine the magnitude of the thermal contact resistance between the polymer and the metal apparatus. Poor thermal contact can introduce significant error into measurement of thermal conductivity. It was said this was shown by a very sharp break in the graph of 'λ' versus temperature in the region of the Tm or Tg depending on whether the polymer was crystalline or amorphous respectively. The break was said to develop as follows : above the freezing temperature, when materials are soft and deformable, they adhere to the plates of the measurement system and good thermal contact is made. Below the melting temperature, the sample is hard and contact is made only at the high spots and a high heat resistance is established between the plates and the sample. This was given as the physical reason for the conductivity dropping sharply at the freezing temperature (see Figure (9)). Even when materials such as oils and fats were used to improve the contact by elimination of the air in the voids, similar low results were obtained.

To illustrate the errors in measurement due to poor thermal contact, the authors compared the results obtained using helium (a gas with a high thermal conductivity), and a vacuum (a perfect vacuum makes interstitial conduction impossible) in the apparatus. Figure (9) shows the results obtained. The steep break occurring when a vacuum was used in the equipment, occurred at the transition point (Tg) of the rubber sample used. The measured values with helium show very little disturbance at the same point, with the same material. Helium was assumed to eliminate the effect of thermal contact resistance, since the gas had a high thermal

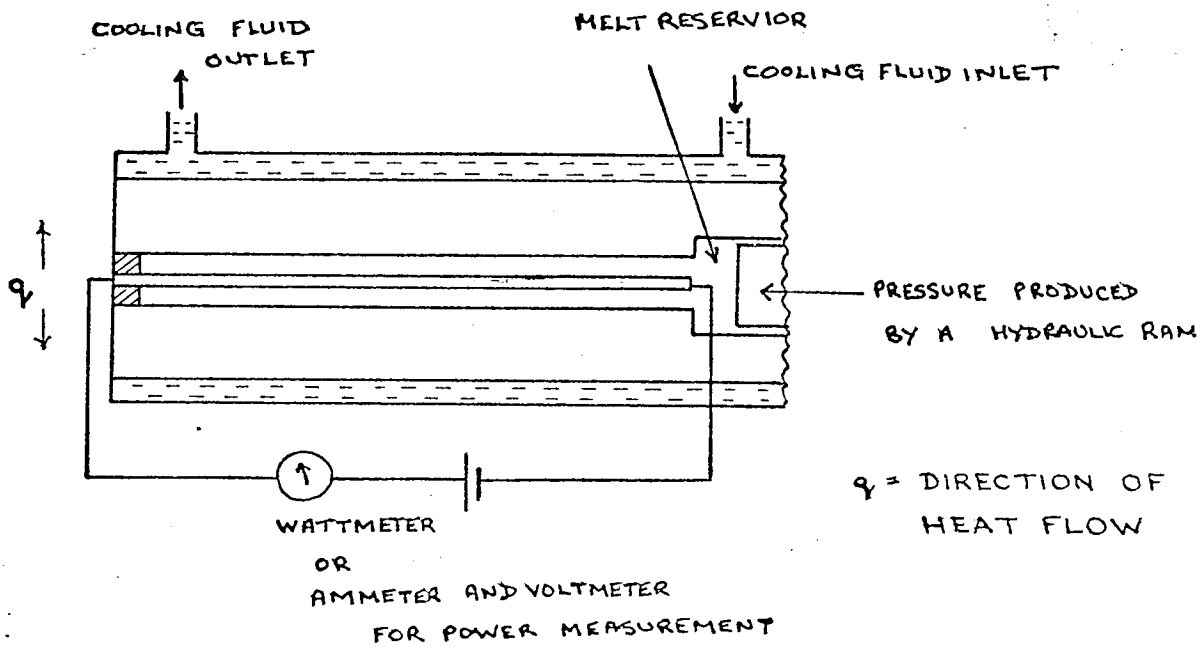

LOHE'S APPARATUS FOR THERMAL CONDUCTIVITY OF POLYMER MELTS

FIG. 10.

CONCENTRIC CYLINDER APPARATUS

CONSTRUCTED BY FULLER AND FRICKE

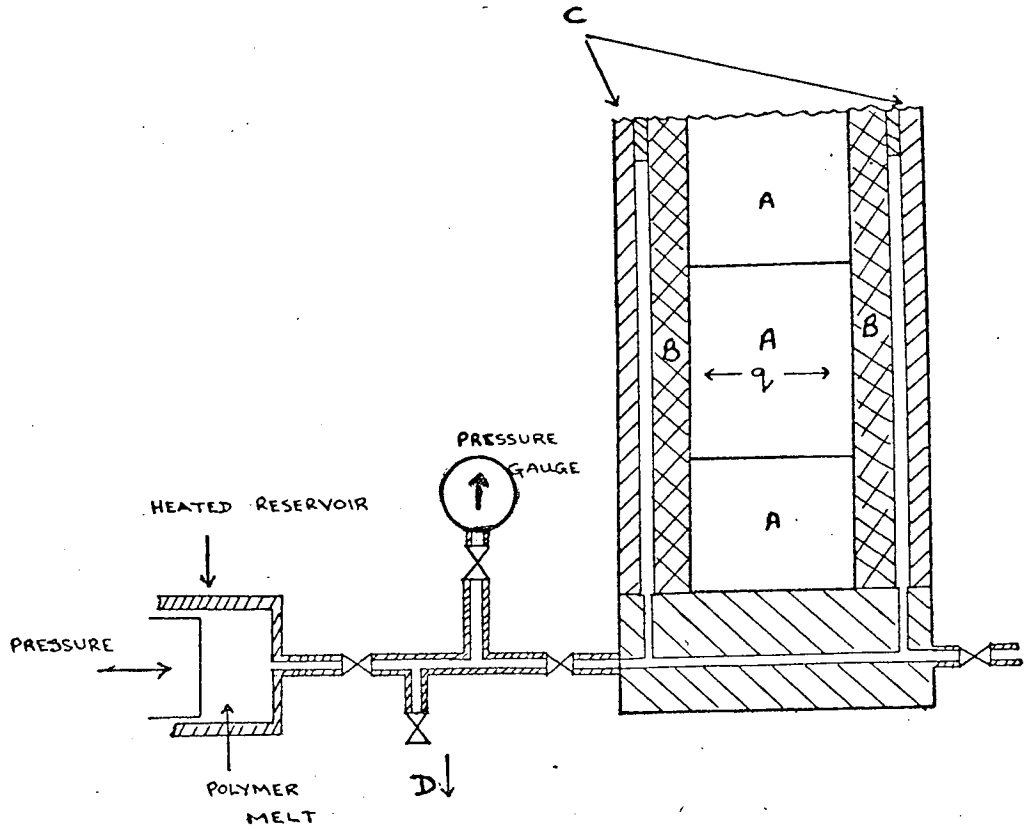

A = HEATERS B = INNER CYLINDER C = OUTER CYLINDER

D = OUTLET TO VACUUM
PUMP FOR REMOVAL OF AIR

FIG. 11.

conductivity and unlike oils and fats it completely fills the voids between the sample and the cell walls.

Molten polymers were investigated by Lohe (5) and Fuller and Fricke (12). The equipment used by these workers is illustrated in Figures (10) and (11) respectively. Lohe found very little change or a slight decrease in conductivity with increasing temperature (in the range 150° - 250°C), depending on whether the polymer was originally crystalline or amorphous. For example, with a crystalline polymer such as polyethylene, no change was observed, but with amorphous polymethylmethacrylate, a decrease in conductivity was observed with increasing temperature. Fuller and Fricke generally found an increase in conductivity with increasing temperature.

2.2.2. Non-Steady State Methods for the Measurement of Thermal Conductivity

Steady state methods have the advantage of being mathematically simple but are very time consuming and the apparatus can be complex and expensive. On the other hand, transient or unsteady state methods usually require relatively simple apparatus and are certainly much more rapid, though mathematically complicated. Basically, transient methods consist of passing heat through a sample from a heat source to a heat sink of known thermal capacity. From the rate of temperature rise of the heat sink, the heat flux can be calculated and thus the conductivity determined. Sometimes the procedure is modified slightly and the heat sink is maintained at a constant temperature and the heat source temperature observed.

Alternatively, the apparatus can be calibrated using standard specimens of known thermal conductivity.

Underwood and McTaggart (13) adapted a 'line source' method for use with plastics. The apparatus consists of a heating wire (i.e. the line source) surrounded by the sample. If the power generated in the wire is determined by measurement of the current and voltage and the temperature rise in the wire is measured, then the conductivity of the sample can be calculated. The rate of temperature rise of the heating wire will depend on the thermal conductivity of the surrounding substance. (The lower the conductivity the faster the temperature of the wire will rise, since the material is not conducting the heat away and conversely the wire temperature will rise slowly if the surrounding material has a high conductivity.) This is a very simple and rapid method, requiring the minimum of apparatus and a matter of seconds to collect sufficient data to perform the necessary calculation. It may also be adapted for use at any required temperature. The following temperature relationships were found by the authors using the above method for low density polyethylene :

$$\lambda = 0.169 + (1.204 \times 10^{-4})\, t - (1.73 \times 10^{-6})\, t^2 \quad \ldots 30^\circ - 220^\circ F$$

$$\lambda = -0.368 - (1.48 \times 10^{-3})\, t + (5.42 \times 10^{-2})\, t^{\frac{1}{2}} \quad \ldots 220^\circ - 375^\circ F$$

Units of λ = BTU/ft.hr.$^\circ$F.

The discontinuity of the temperature behaviour, as shown by the need for two equations, seems to correspond to the "melt temperature" of the polyethylene ($105^\circ - 120^\circ C$; $221^\circ - 248^\circ F$). The results given by these emperical equations

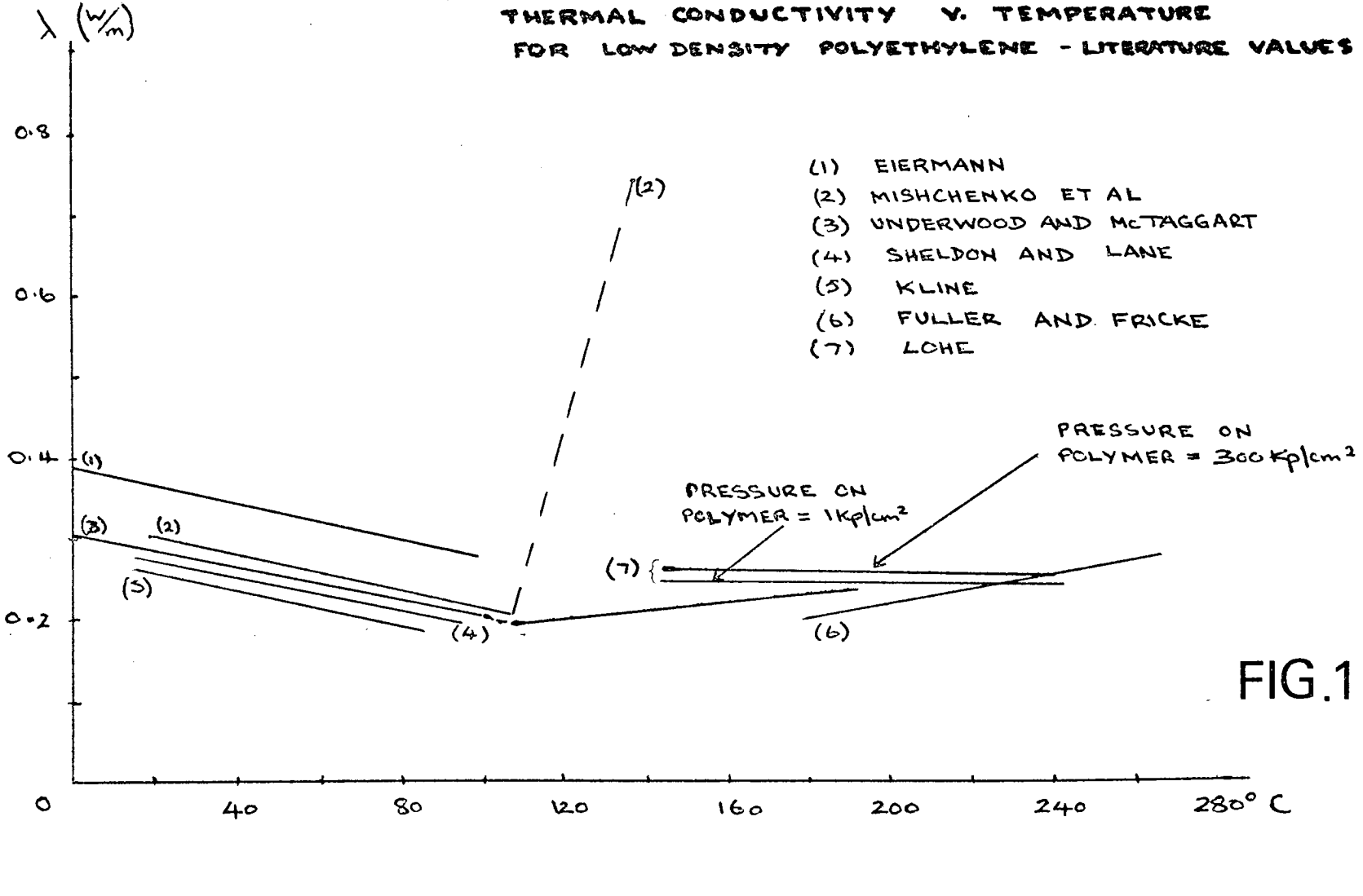
λ (W/m)
THERMAL CONDUCTIVITY V. TEMPERATURE
FOR LOW DENSITY POLYETHYLENE - LITERATURE VALUES
(1) EIERMANN
(2) MISHCHENKO ET AL
(3) UNDERWOOD AND McTAGGART
(4) SHELDON AND LANE
(5) KLINE
(6) FULLER AND FRICKE
(7) LOHE
PRESSURE ON POLYMER = 300 Kp/cm²
PRESSURE ON POLYMER = 1 Kp/cm²
0·8
0·6
0·4
0·2
0
40
80
120
160
200
240
280° C

FIG.12.

THERMAL DIFFUSIVITY V. TEMPERATURE
FOR LOW DENSITY POLYETHYLENE - LITERATURE VALUES

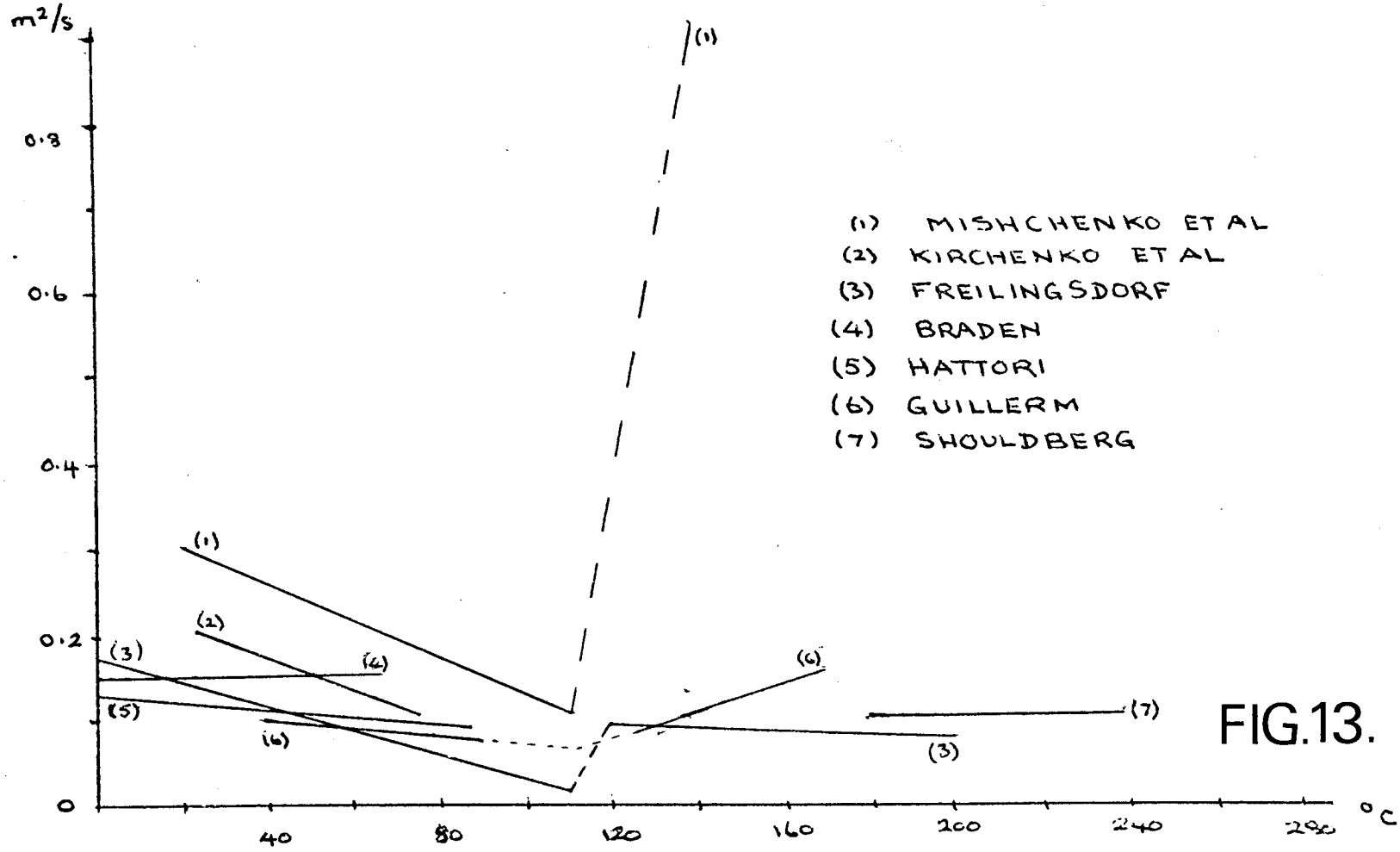

FIG.13.

are plotted in Figure (12) and show a good agreement with other workers.

The line source method was critically analysed by Vos (14). The effects of various errors which may arise are discussed, for example the effects of the finite radius of the line source and too small a sample (in the radial direction).

Beatty, Armstrong and Schoenborn (15) developed a method using a flat plate apparatus with the heat sink and samples surrounded by a heat source as shown in Figure (14). During the experiments, the temperatures of the heat sources and the heat sink are measured continuously from the time when the samples first contact the heated platens. The sample thickness is not important but the thicker the specimen the longer the experiment will take, for example a 0.5" (12.7 mm) thick sample of polymeric material requires a minimum time of 12 minutes for sufficient data to be collected. From the results it was possible to obtain a value for the product of density (ρ) and specific heat (C_p) for the material and for the thermal diffusivity (α).

Now since : $\alpha = \lambda / \rho . C_p$ the thermal conductivity can be calculated. The accuracy of the method was limited by the estimation of the value of ($\rho . C_p$) since this was determined graphically.

A "quasi-stationary" method was used by Gast, Hellwege and Kolheppe (16) for measurements on PVC in the temperature range 70 - 360 K

BASIC ARRANGEMENT USED BY BEATTY ET AL

FOR UNSTEADY STATE MEASUREMENT OF THERMAL CONDUCTIVITY

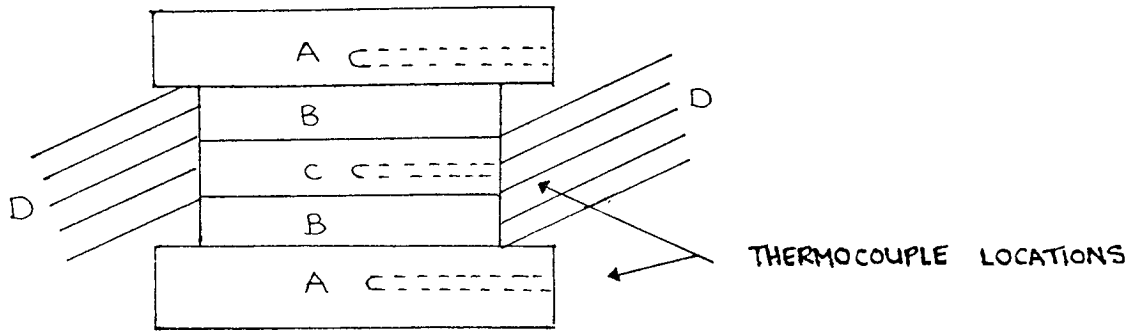

A = HEAT SOURCES
B = SAMPLES
C = HEAT SINK
D = INSULATION TO PREVENT HEAT LOSSES FROM SIDES OF HEAT SINK AND SAMPLES.

FIG. 14.

(-203° to 87°C). The basis of the method was the maintenance of a constant temperature gradient across the sample irrespective of the average temperature. The conductivity of the sample was then said to be proportional to the heat flow through the sample.

Mischenko, Samilov and Buchatskii (17) were able to obtain thermal conductivity and thermal diffusivity from their experiments, hence the method was probably a transient one, though details of the technique were not given. The results for low density polyethylene, above the melt temperature increased rapidly and soon became far higher than any other results reported in the literature. It was not possible to determine why this occurred since so little information was given in the paper. The results obtained are shown in Figures(12) and (13).

2.3. THE MEASUREMENT OF THERMAL DIFFUSIVITY

The measurement of thermal diffusivity (α) has received less attention than thermal conductivity. This is somewhat surprising since it is easier to measure, requiring only the measurement of the change of temperature with time at two points in the sample. The heat flux through the material need not be known. In addition, it could be argued, that it has greater practical significance than conductivity because it is directly related to heating and cooling situations encountered

in processing. In other words, diffusivity is a transient property and the methods of measurement are therefore unsteady state techniques.

Braden (18) made measurements with polymethylmethacrylate (PMMA), polyethylene and polysulphide rubbers using a small rectangular block of the materials. A thermocouple was located at the centre of the block and the whole arrangement immersed in a constant temperature bath. Measurements were made in the temperature range 0° - $70^{\circ}C$ and no change in 'α' was observed. The method was obviously limited to relatively low temperatures as far as polymers were concerned because on approaching the melt or softening temperature the sample would not retain its shape.

A similar technique, but with cylindrical samples was used by Frielingsdorf (19). The experiments were conducted over a temperature range of 20° - $200^{\circ}C$ using oil baths and liquids of known boiling points to provide the constant temperature environments in which to immerse the specimens. The method could be used at high temperatures because the samples were contained in a copper cylinder. This however, raises the question of thermal contact between the polymer and the cylinder. It was claimed that good contact could be obtained by using samples 0.2mm larger than the inside diameter of the copper tube. The samples were inserted by cooling to $-20^{\circ}C$. The results of this work are shown graphically in Figure (13).

Guillerm (20), Hattori (21) and Kirchenko et al (22) all used cylindrical geometry for their measurements and obtained comparable results (see

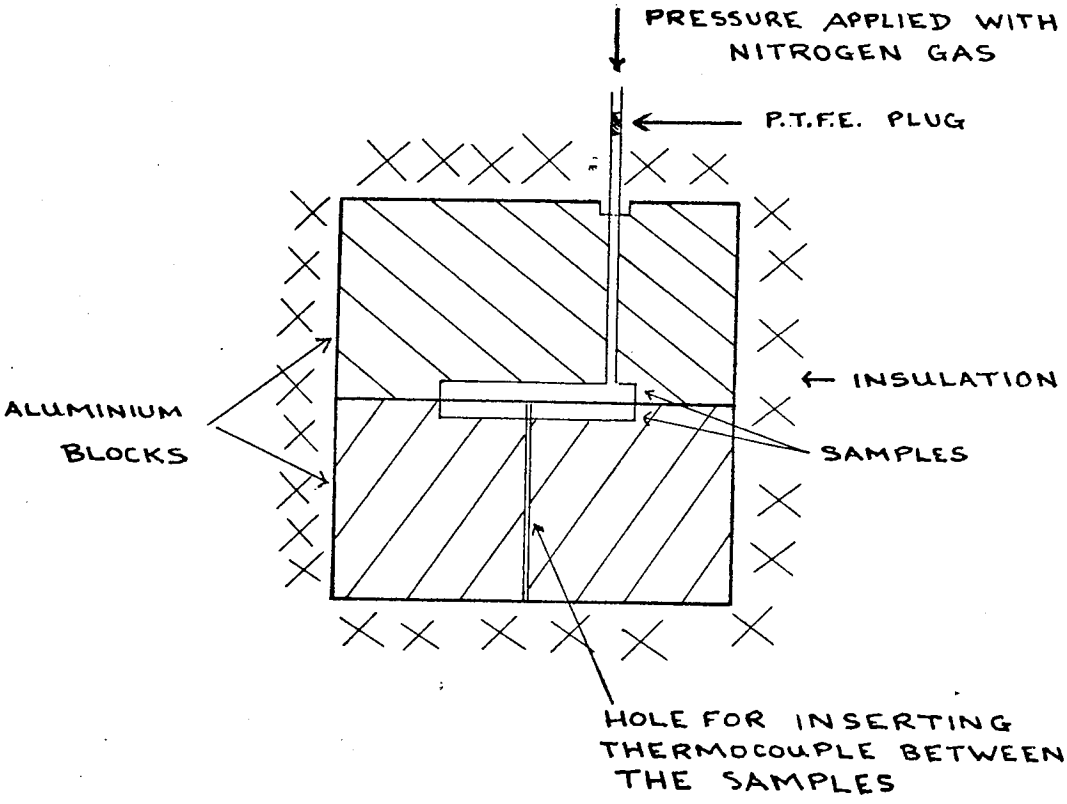

SHOULDBERG'S APPARATUS

FIG.15.

Figure (13)).

Shouldberg (23) concentrated on polymer melts with apparatus which was relatively complex (see Figure (15)). Two disc shaped samples were used with a thermocouple sandwiched between them. The thermocouple measured the sample temperature. The ratio of the diameter to thickness of the discs was large enough for radial heat flow to be ignored. To obtain good thermal contact between polymer and metal surfaces the samples were heated to about 20°C above the glass transition or melt temperature (depending on the properties of the material used) and a pressure of 500 lb/in^2 applied to force it into intimate contact with the cell walls.

The conclusions drawn from this work were :

(a) The diffusivity values of a wide variety of polymers differ by less than a factor of two.

(b) In the absence of degradation, 'α' does not change significantly over a wide temperature range.

(c) Small differences in composition or molecular weight had no significant affect on 'α'.

Point (c) was illustrated by a comparison of the thermal diffusivities of n-octane C_8H_{18} at 30°C and polyethylene melt.

i.e.

Octane	α =	0.093×10^{-6} m^2/s
Polyethylene	α =	0.104×10^{-6} m^2/s

2.4. THE EFFECT OF TEMPERATURE ON THERMAL DIFFUSIVITY (α) AND THERMAL CONDUCTIVITY (λ)

Figures (12) and (13) show the effect of temperature on the values of 'α' and 'λ' for low density polyethylene. Figure (5) indicates the general behaviour of a typical amorphous polymer (polymethylmethacrylate) and a typical crystalline polymer (low density polyethylene) over a wide temperature range. Both 'α' and 'λ' for many polymers are reasonably well defined in the solid state, although the results obtained do not always show agreement. In the melt state, significantly less work has been done,which is not surprising since under these conditions measurements are more difficult to make. Generally speaking the literature values for molten polymers show less change with temperature than in the solid state.

2.5 RHEOLOGICAL BEHAVIOUR OF MATERIALS

Before dealing with the viscous heating of polymers it was thought relevant to deal with the differences between elastic, viscous and viscoelastic materials.

A Hookean body (i.e. a body which obeys Hook's Law stress $\propto$ strain) is perfectly elastic. Any deformation which the body undergoes is completely recoverable, the body will return to its original state and no energy will be lost, providing the applied stress does not exceed the yield point of the material.

DEFORMATIONAL BEHAVIOUR OF
POLYSTYRENE WITH TEMPERATURE

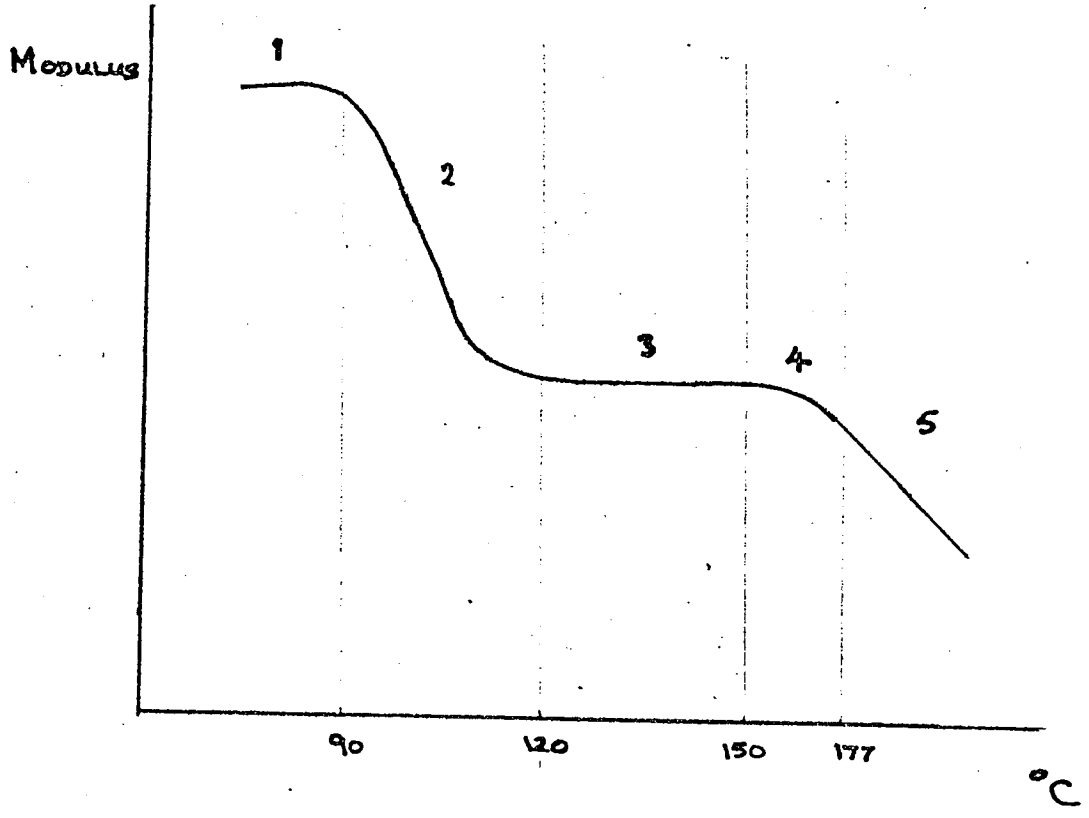

REGION 1 - GLASSY STATE - ELASTIC BEHAVIOUR
REGION 2 - GLASS-RUBBER TRANSITION
REGION 3 - RUBBERY-PLATEAU
REGION 4 - RUBBER-LIQUID TRANSITION
REGION 5 - LIQUID STATE - VERY LITTLE ELASTIC RECOVERY

FIG.16.

A Newtonian fluid (shear stress $\propto$ shear rate) is said to be a viscous fluid. Deformational work done on the fluid cannot be recovered, it is dissipated as heat, hence the term viscous heating.

Between an elastic body and a viscous fluid there are materials which are described as viscoelastic. Some of the deformational work done on these materials is converted to heat as viscous heating and some is recoverable as stored elastic energy. The elastic energy is not recoverable instantaneously, as with Hookean bodies, but the recovery takes place over a period of time which is known as the relaxation time.

Polymers, in general, fall into the category of viscoelastic materials. The precise behaviour would be different for each material and would be principally determined by the molecular weight, molecular weight distribution and the length and nature of any chain branching present. For example, the higher the molecular weight of the polymer the more elasticity it could be expected to exhibit, since the longer the molecular chain the more it can become entangled with other chains.

Tobolsky (24) described the overall molecular behaviour of polymers with respect to temperature, with a graph such as Figure (16) for polystyrene.

Region (1) up to 90°C the material is brittle and exhibits classical elastic behaviour. It is said to be in the "glassy" state. The molecular chains are "frozen" in fixed positions and they undergo little, if any, diffusional motion characteristic of liquids.

Region 2 is the transition zone where some diffusional motion occurs. The temperature range over which this region spans was said to be the "leathery region" or glass - rubber transition zone.

In the "rubbery plateau", region 3, there is rapid diffusional motion. However, the motions of the molecules as a whole are retarded, particularly by entanglements between chains which act as temporary cross-links.

In the region of "rubbery flow" (region 4 , the rubber-liquid transition zone) the motion of the molecules as a whole is important, major configurational changes of the entire molecule occur, including slippage of entanglements.

Region 5 is the area of "liquid flow" where configurational changes occur so rapidly that elastic recovery is almost negligible for stresses which are maintained longer than the retardation time (which is very short at these high temperatures).

The retardation time is the time delay from the application of a stress to the final resultant deformation of the material. Unlike purely elastic or purely viscous material, the effect of stress in a viscoelastic material (i.e. polymer) is not instantaneous, there is a period of time over which the deformation increases to its maximum and this is the retardation time. This period varies with temperature, decreasing with increasing temperature.

In this project a temperature range of 130°C - 230°C was used and

ILLUSTRATION OF NOMENCLATURE USED IN DESCRIBING EXTRUDER OPERATION

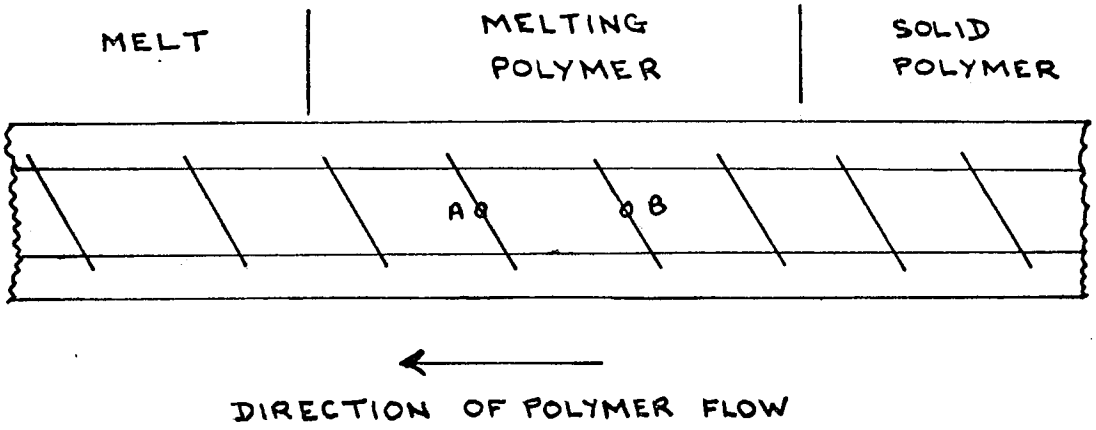

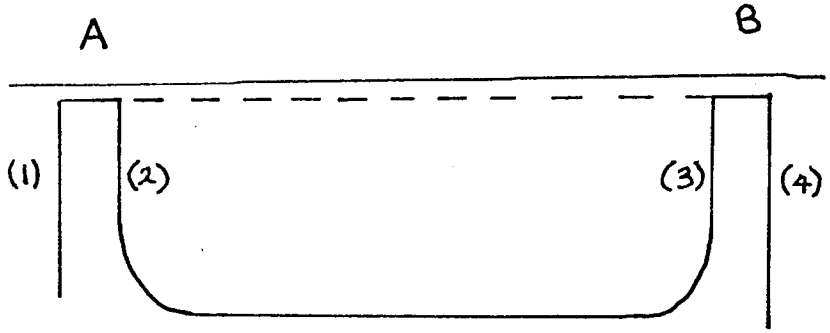

(1) = FORWARD EDGE OF FORWARD FLIGHT
(2) = REAR EDGE OF FORWARD FLIGHT
(3) = FORWARD EDGE OF REAR FLIGHT
(4) = REAR EDGE OF REAR FLIGHT

FIG.17.

FLOW PATTERNS OBSERVED BY STREET.

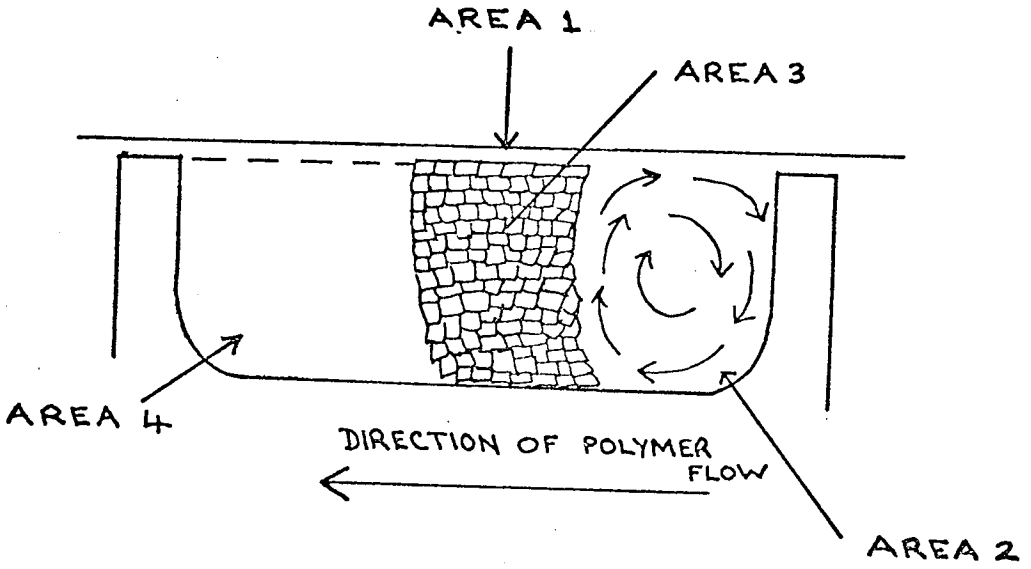

FIG. 18.

for polyethylene this would probably cover the regions 3 - 5 as described above.

2.6 MELTING, HEAT TRANSFER AND VISCOUS HEATING IN EXTRUSION

In 1961 Street (25) investigated the process of melting of the polymer during extrusion. Consideration was given to a section of the channel in the screw which contained two parts of the screw flight (see Figure (17)). These are referred to as the forward and rear flights respectively. This section (Figure (18)) was divided into four areas. Figure (18) should be referred to when considering the following descriptions :

Area 1 : Above the cold granules a coating of molten material on the barrel wall which has been melted by conducted heat.

Area 2 : A portion of fully 'plasticised' melt is held between the forward edge of the rear flight and the remaining material in the channel. The quantity of this material increases as the polymer approaches the extruder die and should finally fill the channel.

Area 3 : Adjacent to the molten material there is a zone where the pellets are warm enough to adhere to each other and to the molten material. At the boundary between the areas (2) and (3) pellets are continually melted and become part of the circulating mass in area (2).

Area 4 : Starting at the rear face of the forward flight there is unplasticised material which advances down the screw eventually to progress into melt via the other three areas previously mentioned.

It was concluded that there were two mechanisms of melting namely :

(a) Conduction from the barrel wall (forming area (1)).

(b) The melting initiated by (a).

i.e. the melting due to the heat transfer and erosion by the circulating mass of area (2).

Menges and Klenk (26) divided the melting process for thermoplastics into two mechanisms, one for "wetting" polymers and one for "non-wetting" polymers (a wetting polymer can be defined as one which tends to adhere to metallic surfaces and non-wetting polymers are therefore ones which do not tend to adhere to metal surfaces.) Wetting materials are exemplified by polyethylene, polystyrene and highly plasticised PVC compounds, while examples of non-wetting materials are unplasticised PVC and ultra-high molecular weight polyolefins.

The mechanism for wetting polymers which is basically the same as that of Street (25) was summarised as follows and the zones are illustrated in Figure (19).

MELTING MECHANISM FOR WETTING THERMOPLASTICS AS OBSERVED BY MENGES AND KLENK

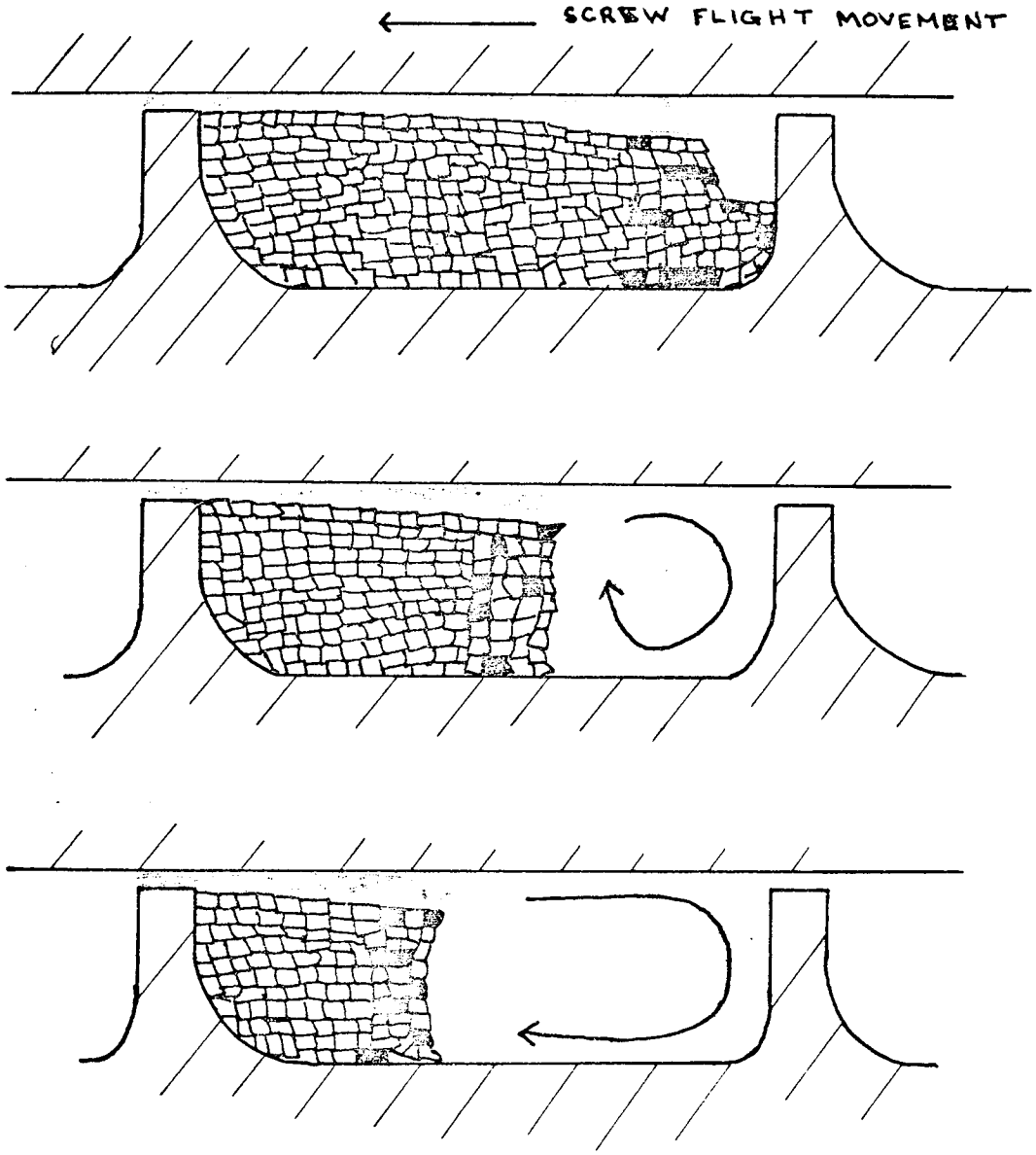

ZONE 1 - THIN LAYER OF MELT

ZONE 2 - MOLTEN POLYMER SCRAPED OFF BY THE ADVANCING SCREW FLIGHT

ZONE 3 - PARTIALLY MELTED POLYMER

ZONE 4 - SOLID POLYMER PARTICLES

FIG. 19.

Zone 1 - The cold material is covered with a thin layer of melt which is formed through direct contact with the barrel wall.

Zone 2 - The following screw flight (forward edge of the rear flight) scrapes the film of melted polymer off the inside of the barrel wall. This forms a zone of plasticised material which circulates on the forward side of the rear screw flight. This zone becomes larger as it passes along the barrel within the screw flight until it completely fills the channel.

Zone 3 - In this transition zone the solid polymer (in the form of granules or powder) is heated by the circulating mass, softened and partially melted by an erosion mechanism.

Zone 4 - Cold particles are found in this area. They completely fill the region up to the rear side of the forward flight, gradually being transformed to zones 2 and 3.

Sometimes non-wetting and high viscosity polymers do not process efficiently on single screw extruders. Figure (20) shows the behaviour found for these polymers. It is quite obvious that the fusion mechanism has changed from that illustrated in Figure (19). The former mechanism is called "rear channel fusion" and therefore it was logical to call the latter mechanism "forward channel fusion".

Zone 1 is shown in Figure (20). The polymer in this region is sintered by conducted heat from the surroundings. The sintered material is converted

MELTING MECHANISM FOR NON-WETTING THERMOPLASTICS (MENGES AND KLENK)

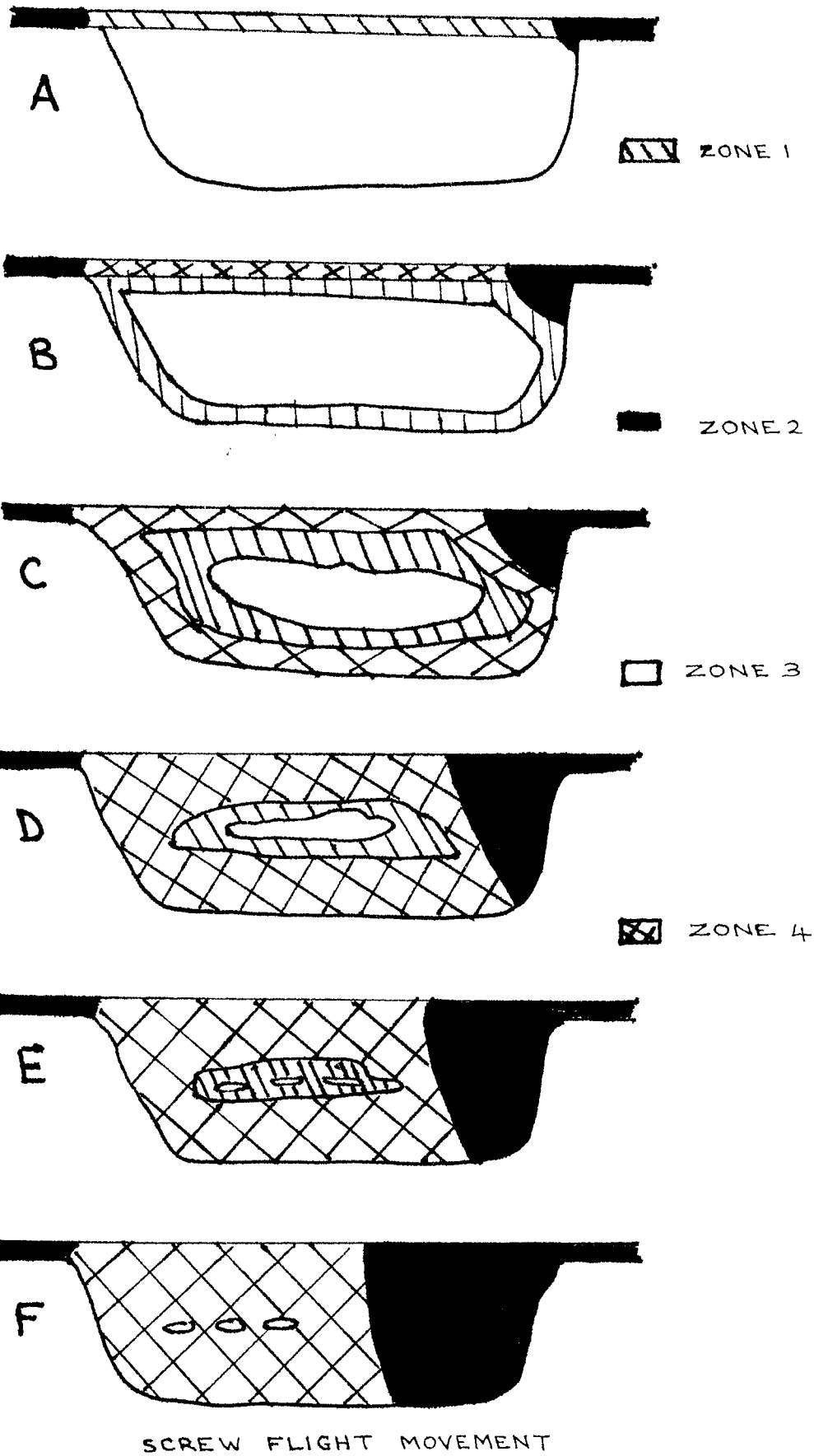

FIG.20

into the plastic state upon reaching a certain temperature which is influenced by the melt pressure and composition of the material (see Figure (20) b-f, zone 4). The sintering process continues towards the channel centre (zone 1, Figure (20) b-e). The screw is filled along some considerable distance both with homogeneously plasticised material on the passive (rear side of the forward flight - zone 2), as well as material which has been softened by conducted and shear heating (i.e. zone 4), with sintered material (zone 1) and with solid (zone 3). In consequence of the poor melting, mixing is also poor, effectively none occurring in zones 1, 3 and 4 (only in zone 2 is material satisfactorily homogenised). This mechanism is undesirable and inefficient compared to "rear channel fusion".

Gale (27) has carried out a considerable amount of work on the processing of rigid PVC dry blends. In this work, the two mechanisms described by Menges and Klenk were observed for PVC compounds. The mechanisms which occurred appeared to depend on the type of lubricant used in the compound. Compatible lubricants such as glycerol monostearate (GMS) tended to produce "rear channel fusion" whereas external or incompatible lubricants such as stearic acid tended to produce "forward channel fusion".

A model which provides equations which enable the length of the melting zone to be calculated was produced by Tadmor (28). The following assumptions were made :

(1) Steady state temperatures and velocities were assumed, implying that at any cross section of the channel the solid/melt interface remains in the

same position.

(2) Sharp boundaries, i.e. sharp melting point for the plastic material rather than a softening range.

(3) The solid bed was considered homogeneous and continuous.

(4) The polymer melt was assumed to be Newtonian.

Condition (1) means that temperatures and velocities do not change, this assumption is probably valid once the extrusion machine has settled to steady operating conditions. The assumption of a sharp melting point (2) was obviously in error even for highly crystalline polymers. A homogeneous solid bed (3) is probably never true as can be seen from the work of Street (25), Gale (27) and Menges and Klenk (26), air will almost certainly be occluded in the semi-fused solid. Assumption (4) is also incorrect since polymers are not Newtonian but probably more closely described by a power law under processing conditions. However, in spite of these assumptions the work is still useful and indeed it would be exceedingly difficult to analyse the situation at all if simplifying assumptions were not made.

The most important conclusions as far as this project is concerned was the estimate that about 35 - 46% of the heat of melting came from viscous heating.

Tanner (29) described the attractions of viscous heating as :

(1) The heat would be available at the point where it was required. If it were

possible to carry out accurate local temperature measurements, instantaneous heat control could be effected by changing the screw speed.

(2) Heat build up could occur only within the material, the barrel and screw would be available to disperse any excess heat.

(3) Heating up times would be shortened.

The experiments carried out by Tanner indicated that since heat generation by viscous heating was not controllable, extensive degradation occurred in the extrudate. As a consequence of these experiments five points were suggested which an extruder should fulfil if operated by the use of viscous heating alone. These conditions were :

(1) There must only be a thin layer of material between the screw and the wall of the barrel. It was said that this prevents "laminar tearing" between the rotating material and the material adhering to the wall. It would seem that "laminar tearing" or interlaminar shear between moving and stationary material would always occur but if the stationary layer on the barrel wall is thin then the heat generated can more easily be conducted away through the barrel wall.

(2) There must not be a high temperature gradient between the bulk of the material and the wall of the barrel since the polymer close to the wall would become molten too quickly and the "laminar tearing" mentioned above would result. This is due to the viscosity of the polymer becoming

comparatively low in that region and therefore offering less resistance to relative rotation.

(3) The extruder must be carefully designed so that the flow of the material is smooth and there are no points of stagnation or hindrance to flow which would lead to local over-heating. This, of course, is important in conventional extruders but was emphasised presumably because it would be more important in an extruder operated by viscous heating alone.

(4) There should be practically no leakage flow (i.e. the flow of material back along the screw) as this would lead to additional heat generation.

(5) It must be possible to take accurate temperature measurements of the material. Measurements on the barrel respond too slowly and make it impossible to control the extruder accurately.

It is extremely difficult to satisfy all these conditions especially (4) and (5). Direct temperature measurements were considered almost impossible at the time of publication of Tanner's paper, however, in recent years it has become possible to measure the temperature of flowing polymer melts more accurately.

The elimination of leakage flow as condition (4) requires, would probably have serious effects on the mixing efficiency of the extruder. Tanner concluded that since the above conditions could not be satisfied operation of an extruder using viscous heating as the major heat source was not a practical proposition.

According to Janeschitz-Kriegel and Schijf (30) the problem of heat transfer in an extruder is much too difficult to solve in purely mathematical terms, even when a computer is used. This was the justification for considering only a part of the heat transfer process. In fact the radial heat transfer by conduction between the screw and the barrel was considered. The investigation used the "wiping effect" described by Jepson (31) and assumed that the heat source was situated in the screw. Jepson's wiping effect is a mechanism postulated for the melting of polymers in an extruder. It states that the moment the screw land wipes the barrel a fresh layer of polymer is deposited and remains there for approximately one revolution of the screw. The amount of heat penetrating the layer during that time by conduction is then removed with the polymer layer. The heat from the wiped polymer was thought to be homogeneously distributed over the screw channel. This mechanism is probably reasonable accurate when the polymer is completely molten but there would probably be a time lag for the distribution of the heat in the screw channel. In the compression zone where the polymer is not completely molten then the heat is certainly not evenly distributed in the screw channel.

In one revolution the heat penetrating from the barrel wall into the polymer was said to be given by :

$$q = \Delta T_o \, 2 k_c \sqrt{t} / \sqrt{(\pi a)}$$

Where q = heat flow unit area .... J/m^2

k_c = thermal conductivity ...$W/m\,^{\circ}C$

t = time required for one revolution of the screw .... seconds(s)

a = thermal diffusivity ... m^2/s

The relationship between the temperature difference and the heat transferred is :

$$\Delta T_o = Q\sqrt{(\pi a)} / 2K_c\sqrt{n}$$

Where Q = heat flow/unit area/ unit time .... W/m^2

n = number of revolutions/unit time .... s^{-1}

The depth of penetration of conducted heat during one revolution was :

$$\Delta_d = 4\sqrt{\frac{a}{n}}$$

Where : Δ_d = thickness of molten polymer film ....m .or cm.

An example was given by Janeschitz - Kriegel et al. It was assumed that :

$\alpha = 0.1 \times 10^{-6}\ m^2/s$

n = 100 revs/min.

It was found that :

$\Delta_{d(100)} = = 0.1$ cm

This illustrates very well the low efficiency of the heat conduction

process, only 0.1 cm of polymer was heated during one revolution. In the experiments performed, the complications of viscous heating were eliminated by the use of a low viscosity polymer mixed with a high proportion of lubricant (low density polyethylene 80% and paraffin oil 20%).

2.7 HEAT TRANSFER TO MOLTEN FLOWING POLYMERS

Griskey and Wiehe (32) developed a method of measuring the temperature profiles in molten flowing polymers, which is important in operations such as extrusion and injection moulding. The situation is complex because molten polymers are compressible and also exhibit viscoelastic characteristics. The technique used an extruder with an adapter fitted at the die exit. The adapter being a 3/8" pipe wrapped with electrical heating tape and fitted with thermocouples in the wall at known radial distances in the pipe. The thermocouples were positioned parallel to the flow stream so that disturbances were reduced to a minimum. Results were plotted as temperature (in dimensionless form) versus radius (reduced radius r/R) as shown in Figure (21). The only term changing in the Graetz number (N_{Gz} = $wCp/\lambda L$ where w = weight flow rate, L = length of the tube, Cp = specific heat of polymer and λ = thermal conductivity of the polymer) is the weight flow rate since all the other terms are constant. Some of these assumptions are not strictly true since the thermal conductivity and specific heat do change with temperature, although probably not significantly in the melt state. Increasing Graetz number means an increasing flow rate and less residence time for the polymer, hence

DATA OBTAINED BY
GRISKEY AND WIEHE

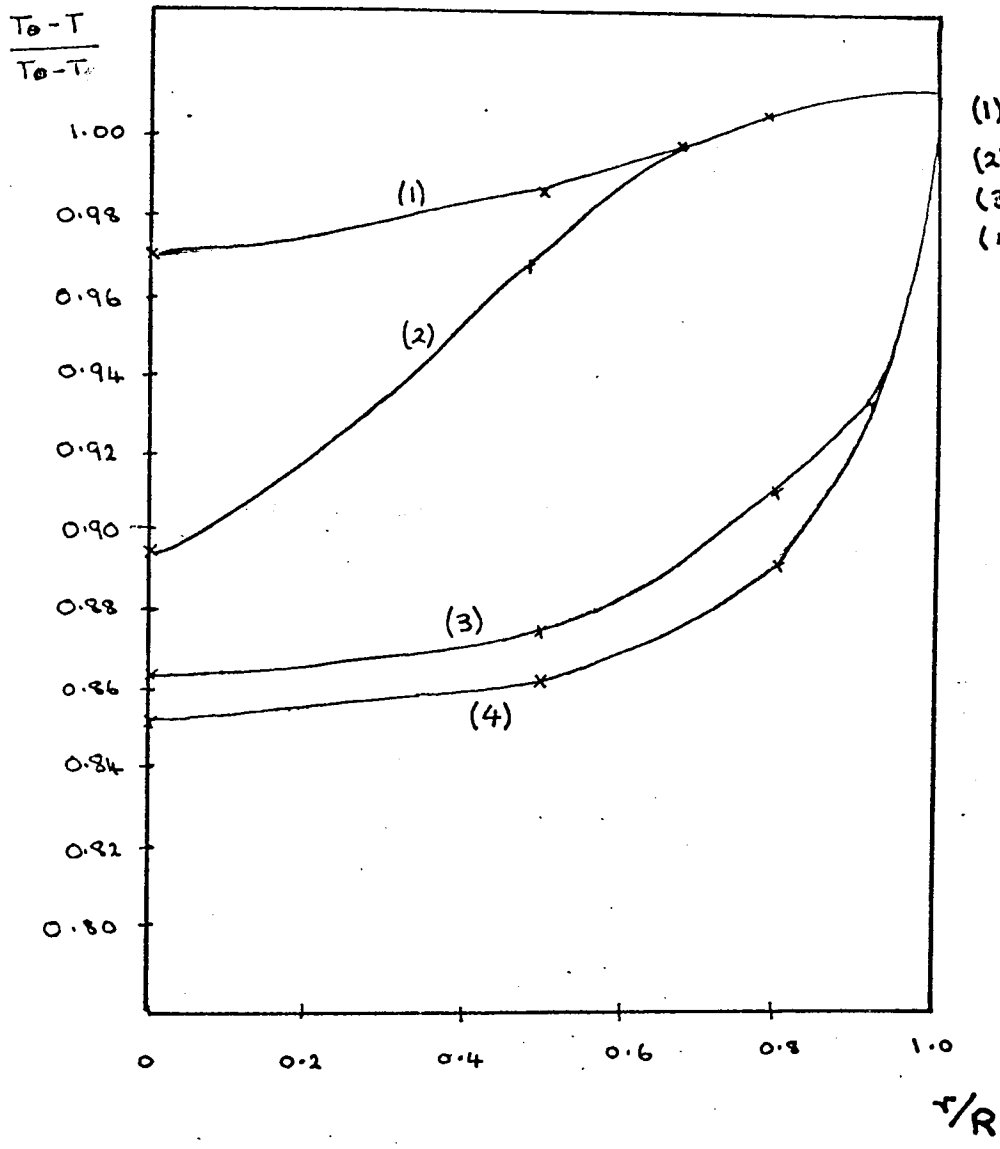

(1) $N_{Gz} = 4.87$
(2) $N_{Gz} = 3.26$
(3) $N_{Gz} = 1.50$
(4) $N_{Gz} = 0.752$
N_{Gz} = GRAETZ NUMBER

T_0 = POINT TEMPERATURE
T = AVERAGE FLUID INLET TEMPERATURE
T_∞ = WALL TEMPERATURE
r = POINT RADIUS
R = TUBE RADIUS

FIG.21.

less opportunity for energy to be transferred to the melt. From Figure (21) it can be seen that the temperature increases with increasing Graetz number which seems to be in direct contradiction to the above reasoning. However, if viscous dissipation (shear heating) is considered the results then become sensible.

The major conclusion as far as this project is concerned was that the shear heating would be lower than predicted by the viscous model used in the calculations. One reason could be that polymers are viscoelastic materials and therefore do not convert all the imposed mechanical work into heat, some energy is stored as elastic potential energy.

3.0 THEORY

The apparatus used for this work consisted of concentric cylinders and the following theory was developed to describe the thermal conduction and viscous heating processes occurring in the apparatus.

3.1. MATHEMATICAL DESCRIPTION OF THE CONDUCTION PROCESS IN THE APPARATUS

If concentric cylinders such as those shown in Figure (22) are considered, then the appropriate heat transfer equation to describe heat conduction from 'a' to 'b' under transient conditions is :

$$\frac{\partial \theta}{\partial t} = \frac{\alpha}{r} \cdot \frac{\partial}{\partial r}\left(r \cdot \frac{\partial \theta}{\partial r}\right) \qquad \ldots\ldots\ldots\ldots\ldots (1)$$

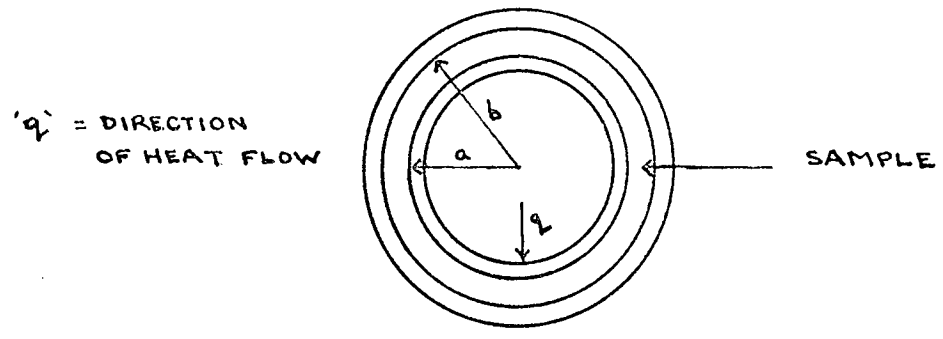

FIG. 22

That is, the heat transfer was assumed to be radially across the cylinders, no heat was assumed to flow axially. This was justifiable because a high L:D ratio was used

in the apparatus (16:1) and it was shown by Kline (10) that axial heat flow could be neglected if the L:D ratio was at least 12:1 .

The boundary conditions for the solution of the above differential equation were :-

$t = 0$, $\Theta = \Theta_o$ for all values of 'r' from r = a to r = b .

$t > 0$, $r = a$; a constant heat flux is supplied to the sample via a known thermal capacity (the inner cylinder);

$r = b$; the heat flux is absorbed into a known thermal capacity (the outer cylinder).

Let 'Ca' and 'Cb' be the total heat capacities of the two cylinders of radius 'a' and 'b' respectively.

Let 'F' be the heat flow rate per unit length (W/m) supplied at r = a .

The heat balance at r = a is then :

$$F = C_a \left(\frac{\partial \theta}{\partial t}\right)_a - 2\pi a \lambda \left(\frac{\partial \theta}{\partial r}\right)_a \qquad \ldots\ldots\ldots\ldots (2)$$

Where :

$C_a \left(\frac{\partial \theta}{\partial t}\right)_a$ = rate of energy absorption by the thermal capacity of the inner cylinder.

$2\pi a \lambda \left(\frac{\partial \theta}{\partial r}\right)_a$ = rate of heat conduction through the specimen.

The heat balance at $r = b$ is :

$$2\pi b\lambda\left(\frac{\partial\theta}{\partial r}\right)_b + C_b\left(\frac{\partial\theta}{\partial t}\right)_b = 0 \qquad \ldots\ldots\ldots (3)$$

Where the terms have the respective significance given above.

Two methods of approach were available for the solution of the differential equations (1), (2) and (3) given above. For an exact mathematical solution an analytical approach was required but the complexity of the mathematics involved would probably have increased the difficulties of the project unnecessarily. The alternative was to use a finite difference approximation for the differential equations which of course does not yield an exact solution but the technique is easier to use, much quicker if computers are used for the calculations and the answers obtained are usually very close to the 'real' solution.

Before equation (1) was converted to its finite difference form a substitution was made which had been shown (33) to simplify problems of this nature.

For a hollow cylinder :

$$x = \ln(r/a) \qquad \ldots\ldots\ldots (4)$$

$$\therefore \quad e^x = r/a \qquad \ldots\ldots\ldots (5)$$

$$\therefore \quad r = ae^x \qquad \ldots\ldots\ldots (6)$$

Then (1) becomes :

$$\frac{\partial \theta}{\partial t} = \alpha \frac{e^{-2x}}{a^2} \frac{\partial^2 \theta}{\partial x^2} \qquad \text{for } x = 0 \text{ to } \ln(b/a) \qquad \ldots\ldots\ldots (7)$$

The implicit finite difference form of $\left(\frac{\partial \theta}{\partial t}\right)$ in this case was :

$$\left(\frac{\partial \theta}{\partial t}\right)_{i,j} = \left(\frac{\theta_{i,j} - \theta_{i,j-1}}{\Delta t}\right) \qquad \ldots\ldots\ldots (8)$$

$\left(\frac{\partial^2 \theta}{\partial x^2}\right)$ became :

$$\left(\frac{\partial^2 \theta}{\partial x^2}\right)_{i,j} = \frac{\theta_{i-1,j} - 2\theta_{i,j} + \theta_{i+1,j}}{(\Delta x)^2} \qquad \ldots\ldots\ldots (9)$$

Therefore (7) becomes :

$$\frac{\theta_{i,j} - \theta_{i,j-1}}{\Delta t} = \left(\frac{\alpha e^{-2xi}}{a^2}\right) \frac{\theta_{i-1,j} - 2\theta_{i,j} + \theta_{i+1,j}}{(\Delta x)^2} \qquad \ldots\ldots\ldots (10)$$

Now at $i = 0$, $x = 0$, i.e. $x_i = i\Delta x$

Therefore, on making this substitution and re-arranging, (10) becomes :

$$\left(\frac{\Delta x^2 . a^2}{\alpha . \Delta t}\right) e^{i\Delta x} (\theta_{i,j} - \theta_{i,j-1}) = \theta_{i-1,j} - 2\theta_{i,j} + \theta_{i+1,j} \qquad \ldots\ldots\ldots (11)$$

Let $m = \frac{\Delta x^2 . a^2}{\alpha . \Delta t}$

Then (11) becomes :

$$\theta_{i-1,j} - (2 + me^{2i\Delta x})\theta_{i,j} + \theta_{i+1,j} = -me^{2i\Delta x}\theta_{i,j-1} \qquad \ldots\ldots\ldots (12)$$

for $i = 1, 2, 3 \ldots\ldots n-2, n-1$

The heat balance at r = a (i.e. when x = 0) was given by :

$$2\pi a\lambda\left(\frac{\partial\theta}{\partial r}\right)_a - C_a\left(\frac{\partial\theta}{\partial t}\right) = -F \qquad \ldots\ldots\ldots (2)$$

Now :

$$\frac{\partial\theta}{\partial r} = \frac{\partial\theta}{\partial x}\cdot\frac{\partial x}{\partial r} \qquad \ldots\ldots\ldots (13)$$

Differentiating (6) gives :

$$\frac{\partial x}{\partial r} = \frac{1}{r} = \frac{e^{-x}}{a} \qquad \ldots\ldots\ldots (14)$$

Therefore :

$$\left(\frac{\partial\theta}{\partial r}\right)_a = \frac{1}{a}\left(\frac{\partial\theta}{\partial x}\right)_a \qquad \ldots\ldots\ldots (15)$$

$$\left(\frac{\partial\theta}{\partial r}\right)_b = \frac{1}{b}\left(\frac{\partial\theta}{\partial x}\right)_b \qquad \ldots\ldots\ldots (16)$$

Substituting (16) in (2) the result is :

$$2\pi\lambda\left(\frac{\partial\theta}{\partial x}\right)_a - C_a\left(\frac{\partial\theta}{\partial t}\right) = -F \qquad \ldots\ldots\ldots (17)$$

In finite difference from the equation is

$$2\pi\lambda\left(\frac{\theta_{1,j} - \theta_{0,j}}{\Delta x}\right) - C_a\left(\frac{\theta_{0,j} - \theta_{0,j-1}}{\Delta t}\right) = -F \qquad \ldots\ldots\ldots (18)$$

This equation rearranges into':

$$\theta_{1,j} - \theta_{0,j} - \frac{C_a.\Delta x}{2\pi\lambda\Delta t}(\theta_{0,j} - \theta_{0,j-1}) = -\frac{F\Delta x}{2\pi\lambda} \quad \ldots\ldots\ldots(19)$$

Let $p = \frac{C_a.\Delta x}{2\pi\lambda\Delta t}$

Then (19) becomes

$$-(1+p)\theta_{0,j} + \theta_{1,j} = -p\theta_{0,j-1} - \frac{F.\Delta x}{2\pi\lambda} \quad \ldots\ldots\ldots(20)$$

The heat balance at r = b (i.e. when x = ln(b/a)) was given by :

$$2\pi\lambda b\left(\frac{\partial\theta}{\partial r}\right)_b + C_b\left(\frac{\partial\theta}{\partial t}\right) = 0 \quad \ldots\ldots\ldots(3)$$

When (16) is substituted in (3) and the equation rearranged as before, it becomes :

$$-\theta_{n,j} - \theta_{n-1,j} = \frac{C_b.\Delta x}{2\pi\lambda\Delta t}(\theta_{n,j} - \theta_{n,j-1}) \quad \ldots\ldots\ldots(21)$$

Let $q = \frac{C_b.\Delta x}{2\pi\lambda\Delta t}$

Equation (21) then becomes :

$$\theta_{n-1,j} - (1+q)\theta_{n,j} = -q\theta_{n,j-1} \quad \ldots\ldots\ldots(22)$$

There is, therefore, a complete set of 'n' finite difference equations and they are listed below.

Equation (20) is the first equation and it represents the situation at i = 0. Equation (11) is valid from i = 1 to i = n-1 and represents the situation at each of

those points in space. Equation (22) is the n^{th} equation and is valid at the point $i = n$.

The series of equations are :

$$i = 0 \qquad -(1+p)\,\theta_{0,j} + \theta_{1,j} = -p\,\theta_{0,j-1} - \frac{F.\Delta x}{2\pi\lambda}$$

$$i = 1, 2 \ldots n-1 \qquad \theta_{i-1,j} - (2 + m e^{2i\Delta x})\,\theta_{i,j} + \theta_{i+1,j} = -m e^{2i\Delta x}\,\theta_{i,j-1}$$

$$i = n \qquad \theta_{n-1,j} - (1+q)\,\theta_{n,j} = -q\,\theta_{n,j-1}$$

Where : i = space variable $i = 0, 1, 2 \ldots n$

j = time variable $j = 0, 1 \ldots\ldots$ to any required integer.

The solution of the differential equations (1), (2) and (3) was now resolved into 'n' simultaneous equations which were solved using a "Gaussian elimination" technique.

3.2. GAUSSIAN ELIMINATION

The set of finite difference equations can be expressed in general terms in the following way.

$i = 0$ $\qquad b_o \theta_{o,j} + c_o \theta_{1,j} = d_o$

$i = 1, 2 \ldots n-1$ $\qquad a_i \theta_{i-1,j} + b_i \theta_{i,j} + c_i \theta_{i+1,j} = d_i$

$i = n$ $\qquad a_n \theta_{n-1,j} + b_n \theta_{n,j} = d_n$

Where in this case :

$a_o = 0$, $a_i = 1$ for $i = 1, 2 \ldots n$

$b_o = -(1+p)$, $b_i = -(2+me^{2i\Delta x})$ for $i = 1, 2 \ldots n-1$, $b_n = -(1+q)$

$c_o = 1$, for $i = 0, 1 \ldots n-1$, $c_n = 0$

$d_o = -p\theta_{o,j-1}$

$d_i = -me^{2i\Delta x}\, \theta_{i,j-1}$ for $i = 1, 2 \ldots n-1$

$d_n = -q\theta_{n,j-1}$

The known quantities are :

'a', 'b', 'c' and 'd' (In order to make 'b' and 'd' known quantities it is necessary to "quess" values for 'α' and 'λ' respectively.)

The unknown quantities are : $\theta_{o,j}, \theta_{1,j} \ldots\ldots \theta_{n,j}$

At $i = 0$ $\qquad b_o \theta_o + c_o \theta_1 = do$ $\qquad \ldots\ldots\ldots (23)$

Therefore : $\theta_o = \dfrac{(d_o - c_o\theta_1)}{b_o}$ ..... (24)

Now at i = 1 the equation is :

$$a_1\theta_o + b_1\theta_1 + c_1\theta_2 = d_1 \quad \text{..... (25)}$$

Substituting the value of θ_o obtained from (24), (25) becomes :

$$a_1 \frac{(d_o - c_o\theta_1)}{b_o} + b_1\theta_1 + c_1\theta_2 = d_1 \quad \text{..... (26)}$$

This equation rearranges into :

$$\theta_1 = \frac{(d_1 - a_1d_o/b_o) - c_1\theta_2}{b_1 - a_1c_o/b_o} \quad \text{..... (27)}$$

Similarly :

$$\theta_2 = \frac{(d_2 - a_2d_1/b_1) - c_2\theta_3}{b_2 - a_2c_1/b_1} \quad \text{..... (28)}$$

Therefore in general :

$$\theta_i = \frac{(d_i - a_id_{i-1}/b_{i-1}) - c_i\theta_{i+1}}{b_i - a_ic_{i-1}/b_{i-1}} \quad \text{..... (29)}$$

Let $\beta_i = (b_i - a_ic_{i-1}/b_{i-1})$ N.B. $\beta_o = b_o$ ..... (30)

$$\delta_i = (d_i - a_id_{i-1}/b_{i-1}) \quad \text{N.B.} \quad \delta_o = d_o \quad \text{..... (31)}$$

Therefore (29) becomes :

$$\theta_i = (\delta_i - c_i \theta_{i+1}) / \beta_i \qquad \ldots\ldots\ldots\ldots (32)$$

The procedure for solving the equations is as follows :

(It will be seen that in the above equation 'j' has been omitted from the 'θ' values, this is because it is constant in each evaluation. That is for each evaluation time it is constant (j = constant), the evaluation can be repeated for every time step (j = 0, 1...m; where 'm' is any required integer.)).

(1) Calculate β_i values from i = 0, 1, 2...n; from (30)

(2) Calculate δ_i values from i = 0, 1,2...n; from (31)

(3) It is necessary to calculate 'θ' values starting at i = n and then proceeding to i = n-1, i = n-2 and so on until i = 0 is reached. This is so because of the θ_{n+1} term which appears in (32).

Now : $$\theta_n = \frac{\delta_n - c_n \theta_{n+1}}{\beta_n}$$

But $c_n = 0$

Therefore : $$\theta_n = \frac{\delta_n}{\beta_n} \qquad \ldots\ldots\ldots\ldots (33)$$

Now θ_{n-1} can be calculated because θ_n has been calculated from (33), the procedure continues until θ_o is reached. At this stage the method has produced

a temperature profile across the sample at the time represented by the value of 'j'. The temperature profile at the next time interval can be found by repeating the procedure with $j = j+1$. Changing the value of 'j' affects the 'd' terms because the $\theta_{i_1 j-1}$ will change. The process can continue until the required length of time is reached (time = $\Delta t.j$).

If this method alone is used to solve the equations then at the end of the time ($\Delta t.j$) the temperature profile obtained with the guessed values of 'α' and 'λ' has to be compared manually with the experimental temperature profile. Adjustments to the valuesof 'α' and 'λ' are made until the profiles agree. This, of course, could prove to be a long and tedious process and the following section describes how to avoid the "hand optimisation" of the quantities 'α' and 'λ'.

3.3. THE USE OF NON-LINEAR OPTIMISATION

To avoid using the trial and error method discussed in the previous section the finite difference approximation was combined with a non-linear optimisation technique (34). The optimisation procedure basically achieves the same result as the trial and error method, but with the aid of a computer, in a fraction of the time.

The method employed was called the 'Simplex Method'. Most optimisations reduce to a mathematical problem of maximising or minimising a function (usually

called the objective function.) In this case the sum of the squares of the differences between the experimental and calculated temperatures.

The 'simplex method' evaluates the objective function at 'n + 1' mutually equidistant points in the space of 'n' independent variables (i.e. the variables to be optimised, in this case thermal diffusivity and thermal conductivity). The 'n + 1' points are said to form the vertices of a regular simplex. Therefore, a regular simplex in two dimensions consists of an equilateral triangle, whilst that in three dimensions consists of a regular tetrahedon.

The method is initiated by setting up a regular simplex in the space of the 'n' independent variables and evaluating the objective function at each vertex. The basic iteration proceeds according to the following rules :

(1) Determine the vertex at which the objective function takes on the largest value and reflect this vertex in the centroid of the remaining 'n' vertices, thus forming a new simplex.

(2) Evaluate the objective function at this new vertex and revert to step (1).

If the new vertex happened to be the vertex of greatest function value in the new simplex, this search procedure would cease to progress and mere oscillation between the last two simplexes would occur. To prevent such an occurrence, a new rule is introduced :

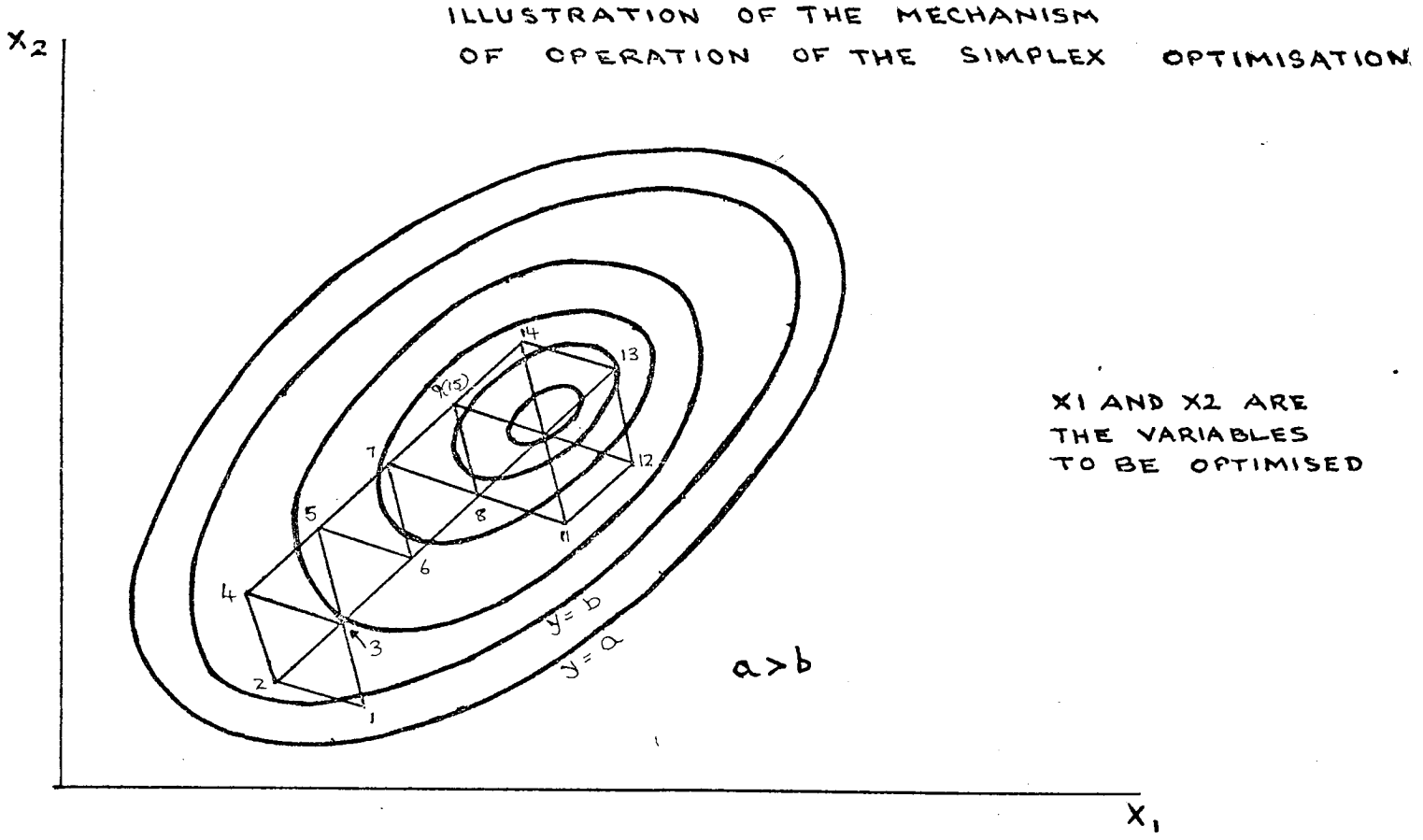
ILLUSTRATION OF THE MECHANISM
OF OPERATION OF THE SIMPLEX OPTIMISATION
X2
X1
X1 AND X2 ARE
THE VARIABLES
TO BE OPTIMISED
a>b
y=b
y=a
1
2
3
4
5
6
7
8
11
12
13
14
X(15)

FIG. 23.

(3) If, at any stage, the vertex selected by (1) is the most recently introduced vertex of the current simplex, reflect the vertex of the next largest function value instead.

A typical performance of the procedure with a function of two variables is illustrated in Figure (23) in which the numbers denote the order in which the vertices were introduced. It will be noticed that rule (3) has been used in the simplex comprising points 8, 10 and 11, point 8 being selected instead of point 11. Vertex 10 is close to the minimum and so the simplex revolves about this point, until vertex 15, which coincides with vertex 9 is obtained. The exact coincidence of points 9 and 15 is a property of equilateral triangles and would not occur in more than two dimensions. This illustrates the point that when a simplex is near a minimum, it is characteristic for one point to constitute a vertex of a large number of consecutive simplexes. A fourth rule is therefore introduced :

(4) If one vertex of the simplex remains unchanged for more than 'M' consecutive iterations, reduce the size of the simplex by halving the distances of the remaining vertices from this vertex and recommence the whole search procedure. 'M' depends on the number of independent variables. Spendley et al suggested the following relationship : $M = 1.65n + 0.05\,n^2$
The search is terminated and convergence assumed when the size of the simplex has been reduced by a specified amount.

The complete programme in Fortran IV is given in Appendix 2 together with its flow chart.

3.4. MATHEMATICAL DESCRIPTION OF THE THERMAL CONDUCTION AND VISCOUS HEATING PROCESSES IN THE APPARATUS

The equation of motion for V_θ in terms of θ is (35) :

$$\rho \frac{\partial V_\theta}{\partial t} = -\frac{1}{r} \cdot \frac{\partial P}{\partial \theta} - \frac{1}{r} \frac{\partial}{\partial r} (r \tau_{r\theta}) + \rho g_\theta \qquad \ldots\ldots\ldots (34)$$

In this case $\frac{\partial P}{\partial \theta} = g_\theta = 0$. This can be assumed because the pressure within the polymer should be uniform and constant during experiments. Gravitational forces represented by 'g_θ' can be ignored because the viscosity of the polymer is so high the effect of gravity on the flow of the material can be neglected.

Therefore,

$$\rho \frac{\partial V_\theta}{\partial t} = \frac{1}{r} \cdot \frac{\partial}{\partial r} (r \tau_{r\theta}) \qquad \ldots\ldots\ldots (35)$$

Now $\tau_{r\theta} = \eta_a \left(\frac{\partial V_\theta}{\partial r}\right)$

Therefore : $$\rho \frac{\partial V_\theta}{\partial t} = \eta \frac{\partial}{\partial r} \left(\frac{1}{r} \frac{\partial}{\partial r} (r V_\theta) \right) \qquad \ldots\ldots\ldots (37)$$

The progression from equations (35) to (37) involves the assumption that 'η' is independent of 'r'.

Viscous heating can be calculated from :

$$\tau . \dot{\gamma} = K(\dot{\gamma})^{n-1} (\dot{\gamma})^2 = K(\dot{\gamma})^{n+1}$$

Where $K(\dot{\gamma})^{n-1} = \eta$ = apparent viscosity

$\dot{\gamma} = \left(\frac{\partial V_\theta}{\partial r}\right)$ = shear rate

However, in cylindrical co-ordinates the shear rate term becomes:

$$\phi_v = r \cdot \frac{\partial}{\partial r}\left(\frac{V_\theta}{r}\right)$$

Therefore the viscous heating term becomes:

$$\eta\left(r \frac{\partial}{\partial r}\left(\frac{V_\theta}{r}\right)\right)^2 \quad \text{or} \quad \eta r^2\left(\frac{\partial}{\partial r}\left(\frac{V_\theta}{r}\right)^2\right)$$

Hence there are two equations which describe the situation, equation (37) and the following heat conduction equation with a source term for viscous heating;

$$\frac{\partial T}{\partial t} = \alpha \cdot \frac{\partial}{\partial r}\left[\frac{1}{r}\frac{\partial}{\partial r}\left(r \frac{\partial T}{\partial r}\right)\right] + \frac{\eta r^2}{\rho C_p}\left[\frac{\partial}{\partial r}\left(\frac{V_\theta}{r}\right)\right]^2 \qquad \ldots\ldots\ldots (38)$$

Boundary conditions :

$t = 0,\ V_\theta = 0,\ T = T_o$ for all 'r'

$t > 0$, at $r = a,\ V_\theta = Va$)
) for all
at $r = b,\ V_\theta = 0$) T, t

Now :

$$\eta = K\left(\frac{\partial V_\theta}{\partial r}\right)^{n-1} \qquad \ldots\ldots\ldots (39)$$

Where : η = apparent viscosity

K = consistency index

$\left(\frac{\partial V_\theta}{\partial r}\right)$ = shear rate

n = flow behaviour index

The temperature dependence of 'η' is given by (36).

$$\eta = K_o \left(\frac{\partial V_\theta}{\partial r}\right)^{n-1} \cdot B e^{A/(T+273.2)} \qquad \ldots\ldots\ldots (40)$$

B = constant for each polymer used

A = constant

K_o = consistency index at a chosen reference temperature 'T'.

For a first approximation :

$$\frac{\partial V_\theta}{\partial t} = 0 \qquad \text{and} \qquad K = \text{constant}$$

Equation (37) becomes:

$$\left(\frac{\partial V_\theta}{\partial r}\right)^{n-1} \frac{\partial}{\partial r}\left[\frac{1}{r}\frac{\partial}{\partial r}(r V_\theta)\right] = 0 \qquad \ldots\ldots\ldots (41)$$

but

$$\frac{\partial V_\theta}{\partial r} \neq 0 \qquad \text{for } r = a \text{ to } r = b$$

Therefore : $\frac{1}{r}\frac{\partial}{\partial r}(r V_\theta) = 2C_1$ (i.e. constant)

Integrating : $rV_\theta = C_1 r^2 + C_2$

At $r = a$, $V_\theta = V_a$. $aV_a = C_1 a^2 + C_2$

At $r = b$, $V_\theta = 0$. $= C_1 b^2 + C_2$

$$C_2 = -C_1 b^2$$

$$aV_a = -C_1 (b^2 - a^2)$$

$$rV_\theta = -C_1 (b^2 - r^2)$$

$$\frac{aV_a}{rV_\theta} = \frac{b^2 - a^2}{b^2 - r^2} \qquad \ldots\ldots\ldots (42)$$

$$\frac{V_\theta}{V_a} = \frac{a(b^2 - r^2)}{r(b^2 - a^2)} \qquad \ldots\ldots\ldots (43)$$

Differentiating :

$$\frac{\partial V_\theta}{\partial r} = \frac{aV_a}{b^2 - a^2} \frac{\partial}{\partial r}\left(\frac{b^2 - r^2}{r}\right)$$

$$= \frac{aV_a}{b^2 - a^2}\left(\frac{r^2 + b^2}{r^2}\right) \qquad \ldots\ldots\ldots (44)$$

$$\frac{\partial}{\partial r}\left(\frac{V_\theta}{r}\right) = \frac{aV_a}{(b^2 - a^2)} \frac{\partial}{\partial r} \frac{b^2 - r^2}{r^2} \qquad \ldots\ldots\ldots (45)$$

$$= \frac{aV_a}{(b^2 - a^2)}\left(-\frac{2b^2}{r^3}\right) \qquad \ldots\ldots\ldots (46)$$

Now the viscous heating term is :

$$\eta r^2 \left[\frac{\partial}{\partial r}\left(\frac{V_\theta}{r}\right)\right]^2 = K\left(\frac{\partial V_\theta}{\partial r}\right)^{n-1}\left(\frac{aV_a}{b^2 - a^2}\right) 4\left(\frac{b}{r}\right)^4$$

$$= K\left(\frac{aV_a}{b^2 - a^2}\right)^{n+1} 4\left(\frac{b}{r}\right)^4 \left(\frac{r^2 + b^2}{r^2}\right)^{n+1} \qquad \ldots\ldots\ldots (47)$$

Therefore :

$$\frac{\partial T}{\partial t} = \alpha \frac{\partial}{\partial r}\left[\frac{1}{r}\frac{\partial}{\partial r}\left(r.\frac{\partial T}{\partial r}\right)\right] + \frac{K_o B e^{A/(T+273.2)}}{\rho C_p} 4\left(\frac{b}{r}\right)^4 \left(\frac{aV_a}{b^2-a^2}\right)^{n+1}\left(\frac{(r^2+b^2)}{r^2}\right)^{n-1} \quad (48)$$

Substituting $x = \ln (r/a)$ i.e. $r = ae^x$

$$\frac{\partial T}{\partial t} = \alpha.\frac{e^{-2x}}{a^2}\frac{\partial^2 T}{\partial x^2} + M\left[\frac{(a^2 e^{2x}+b^2)^{n-1}}{a^{2n+2}.e^{(2n+2)x}}\right] e^{A/(T+273.2)} \quad \ldots\ldots (49)$$

where $M = \frac{K_o}{\rho C_p}\left(\frac{aV_a}{b^2-a^2}\right)^{n+1}.4b^4$

Boundary conditions : $t = 0,\ T = T_o$ for all r, $a \leqslant r \leqslant b$

$V_\theta = 0$

$t > 0,\ V_\theta = V_a$ at $r = a$)
$V_\theta = 0$ at $r = b$) for all T, t

As in section 3.1. there are heat balances at the boundaries.

At $r = a$ $\quad F = -2\pi a\lambda\left(\frac{\partial T}{\partial r}\right)_a + C_a\left(\frac{\partial T}{\partial r}\right)_a \quad \ldots\ldots (50)$

At $r = b$ $\quad 0 = 2\pi b\lambda\left(\frac{\partial T}{\partial r}\right)_b - C_b\left(\frac{\partial T}{\partial t}\right)_b \quad \ldots\ldots (51)$

As before, an implicit finite difference technique was used because of its stability, irrespective of the chosen sizes for the time and space steps.

In this case the notation of Crank and Nicholson was used. Figure (24) shows the difference between the two approximations.

FIGURE 24

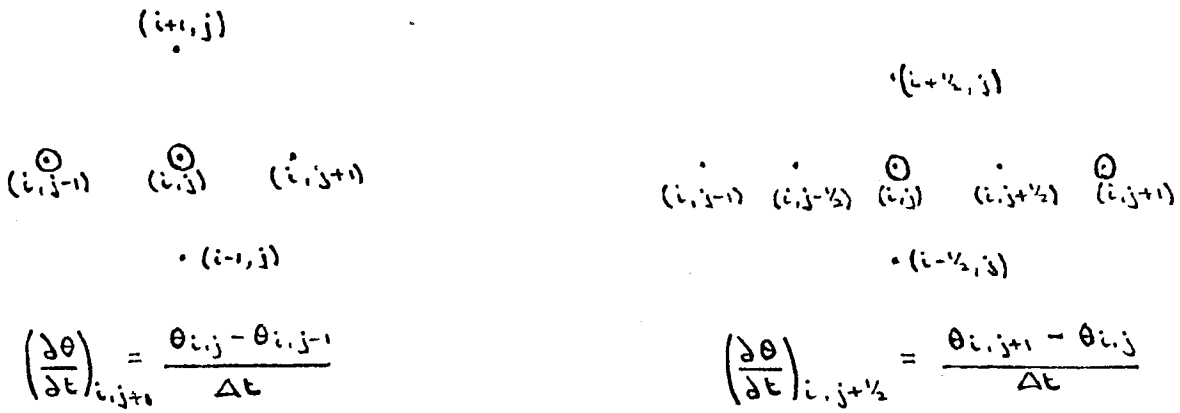

Finite difference used for the conduction calculations.

Crank-Nicholson approximation used for calculation of the viscous heating.

The ringed points are the ones used to predict the next point.

There was no outstanding reason for the change of notation except that it would indirectly provide an extra check on the conduction calculations. The check could be made by performing the same calculation using both methods and comparing the results.

Using the Crank-Nicholson definitions :

$$\left(\frac{\partial T}{\partial t}\right)_{i,j+\frac{1}{2}} = \frac{T_{i,j+1} - T_{i,j}}{\Delta t}$$

$$\left(\frac{\partial^2 T}{\partial x^2}\right)_{i,j+\frac{1}{2}} = \frac{1}{\Delta x^2}\left[\frac{(T_{i-1,j} + T_{i-1,j+1}) - (T_{i,j} + T_{i,j+1}) + (T_{i+1,j} + T_{i+1,j+1})}{2}\right]$$

The exponential term present in equation (49)

i.e. $e^{A/(T_{i,j+\frac{1}{2}}+273.2)}$

was assumed to become : $\frac{1}{2}\, e^{A/(T_{i,j+1}+273.2)} + \frac{1}{2}\, e^{A/(T_{i,j-1}+273.2)}$

Then equation (49) in finite difference form is :

$$\frac{T_{i,j+1}-T_{i,j}}{\Delta t} = \frac{\alpha\, e^{-2x_i}}{2a^2\Delta x^2}\left[(T_{i-1,j+1}-2T_{i,j+1}+T_{i+1,j+1})+(T_{i-1,j}-2T_{i,j}+T_{i+1,j})\right] + \frac{M\phi}{2}\left[e^{A/(T_{i,j+1}+273.2)} + e^{A/(T_{i,j-1}+273.2)}\right] \quad (52)$$

$$2T_{i,j+1}-2T_{i,j} = \frac{\alpha\Delta t}{a^2\Delta x^2}\, e^{-2x_i}\left[(T_{i-1,j+1}-2T_{i,j+1}+T_{i+1,j+1})+(T_{i-1,j}-2T_{i,j}+T_{i+1,j})\right] + M\phi\,\frac{\Delta x^2 a^2}{\alpha}\left(\frac{\alpha\Delta t}{a^2\Delta x^2}\right)\left[e^{A/(T_{i,j+1}+273.2)} + e^{A/(T_{i,j}+273.2)}\right] \quad (53)$$

Thus :

$$-T_{i-1,j+1}+(2\mu e^{2x_i}+2)T_{i,j+1} - \frac{M\phi\Delta x^2 a^2}{\lambda}\, e^{2x_i}\, e^{A/(T_{i,j+1}+273.2)} - T_{i+1,j+1}$$

$$= T_{i-1,j}+(2\mu e^{2x_i}-2)T_{i,j} + \frac{M\phi\Delta x^2 a^2}{\lambda}\, e^{2x_i}\, e^{A/(T_{i,j}+273.2)} \quad \ldots\ldots\ldots (54)$$

Now : $x_i = i\Delta x$

$n\Delta x = \ln\left(\frac{b}{a}\right)$

Boundary conditions :

$t = 0$, $T = 0$ for all 'r' from $b \geqslant r \geqslant a$

$t > 0$, and $r = a$. a constant heat flux is supplied to the sample via a known thermal capacity.

$r = b$ heat flux absorbed by the thermal capacity at 'b'.

At r = a there is the heat balance given by equation (50) which in finite difference form becomes :

$$F = \pi\lambda\left[\frac{T_{-1,j+1} + T_{-1,j} - T_{1,j+1} - T_{1,j}}{2\Delta x}\right] + Ca\left[\frac{T_{0,j+1} - T_{0,j}}{\Delta t}\right] \quad (55)$$

Since :
$$\frac{\partial T}{\partial r} = \frac{\partial T}{\partial x} \cdot \frac{\partial x}{\partial r}$$
$$= \frac{\partial T}{\partial x} \cdot \frac{\partial}{\partial r}\left[\ln\left(\frac{r}{a}\right)\right]$$
$$= \frac{\partial T}{\partial x}\left(\frac{1}{a} \cdot \frac{a}{r}\right) = \frac{e^{-x_i}}{a}\left(\frac{\partial T}{\partial x}\right)$$

Combining equation (54) with equation (55) with i = 0, and eliminating the indeterminate 'T_{-1}' terms.

$$2T_{1,j+1} - (p + 2(\mu+1))\,T_{0,j+1} + Ee^{A/(T_{0,j+1}+273.2)}$$
$$= 2T_{1,j} - (p + 2(\mu-1))T_{0,j} - \frac{2F\Delta x}{\pi\lambda} - M\phi\frac{a^2\Delta x^2}{\lambda}\,e^{A/(T_{0,j}+273.2)} \quad \ldots\ldots(56)$$

Where :

$$P = \frac{2Ca\,\Delta x}{\pi\lambda\Delta t} \qquad \left(q = P \cdot \frac{Cb}{Ca}\right)$$
$$\mu = \frac{a^2 \cdot \Delta x^2}{\alpha \cdot \Delta t}$$

Similarly the heat balance at r = b (i = n) equation (51) becomes :

$$2T_{n,j+1} - (q + 2(\mu e^{2n\Delta x} + 1))\,T_{n+1,j+1} + M\phi\frac{a^2\cdot\Delta x^2}{\lambda}\,e^{A/(T_{n,j+1}+273.2)} \cdot e^{2n\Delta x}$$
$$= -2T_{n,j} - (q + 2(\mu e^{2n\Delta x} - 1))T_{n+1,j} - M\phi\frac{a^2\cdot\Delta x^2}{\lambda}\,e^{A/(T_{n,j}+273.2)} \cdot e^{2n\Delta x} \quad \ldots\ldots(57)$$

The complete set of finite difference equations are :

$$i = 0: \quad 2T_{i,j+1} - (p+2(\mu+1))T_{o,j} + M\phi\frac{a^2.\Delta x^2}{\lambda} e^{A/(T_{o,j+1}+273.2)}$$

$$= -2T_{i,j} - (p+2(\mu-1))T_{o,j} - \frac{2F\Delta x}{\pi\lambda} - M\phi\frac{a^2.\Delta x^2}{\lambda} e^{A/(T_{o,j}+273.2)} \quad \ldots\ldots(58)$$

$$i = 1,2\ldots n-1:$$

$$T_{i-1,j+1} - (2\mu e^{2i\Delta x}+2)T_{i,j+1} + M\phi\frac{\Delta x^2.a^2}{\lambda}.e^{A/(T_{i,j+1}+273.2)}.e^{2i\Delta x} + T_{i+1,j+1}$$

$$= -T_{i-1,j} - (2\mu e^{2i\Delta x}-2)T_{i,j} - M\phi\frac{\Delta x^2.a^2}{\lambda} e^{A/(T_{i,j}+273.2)}.e^{2i\Delta x} \quad \ldots\ldots\ldots(59)$$

$$i = n:$$

$$2T_{n,j+1} - (q+2(\mu e^{2n\Delta x}+1))T_{n+1,j+1} + M\phi\frac{a^2.\Delta x^2}{\lambda} e^{A/(T_{n,j+1}+273.2)}.e^{2n\Delta x}$$

$$= -2T_{n,j} - (q+2(\mu e^{2n\Delta x}-1))T_{n+1,j} - M\phi\frac{a^2.\Delta x^2}{\lambda}.e^{A/(T_{n,j}+273.2)}.e^{2n\Delta x} \quad \ldots\ldots(60)$$

3.5. SOLUTION OF THE FINITE DIFFERENCE EQUATIONS

There are, as before, 'n' finite difference equations, previously these were solved by "Gaussian elimination". In this case, however, the solution cannot be found by immediate use of this technique, because the equations are non-linear with respect to the unknown temperatures. The non-linearity is due to the presence of the exponential term for the temperature dependence of viscosity.

If the equations could be reduced to a linear form then the elimination technique could be used.

The finite difference equations could be represented in general terms as :

$$\left.\begin{aligned}
f_0(T) &= + b_0 T_{0,j+1} + c_0 T_{1,j+1} - d_0 = 0 \\
f_1(T) &= a_1 T_{0,j+1} + b_1 T_{1,j+1} + c_1 T_{2,j+1} + K.E.e^{2\Delta x} e^{A/(T_{1,j+1}+273.2)} - d_1 = 0 \\
f_2(T) &= a_2 T_{1,j+1} + b_2 T_{2,j+1} + c_2 T_{3,j+1} + K.E e^{4n\Delta x} e^{A/(T_{2,j+1}+273.2)} - d_2 = 0 \\
&\vdots \\
f_{n-1}(T) &= a_{n-1} T_{n-1,j+1} + b_{n-1} T_{n,j+1} + c_{n-1} T_{n+1} + K.E e^{2(n-1)\Delta x} e^{A/(T_{n-1,j+1}+273.2)} - d_{n-1} = 0 \\
f_n(T) &= a_n T_{n-1,j+1} + b_n T_{n,j+1} + KE e^{2n\Delta x} e^{A/(T_{n,j+1}+273.2)} - d_n = 0
\end{aligned}\right\} \quad (61)$$

Where K = consistency index

$$E = \frac{M\phi a^2.\Delta x^2}{\lambda}$$

$d_0, d_1 \ldots d_n$ = left hand sides of equations (58), (59) and (60)

$$a_1 \ldots a_{n-1} = 1$$

$$a_n = 2$$

$$b_o = -(p+2(\mu+1)), \quad b_i = -(2(\mu e^{2i\Delta x}+1)), \quad b_n = -(q+2(\mu e^{2n\Delta x}+1))$$

$$c_o = 2, \quad c_i = 1$$

At:

$$\left.\begin{aligned}
i = 0 \quad & f_0(T) \longrightarrow \frac{\partial f_0}{\partial T_0} = b_0, \quad \frac{\partial f_0}{\partial T_1} = C_0 \\
i = 1 \quad & f_1(T) \longrightarrow \frac{\partial f_1}{\partial T_0} = a_1, \quad \frac{\partial f_1}{\partial T_1} = b_1 + K.E\, e^{2\Delta x}.e^{A/(T_{1,j+1}+273.2)}, \\
& \frac{\partial f_1}{\partial T_2} = C_1
\end{aligned}\right\} \quad (62)$$

$$
\left.
\begin{array}{lll}
i = i & f_i(T) \text{ —} & \dfrac{\partial f_i}{\partial T_{i-1}} = a_i \;, \quad \dfrac{\partial f_i}{\partial T_i} = b_i + KE.e^{2i\Delta x}.e^{A/(T_{i,j+1}+273.2)} \;, \quad \dfrac{\partial f_i}{\partial T_{i+1}} = c_i \\
i = n & f_n(T) \text{ —} & \dfrac{\partial f_n}{\partial T_{n-1}} = a_{n-1} \;, \quad \dfrac{\partial f_n}{\partial T_n} = b_n + KE\, e^{2n\Delta x}.e^{A/(T_{n,j+1}+273.2)}
\end{array}
\right\} \quad (62)
$$

Using a Newton-Raphson technique .

$$
\left.
\begin{aligned}
f_0' &= f_0^\circ + \frac{\partial f_0}{\partial T_0}(T_0'-T^\circ) + \frac{\partial f_0}{\partial T_1}(T_1'-T_1^\circ) \\
f_1' &= f_1^\circ + \frac{\partial f_1}{\partial T_0}(T_0'-T_0) + \frac{\partial f_1}{\partial T_1}(T_1'-T_1^\circ) + \frac{\partial f_1}{\partial T_2}(T_2'-T_2^\circ) \\
&\vdots \\
f_i' &= f_i^\circ + \frac{\partial f_i}{\partial T_{i-1}}(T_{i-1}'-T_{i-1}^\circ) + \frac{\partial f_i}{\partial T_i}(T_i'-T_i^\circ) + \frac{\partial f_i}{\partial T_{i+1}}(T_{i+1}'-T_{i+1}^\circ) \\
&\vdots \\
f_n' &= f_n^\circ + \frac{\partial f_n}{\partial T_{n-1}}(T_{n-1}'-T_{n-1}^\circ) + \frac{\partial f_n}{\partial T_n}(T_n'-T_n^\circ)
\end{aligned}
\right\} \quad (63)
$$

Now let $f_0' \ldots\ldots f_i' \ldots\ldots f_n' = 0$ = differentials of right hand side of above equations.

Then :

$$
\left.
\begin{aligned}
\frac{\partial f_0}{\partial T_0}\Delta T_0 + \frac{\partial f_0}{\partial T_1}\Delta T_1 &= -f_0^\circ \\
\frac{\partial f_1}{\partial T_0}\Delta T_0 + \frac{\partial f_1}{\partial T_1}\Delta T_1 + \frac{\partial f_1}{\partial T_2}\Delta T_2 &= -f_1^\circ \\
\frac{\partial f_i}{\partial T_{i-1}}\Delta T_{i-1} + \frac{\partial f_i}{\partial T_i}\Delta T_i + \frac{\partial f_i}{\partial T_{i+1}}\Delta T_{i+1} &= -f_i^\circ \\
\frac{\partial f_n}{\partial T_{n-1}}\Delta T_{n-1} + \frac{\partial f_n}{\partial T_n}\Delta T_n &= -f_n^\circ
\end{aligned}
\right\} \quad (64)
$$

The above equations can be written in general terms as :

$$
\left.
\begin{aligned}
+ b_0 \Delta T_0 + c_0 \Delta T_1 &= -f_0^\circ \\
a_1 \Delta T_0 + b_1 \Delta T_1 + c_1 \Delta T_2 &= -f_1^\circ \\
a_i \Delta T_{i-1} + b_i \Delta T_i + c_i \Delta T_{i+1} &= -f_i^\circ \\
a_n \Delta T_{n-1} + b_n \Delta T_n &= -f_n^\circ
\end{aligned}
\right\} \qquad (65)
$$

The above equations are now linear in terms of the temperature differences (ΔT) and Gaussian elimination can be used.

The flow diagram and computer programme used for the solution of these equations are given in Appendix 3.

The programme in Appendix 3 calculates the temperature profile and these were compared manually with the experimental temperatures.

4.0. EXPERIMENTAL WORK AND RESULTS

In this section the apparatus used in the project is described. Two pieces of equipment were built. The "static" apparatus was used to check the stability of the computer programme and to determine the dimensions and design which was required to obtain reliable results.

Additional experiments which were necessary are also described, together with some later modifications to the dynamic apparatus.

4.1. STATIC APPARATUS

4.1.1. Description of the Static Apparatus

With reference to Figure (25) the apparatus can be seen to consist of two 7" (177.8 mm)long aluminium cylinders (A and B). The inner cylinder 'A' was 3/8" (9.525 mm) outside diameter and the outer cylinder 'B' was 5/8" (15.875 mm) outside diameter both having a wall thickness of 1/16" (1.5875 mm). Thermocouples were fitted to the two cylinders, the inner one being cemented with epoxide resin into a small hole of 1/32" (0.794 mm) diameter in the wall of the inner cylinder. The outer thermocouple was attached in the same manner in a shallow groove on the surface of the cylinder 'B'.

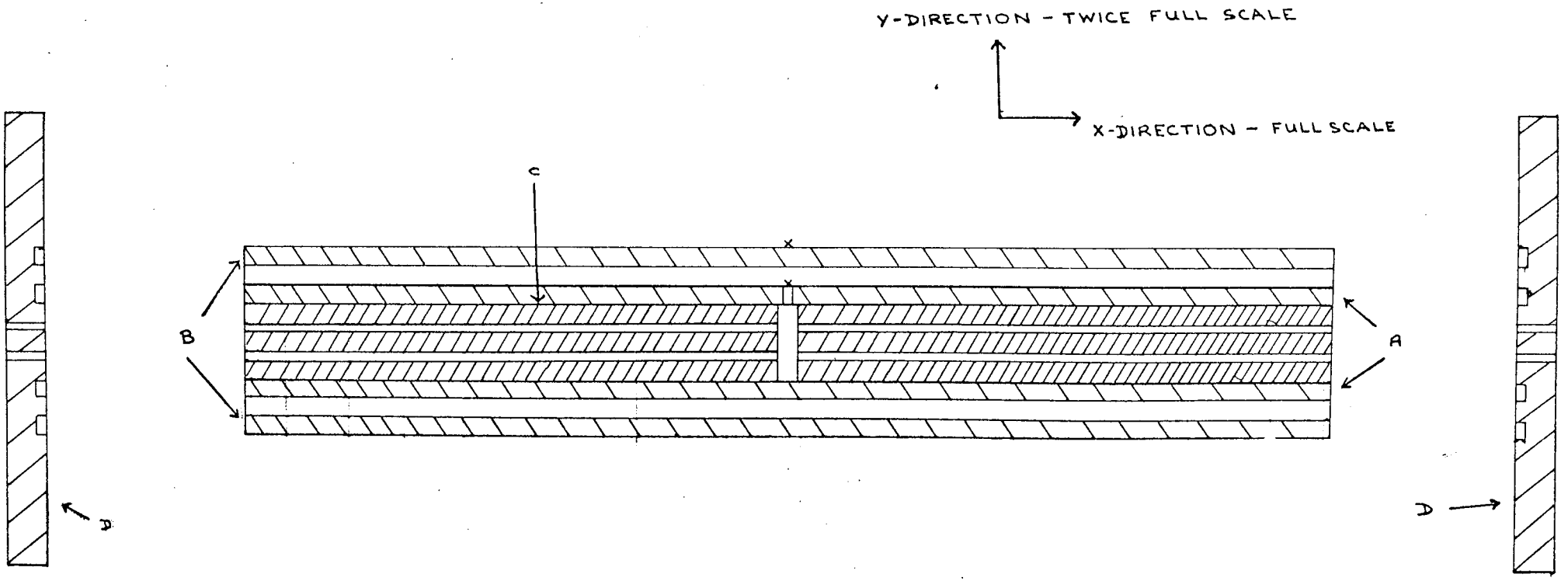
Y-DIRECTION - TWICE FULL SCALE
X-DIRECTION - FULL SCALE
C
X
X
B
A
A
D

FIG. 25.

The cylinders were maintained concentric by the PTFE end caps 'D' (machined with annular grooves) into which the cylinders fitted. The end caps were bored to allow the thermocouple and heater wires to pass through so that they could be connected to the appropriate external instruments.

The inner cylinder was heated by a single strand of nichrome wire which would produce a maximum power of 60 watts (maximum voltage = 12 volts, maximum current = 5 amps.)

The heating wire was contained in one bore of the twin bore ceramic tube 'C', this held the wire steady and also insulated it from the inner cylinder. The second bore of the tube'C' was used to carry the thermocouple wires which were cemented in the wall of cylinder 'A'.

The outer cylinder was insulated by surrounding it with loosely packed glass wool in a specially constructed 4" square (101 .6 mm) container (not shown in Figure (25)).

This apparatus was used to check the stability of the computer programme. Various parameters required by the programme were changed, for example, the initial guesses for thermal conductivity and thermal diffusivity were changed drastically to examine the affect on the final computed values for those properties. This type of variation would check that the minimum point reached by the programme was a true minimum and not merely a saddle point.

The samples were extruded tube made from I.C.I. X.D.G. 33 low density polyethylene. The tube was nominally 0.375" (9.525 mm) diameter bore and 0.0625" (1.5875 mm) wall thickness. The tolerance was ± 0.005" (0.127 mm).

4.1.2. Experimental Procedure with the Static Apparatus

(1) The polyethylene samples were cut (using a sharp knife) to the correct length to fit the apparatus. (7.0" or 177.8mm).

(2) The samples were coated with silicone oil to help reduce the thermal contact resistance between the samples and the aluminium cylinders.

(3) The samples were inserted into the apparatus by sliding into the outer cylinder and the arrangement completed by pushing the inner cylinder through the bore of the sample

(4) The PTFE end caps were secured on the ends of the cylinders and the heater and thermocouple wires connected to the power source and potentiometer respectively. The power to the heater was measured with an ammeter and a voltmeter, and controlled by a variac type transformer. The output from the thermocouples was monitored with a two channel potentiometric recorder.

(5) Once sufficient data had been collected, (this was determined by trial and error and it was found that experimental times of about a minute were quite adequate) the apparatus was dismantled and cleaned ready for the next set of measurements. Removal of the sample was best done by heating it to a temperature in excess of its melt temperature and sliding the two cylinders apart. It was virtually impossible to remove the samples when the apparatus was cold if the specimen had been melted during the experimental run.

4.2. ROTATING APPARATUS

4.2.1. Description of the Rotating Apparatus

From Figure (26) and Plate (1) it can be seen that the apparatus consisted of three copper cylinders. Cylinders 'A' and 'B' were 11.5" (292.1mm) in length and 'A' was made an interference fit inside 'B' ('B' had an outside diameter of 0.375" (9.525 mm)). Cylinder 'C' was 8" (203.2 mm) long and had an outside diameter of 0.625" (15.875 mm). The inner bore was reamed until samples would just slide in.

The outer cylinder (C) was held stationary by a retaining peg which passed through one half of the "Sindanyo" casing effectively attaching it to the outer cylinder. ("Sindanyo" is a commercial name for a compressed asbestos.)

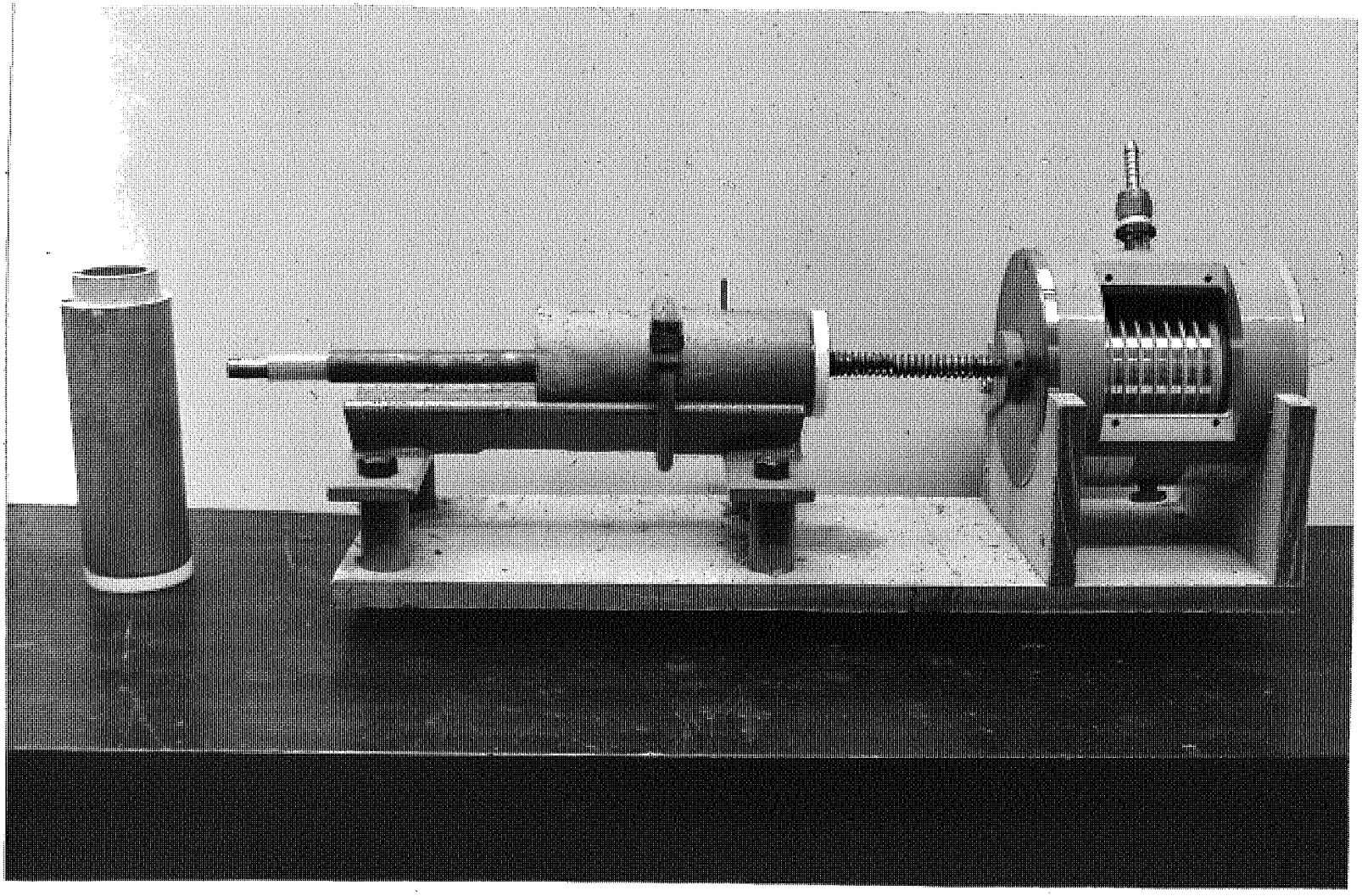

ROTATING APPARATUS

PLATE 1

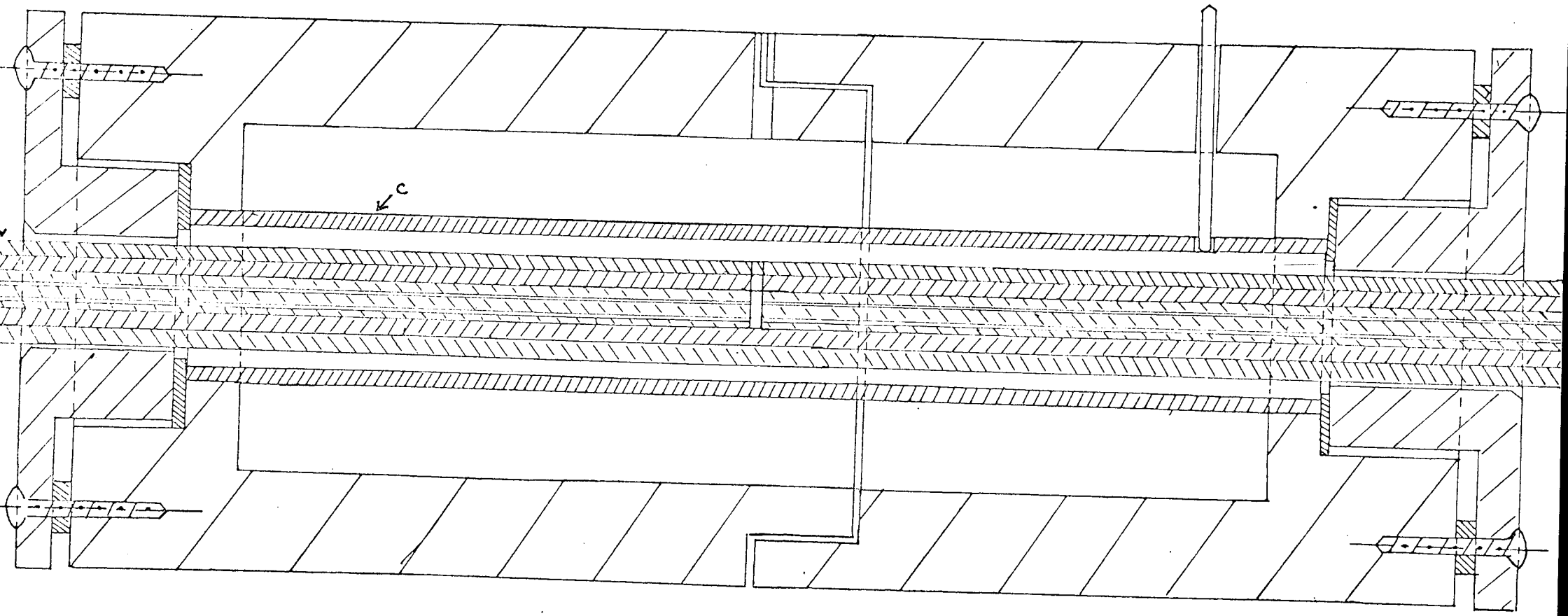

SECTION THROUGH ROTATING APPARATUS

TWICE FULL SCALE

y

x FULL SCALE

FIG. 26

The cylinders were maintained concentric by supporting them in the "Sindanyo" casing which had been fitted with PTFE (polytetrafluoroethylene) bearings at each end. Concentricity was ensured because both bearings and "Sindanyo" were bored simultaneously on a lathe.

The samples were polyethylene as before.

The outer cylinder was heated by a coil of nichrome wire at low voltage (30 volts). The coil was wound round the cylinder and insulated from it by a thin layer of asbestos. The inner cylinder was heated by a single strand of nichrome wire with a total maximum power of 240 watts (60 volts; 4 amps.).

The inner cylinder was driven by a 1/3 H.P. (246 watt) motor with an infinitely variable speed gear box which gave speeds of between 25 - 280 r.p.m. The motor drive was connected to the apparatus by a grub screw and collar.

The thermocouples and heater wires from the rotatable inner cylinder were taken out through a flexible coupling into the slip rings. Figure (27) show the construction of the slip rings. The rotating leads were connected to the rotating terminals which were a continuation of the silver rings inside the unit. The circuit was completed by silver - graphite brushes in contact with the silver rings which were connected to the stationary terminals on the enclosing case of the slip ring unit. The slip rings were cooled with compressed air since it was recommended

FIG. 27.

DIAGRAM OF SLIP RINGS USED FOR MEASUREMENTS ON ROTATING APPARATUS

by the manufacturers that they should not operate above 90°C,

Two types of thermocouples were used with this apparatus, the first consisted of constantan wires soldered to the copper cylinders. The copper cylinder replacing the normally used copper wire. This type of thermocouple was quite satisfactory but in this application the major disadvantage was the insulation of the wires. Woven glass insulation was the most successful but this often failed because of mechanical abrasion. The second type of thermocouple was commercially available, being produced by Pyrotenax Limited.

In this case the thermocouples were chromel-alumel and were conventional thermocouples contained in a stainless steel sheath. The thermocouple wires were insulated from the sheath with magnesia powder. The overall diameter of the thermocouple was 0.021" (0.533 mm). These were satisfactory and were certainly more convenient to use, needing no calibration and being sheathed generally provide a more stable signal than "home-made" thermocouples.

The only disadvantage of using these thermocouples was the tendency of the stainless steel sheath to be brittle, which led to cracking making the thermocouple useless (they could be repaired, if sent to the manufacturers).

The rotating apparatus was used in the static state to determine the thermal conductivity (λ) and thermal diffusivity (α) of the polyethylene samples with the procedure adopted for the static apparatus (see section 4.1.2.). Values

of 'λ' and 'α' were measured at various temperatures in the melt state.

The thermal property values obtained, were used in the second set of experiments, when the inner cylinder was rotated. In these experiments, the heat input to the polymer was from two sources, the heating element and viscous heating due to deformation of the polymer melt. The object was to determine the magnitude of the viscous heating at various temperatures and shear rates.

4.2.2. Experimental Procedure with Rotating Apparatus

(1) The polyethylene samples were cut (with a sharp knife) to the correct length (8" or approximately 203 mm).

(2) The sample was inserted into the apparatus.

(3) The apparatus was completed by surrounding the cylinders with the supporting "Sindanyo" casing.

(4) The thermocouples, heater and motor drive were connected.

(5) The apparatus was heated to the required temperature and the inner and outer cylinder temperature equilibrated by adjustment of the power input and by observation of the temperatures as recorded by the thermocouples.

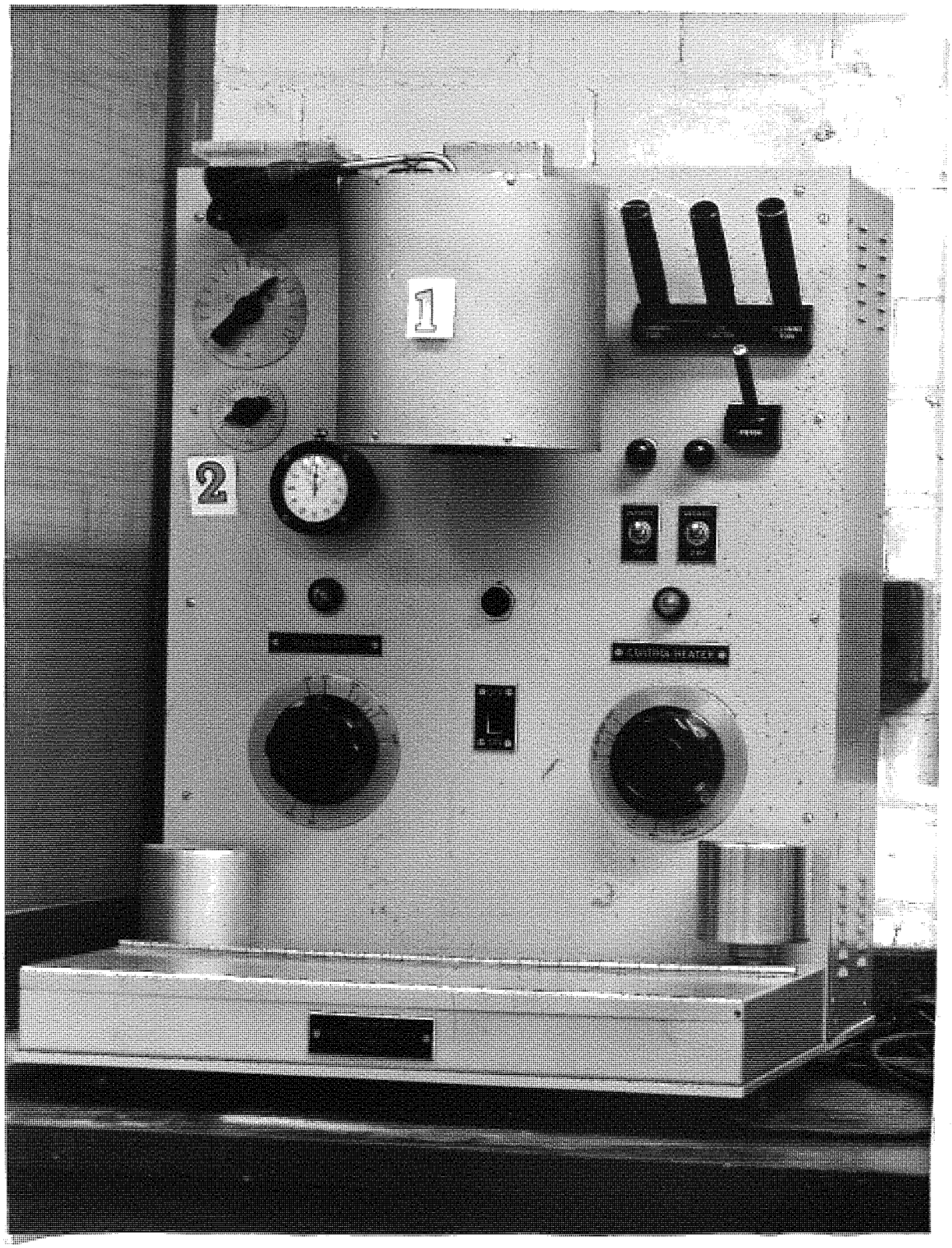

WEIGHT LOADED DAVENPORT RHEOMETER

PLATE 2

4.3. THE SUITABILITY OF COPPER CYLINDERS

As previously mentioned, transition metals such as copper often react with, or catalyse, degradation reactions in polymeric materials. The general type of reaction is :

$$ROOH + Cu^{2+} \longrightarrow RO^{\circ} + {}^{\circ}OH + Cu^{+}$$

which is in practice an acceleration of the breakdown of the hydroperoxide group (-OOH) formed by oxidative attack on the polymer at high temperatures. Many polymers are prone to this type of reaction but the presence of copper ions greatly accelerates an otherwise relatively slow reaction. The initial attack which produces the hydroperoxide groups may, of course, be considerably reduced by addition of anti-oxidants.

To determine if copper could be used in the apparatus samples were held between two cylinders at a temperature of 180°C for one hour. The extent of degradation was estimated by measuring the melt flow index (MFI) before and after the thermal treatment. The apparatus used for this is shown in Plate 2.

The MFI of a material is the number of grams which flow from the cylinder "1" (Plate 2) under a set of standard conditions (in this case 190°C with a load of 2.16 Kg). Also shown in Plate 2 are the heater controls for the thermostatically controlled cylinder (1).

MELT FLOW INDEX - LOW MOLECULAR POLYETHYLENE (ICI-XDG 33)

AT 190°C

INITIAL RESULTS

WEIGHT EXTRUDED (IN 2 MINUTES)

	0.0061 g
	0.0063 g
	0.0059 g
MEAN	0.0061 g

MFI (WEIGHT EXTRUDED IN 10 MINUTES) = 0.031

AFTER 60 MINUTES AT 180°C

WEIGHT EXTRUDED IN 2 MINUTES

	0.0056 g
	0.0054 g
	0.0055 g
MEAN	0.0055 g

MFI = 0.028

N.B. A reduction in MFI indicates an increase in molecular weight (i.e. some crosslinking has probably occurred).

TABLE 2

The results obtained are summarised in Table 2.

No visible change in the polymer could be observed. A small change had, however, taken place since the MFI results had decreased. This indicated that the molecular weight of the sample had increased after undergoing the treatment. This is quite possible since it is known that polyethylene cross-links slightly under such conditions, whereas most other polymers suffer chain scission and therefore a reduction in molecular weight.

4.4. MEASUREMENT OF THERMAL CAPACITY OF THE CYLINDERS

4.4.1. Description of the Apparatus

The apparatus is shown in Figure (28). It consists of a copper calorimeter insulated from the surroundings by polystyrene foam. The equipment also includes an accurate thermometer (capable of measuring to one tenth of a degree centigrade) and a stirrer to ensure a uniform temperature in the water.

4.4.2. Experimental Procedure

A standard calorimetric technique (the method of mixtures) was used to determine the specific heat of the inner and outer cylinders of the apparatus.

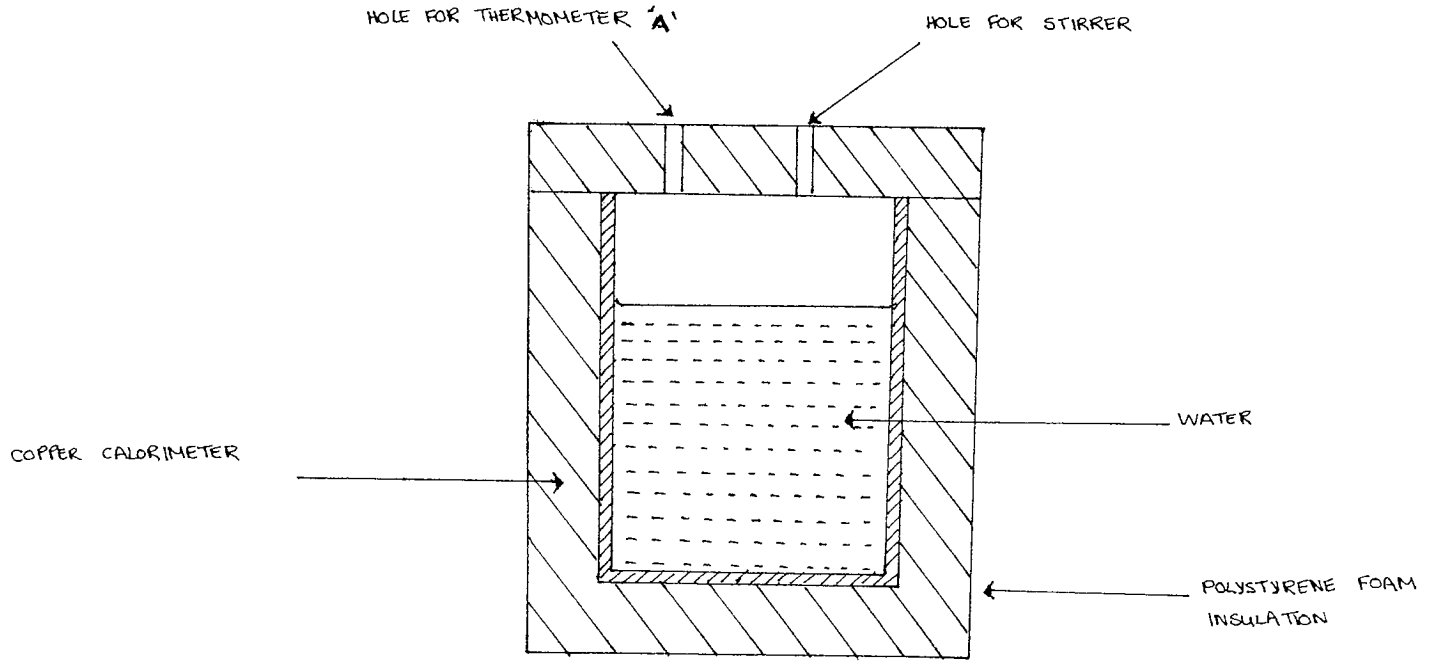
HOLE FOR THERMOMETER 'A'
HOLE FOR STIRRER
WATER
COPPER CALORIMETER
POLYSTYRENE FOAM INSULATION

FIG. 28.

The thermal capacity could then be calculated by multiplying the measured specific heat by the mass of the cylinders.

The experimental procedure was :

(1) The cylinders, in turn, were placed into boiling distilled water and left for sufficient time to attain the temperature of the boiling water (ten minutes immersion time was generally used). The temperature at which pure water boils depends on the barometric pressure, this was recorded for every determination and the necessary correction made using the gas laws.

i.e. $P_1/T_1 = P_2/T_2$

where : P = pressure

T = absolute temperature (K)

(2) After reaching the water temperature the cylinder was transferred to the calorimeter (known specific heat and mass) which contained a known weight of water, at room temperature. Introducing the hot cylinder to the calormeter will cause the temperature of the water to rise and this was detected with the thermometer 'A'. The procedure was repeated several times and the average of the results taken.

The time of transfer of the cylinder to the water was important and

TABLE 3 - ALUMINIUM CYLINDERS (STATIC APPARATUS)

	Specific Heat J/c.g *	Thermal Capacity J/c	Thermal Capacity/Metre J/ m
Inner Cylinder	0.964	29.1	164.3
Outer Cylinder	0.964	35.1	197.5

* Specific heat taken from Kaye and Laby, Longmans Press : Al = 0·88 J/c g
Cu = 0·38 J/c g

TABLE 4 - COPPER CYLINDERS (ROTATING APPARATUS)

	Specific Heat J/c.g *	Thermal Capacity J/c	Thermal Capacity/Metre J/ m
Inner Cylinder	0.421	48.6	189.9
Outer Cylinder	0.421	55.5	240.2

TABLE 5 - THE EFFECT OF TRANSFER TIME (ALUMINIUM SAMPLE)

Time (sec.)	Specific Heat cal/c.g	Specific Heat J/c.g	Thermal Capacity J/c
1	0.232	0.964	20.4
2	0.232	0.964	20.4
3	0.173	0.723	15.3
4	0.172	0.722	15.2
5	0.172	0.722	15.2

could cause erroneous results if it was too long. Experiments were performed to determine the effect of transfer time on the calculated value of specific heat. This was done by using an object of known specific heat, in this case a piece of aluminium. The transfer was purposely delayed in the time scale 1 - 5 seconds, 1 - 2 seconds was the time taken for transfer under normal experimental conditions. Results are shown in Table (5). Also using this standard metal block the accuracy of the method was determined and an inherent error of approximately 10% was found in the method.

4.5. MEASUREMENT OF TORQUE

In order to estimate the mechanical energy input from the motor to the polymer it was necessary to measure the torque transmitted to the apparatus.

The torque necessary to initiate rotation of the apparatus was measured with a torque wrench. The result from this measurement would be the maximum value which could be obtained, since it gives the torsional force necessary to initiate rotation.

APPARATUS CONSTRUCTED FOR TORQUE MEASUREMENT ON ROTATING CYLINDER

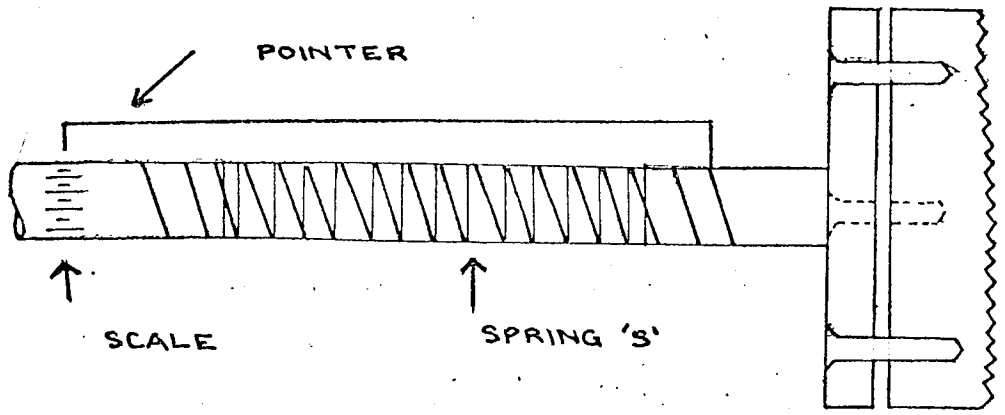

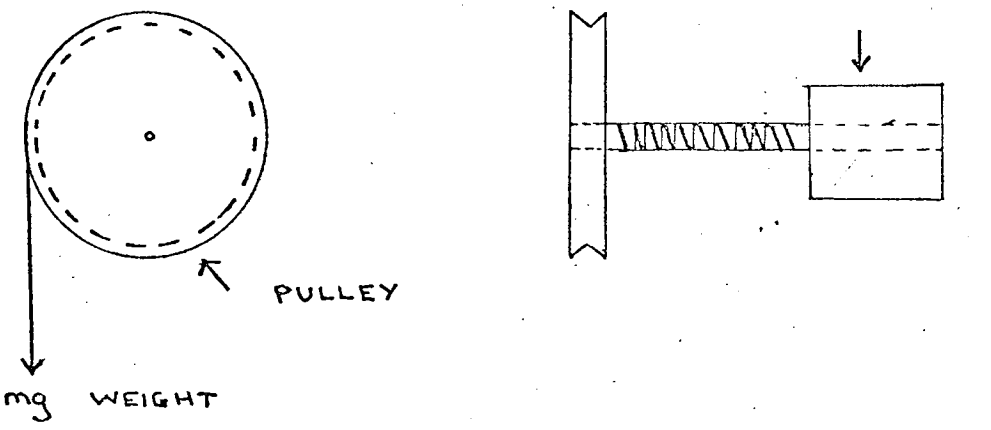

FIG. 29.

To measure the torque at various rotational speeds the apparatus was modified to incorporate a torque measuring device and this is illustrated in Figure (29).

The spring 'S' was calibrated using a pully wheel of known diameter and weights (Figure (29)).

Torque = weight x radius of pully.

The torque was calculated as above and the deflection of the spring marked on a scale attached to the fixed end of the spring.

Experiments at 80 r.p.m., on the apparatus, gave torque readings of 8 in.lbf. (0.91 Nm). However, measurements at higher speeds were not possible with this arrangement, since slippage occurred between the spring and cylinder. Attempts to prevent this by hard soldering failed since this process annealed the spring and it was no longer able to withstand the applied torque.

The torque required to rotate the slip rings was 0.29 Nm. Therefore the overall torque required to rotate the apparatus is 0.62 Nm at 80 r.p.m.

TABLE (7) 80 R.P.M. INITIAL TEMPERATURE 138.0

Shear Rate (s^{-1})	Viscosity (Ns/m^2) x 10^3	Shear Stress (N/m^2) x 10^4	Torque (Nm)	Theoretical Power Input (Watts)
28.4 *	3.7 *	10.5 *	1.78 *	7.45 *
26.2	3.85	10.1	1.72	7.19
23.8	4.10	9.76	1.66	6.94
22.4	4.29	9.6	1.63	6.81
20.8	4.65	9.68	1.65	6.89
19.8 **	4.92 **	9.74 **	1.65 **	6.89 **

* INNER CYLINDER ** OUTER CYLINDER

Measured Torque = 0.62 (at 80 r.p.m.)

$$= 0.62 \frac{80}{60} \pi \text{ Watts}$$

$$= 2.60 \text{ Watts}$$

i.e. approximately 30% of theory. (From Table (7))

The power input from the motor produces temperature rises of :-

inner cylinder = $1.6^{\circ}C$

outer cylinder = $0.8^{\circ}C$

(From Table (12)).

Thermal input from heater = 49.9 W/m

= 49.9 . 0.203 Watts

= 10.15 Watts

Heater input produces temperature rises of :

inner cylinder = 4.6°C

outer cylinder = 0.7°C

mean temperature rise = 2.65°C

Energy inputs per °C rise are :-

thermal conduction = 10.15 Watts/2.65°C

= 3.83 W/°C

viscous heating at = 2.60/1.2°C

80 r.p.m. = 2.17 W/°C

The process of viscous heating in this case is therefore a more efficient form of heating. Less energy per unit temperature rise is required by viscous heating, which is not surprising, since the heat source is within the material and does not have to be transmitted from an outside source.

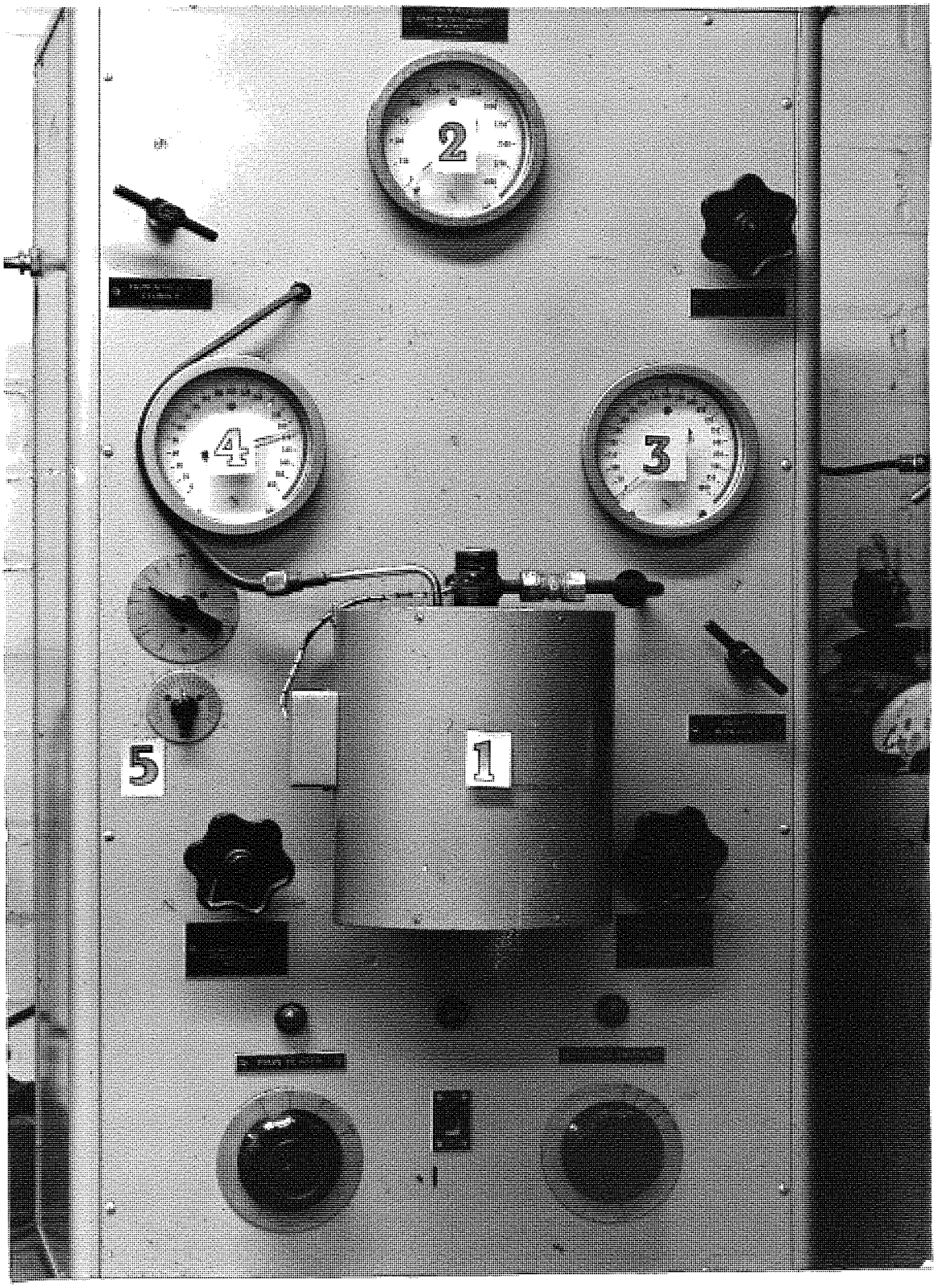

GAS LOADED DAVENPORT RHEOMETER

PLATE 3

4.6. DETERMINATION OF THE FLOW BEHAVIOUR FOR THE POLYMER SAMPLES

It was necessary to calculate viscous heating to determine certain rheological properties of the polymer used. The power law was used to describe the rheological behaviour.

The power law states :

$$\tau = K(\dot{\gamma})^n = \underbrace{K(\dot{\gamma})^{n-1}}_{\eta_a} . \dot{\gamma}$$

where

τ = shear stress

K = consistency index

n = flow behaviour index

$\dot{\gamma}$ = shear rate

η_a = apparent viscosity

This section describes the measurement of 'K' and 'n' over the temperature range 150°C to 230°C.

Flow curves ($\log \tau$ versus $\log \dot{\gamma}$) were also determined so that the relationship between apparent viscosity and shear rate could be deduced.

SECTION THROUGH DAVENPORT RHEOMETER BARREL

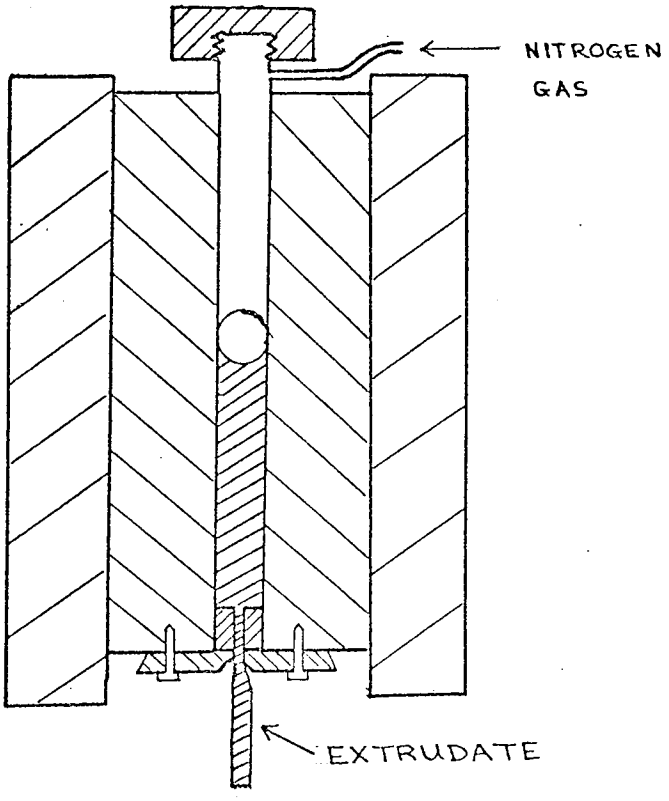

FIG.30.

4.6.1. Apparatus

For these determinations a capillary rheometer was employed and in this case the instrument was a commercially available model produced by Davenport Limited. Plate (3) shows the apparatus used and Figure (30) shows a cross section of the barrel, reservoir and die.

4.6.2. Experimental Procedure

The procedure adopted with the apparatus was :

(1) The barrel (No. 1 in Plate 3) was heated to the required temperature (in this case 190°C) and allowed to stabilise. This procedure usually required about one hour.

(2) The barrel was loaded with the sample granules using the special loading tool supplied with the apparatus. The polymer granules were produced by cutting the extruded tube into small pieces.

(3) The heater control(No. 5 in Plate 3) was turned to boost while the granules were being loaded and returned to normal after loading was completed. When all the polymer had been charged to the barrel the special steel sphere was placed on top of the polymer and the gas tight seal screwed to the top of the barrel.

(4) Pressure was applied to the barrel chamber by means of nitrogen gas, this caused the polymer to be extruded out of the die at a rate which was proportional to the applied pressure. The pressure used was noted. (Pressure gauges 2, 3, 4, Plate 3).

(5) The extrudate was cut from the die face at appropriate time intervals (usually about 30 seconds) using a small spatula.

(6) The extrudate was collected and weighed. The average of five weighings was recommended and they should not differ from each other by more than 10%.

(7) The residual polymer was pushed out of the barrel using the cleaning tool provided and the barrel cleaned with xylene.

The shear stress at the capillary wall was given by :

$$\tau = \Delta p.r/2.l$$

The apparent shear rate at the wall was given by :

$$\dot{\gamma} = 32.Q/\pi D^3 \quad \text{or} \quad 4.Q/\pi r^3$$

Where : Q = Volumetric output rate $cm^3/sec.$ or $m^3/sec.$

r = Radius of the capillary cm. or m.

p = Applied pressure N/m^2

4.6.3. Flow Curve Superposition

Using the capillary rheometer alone, would have been very time consuming, because flow curves at every experimental temperature would have had to be determined. However, the technique described by Mendleson (36) greatly reduces the experimental work, in fact the flow curve need only be determined at one temperature.

Flow curves at various temperatures could be shifted along the shear rate axis to superimpose on a single master curve which corresponds to the flow curve for the arbitarily chosen temperature. The amount by which each curve had to be shifted was known as the shift factor. It was also shown that the shift factor (a_T) did not depend on the molecular weight or molecular weight distribution.

Mendelson showed that :

$$a_T = \gamma_{ref}/\gamma_T \qquad \ldots\ldots\ldots (1)$$

where : a_T = shift factor

γ_{ref} = shear rate at the reference temperature chosen (In this case 200°C)

γ_T = shear rate at any other temperature.

TABLE 6 RESULTS FROM DAVENPORT RHEOMETER

Temperature °C	Applied Pressure p.s.i.	Output g/s	Shear Stress $N/m^2 \times 10^4$	Shear Rate $sec.^{-1}$
150	380	0.0024	6.25	3.90
	500	0.0043	7.23	7.11
	605	0.0061	9.96	10.00
	740	0.0107	12.18	17.50
160	365	0.0026	6.10	4.26
	500	0.0054	8.23	8.86
	600	0.0081	9.88	13.28
	720	0.0127	11.85	20.83
170	340	0.0032	5.60	5.25
	480	0.0069	7.90	11.32
	590	0.1144	9.71	17.06
	700	0.0161	11.52	26.40
180	360	0.0045	5.93	7.38
	480	0.0087	7.90	14.27
	580	0.0134	9.55	21.98
	710	0.0200	11.69	32.80
190	310	0.0048	5.10	7.87
	420	0.0087	6.91	14.27
	560	0.0162	9.22	26.57
	745	0.0289	12.26	47.40
200	50	0.0004	0.82	0.69
	100	0.0006	1.64	1.04
	150	0.0013	2.47	2.14
	195	0.0022	3.21	3.62
	320	0.0060	5.27	9.88
	430	0.0011	7.08	18.27
	590	0.0219	9.71	36.05
	750	0.0364	12.30	59.91
	840	0.0436	13.78	71.50
	850	0.0440	13.99	72.16
210	330	0.0084	5.43	13.78
	470	0.0169	7.74	27.72
	585	0.0274	9.63	44.94
	730	0.0434	12.02	71.18
220	310	0.0095	5.10	15.58
	435	0.0190	7.16	31.16
	575	0.0347	9.46	56.91
	720	0.0548	11.85	89.87
230	250	0.0084	4.12	13.78
	430	0.0249	7.08	40.84
	580	0.0460	9.55	75.44
	720	0.0724	11.85	118.74

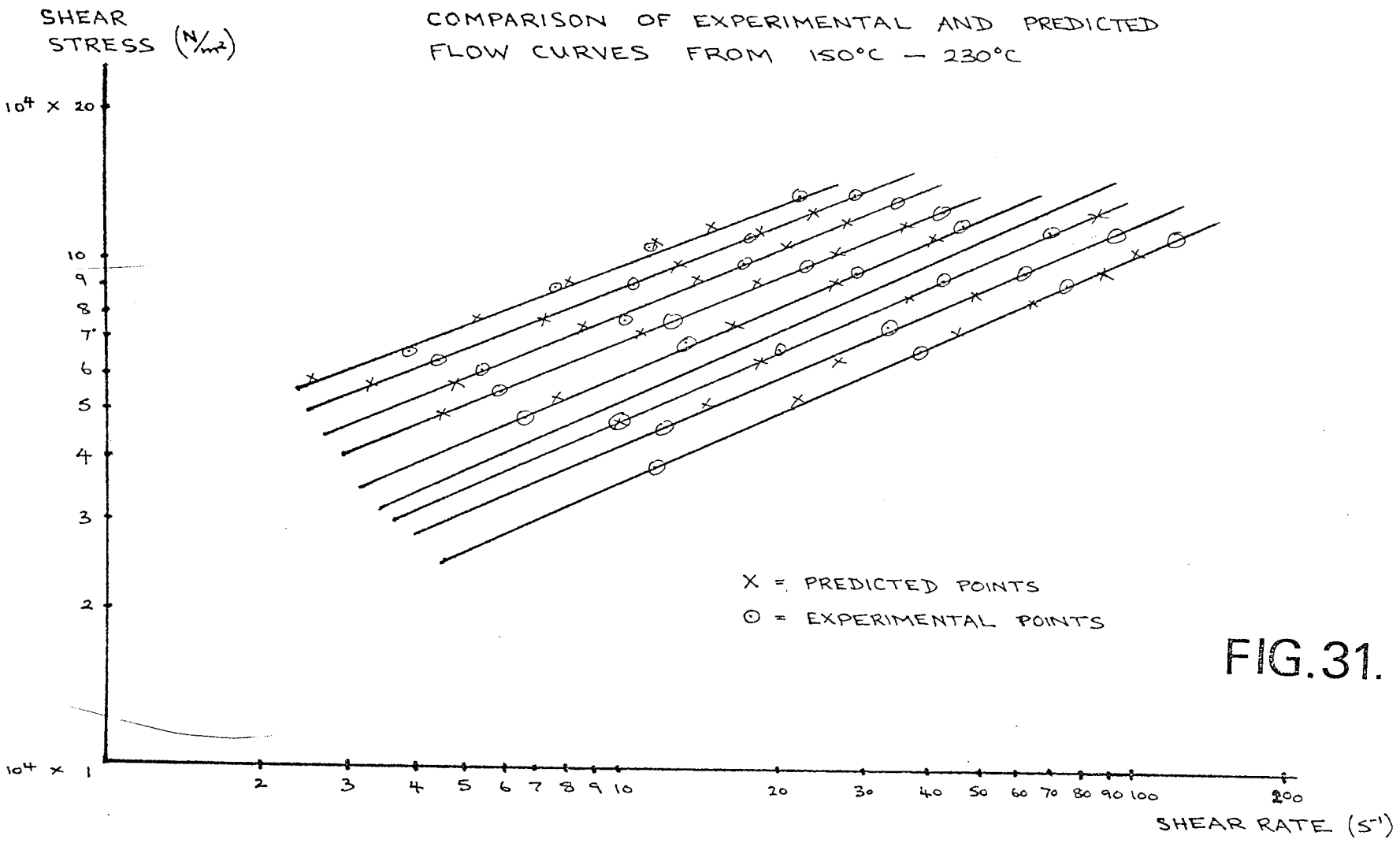
SHEAR STRESS (N/mm²)
COMPARISON OF EXPERIMENTAL AND PREDICTED FLOW CURVES FROM 150°C — 230°C
10⁴ x 20
10
9
8
7
6
5
4
3
2
10⁴ x 1
2 3 4 5 6 7 8 9 10 20 30 40 50 60 70 80 90 100 200
SHEAR RATE (S⁻¹)
X = PREDICTED POINTS
⊙ = EXPERIMENTAL POINTS

FIG.31.

FLOW CURVE AT 200°C FOR
LOW DENSITY POLYETHYLENE
(ICI - YDG 33)

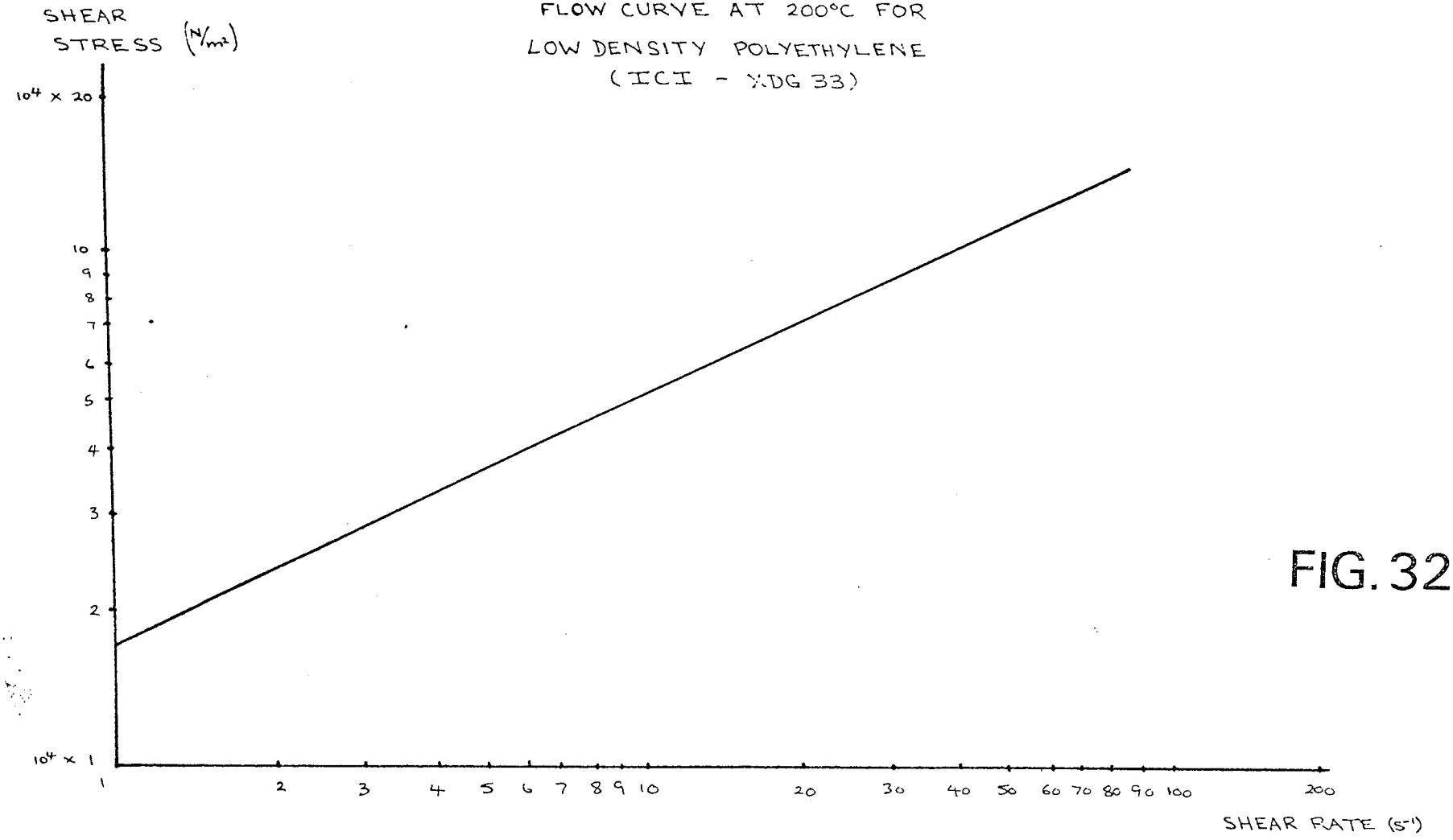

FIG. 32.

The shift factor was shown to be temperature dependent :

$$a_T = B \exp (Ea/RT) \qquad (2)$$

where : B = constant

E_a = activation energy for viscous flow

R = gas constant

T = ^{o}K

The validity of the method was tested by producing flow curves at $10^{o}C$ intervals in the range 150^{o} - $230^{o}C$. Figure (31) shows the experimental curves and the predicted points calculated using the method.

A more complete flow curve at $200^{o}C$ is shown in Figure (32).

4.7. THE USE OF A KEYED OUTER CYLINDER

Observations of the sample in the apparatus, when the inner cylinder was rotating, suggested that slippage could be occurring at the outer cylinder - polymer interface. (The end of the sample could be seen if one side of the "sindanyo" casing was removed.)

To determine if slippage was occurring a new outer cylinder was made, which was keyed as shown in Figure (33). The grooves were approximately 0.005" (0.127 mm) in depth. The object was to operate the apparatus as before,

ILLUSTRATION OF KEYED OUTER CYLINDER

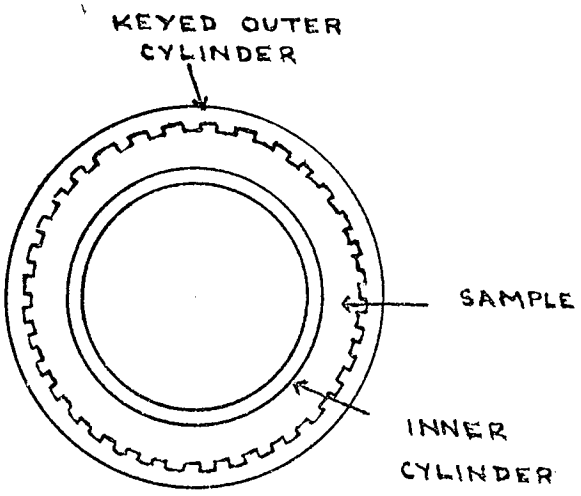

FIG. 33.

but with the increased resistance which the keying provided the observed temperatures should be greater than with the original cylinder. Table (8) shows typical results obtained.

Table (8) shows the temperature differences observed when comparing the smooth and keyed cylinders. (i.e. the increased temperature differences compared to the smooth cylinder.)

The temperature increases are not very large, but significant percentages of the original temperature rises (i.e. with the smooth cylinder). However, the theory indicates that the temperature rises for the polymer at the above speeds and temperatures should be :

17°C for the inner cylinder 13°C for the outer cylinder	at 80 r.p.m. after 30 seconds Initial temperature 156.0°C
25°C for the inner cylinder 20°C for the outer cylinder	at 116 r.p.m. after 30 seconds Initial temperature 155.0°C

From Figures (36) and (37) respectively.

4.8. THE USE OF A TRACER TECHNIQUE

This technique used coloured polyethylene markers which were inserted into the walls of the specimens, and passed completely through the total

TABLE (8)

KEYED CYLINDER: DIFFERENCES IN TEMPERATURE RISES AT SPECIFIED TIMES (°C)

Initial Temperature = 155.0 - 156.0°C

Time(s)	30		60	
Speeds (r.p.m)	80	116	80	116
Inner Cylinder	1.7	2.5	2.5	6.0
Outer Cylinder	1.5	0.5	2.0	2.5

thickness. Several markers were placed at intervals along its length. These samples were subjected to one revolution of the inner cylinder. If the tracers had spread to form a continuous band of colour round the circumference of the sample, it would indicate the polymer had undergone continuous torsional deformation as intended. An intermittent or partial band would have indicated that slippage or non-continuous deformation had occurred.

However, it was impossible to remove samples from the apparatus once the sample had melted without damaging the cylinders. The only way to remove it was to melt the polymer, and slide the cylinders apart. The result, however, was to destroy the sample.

This experiment, therefore, failed in its initial intention but it did suggest that total slippage was not occurring. It seemed unlikely that the sample would be so difficult to remove if there were not strong adhesive forces, and pressure due to expansion, on the cylinder walls. These forces were, in fact, so strong that one half of the polymer sample adhered to the inner cylinder and one half to the outer cylinder, when they were separated.

4.9. RESULTS FROM THE STATIC APPARATUS

The results obtained from the use of this apparatus are shown in Table (9). Column 1 is the heat flow rate from the inner cylinder heater. Column 2 is a measure of the accuracy of the optimised values obtained by the programme. Column 3 is the initial size of the "Simplex", i.e. the initial step sizes the programme will take to begin the optimisation. Column 4 is the final size of the "Simplex", i.e. the smallest step size the programme is allowed to take. Column 5 is the initial (guessed) value of thermal diffusivity (α) which is required to start the programme. Column 6 is the initial (guessed) value of thermal conductivity (λ) which is required to start the programme. Columns 7 and 8 are the optimised values for 'α' and 'λ' respectively. Columns 9 and 10 are the initial temperatures of the inner and outer cylinders respectively. Columns 11 and 12 are the optimised values for the inner and outer cylinders respectively. After 4 minutes heating the observed temperatures are within 0.5°C of the optimised temperatures at worst and more often much closer.

e.g. Average deviation $= \sqrt{\dfrac{\text{Objective Function}}{\text{number of time steps}}}$

number of 30 second time steps in 4 minutes $= 8$

For line (A) Table 9

average deviation $= \sqrt{\dfrac{1.7285}{8}} = \dfrac{1.34}{8}$

$= \underline{\underline{0.161^{\circ}C}}$

TABLE. 9.

RESULTS FROM TESTS OF PROGRAM STABILITY

	1. HEAT FLOW RATE W/m	2. FINAL VALUE OF OBJECTIVE FUNCTION	3. INITIAL SIZE OF SIMPLEX	4. FINAL SIZE OF SIMPLEX	5. STARTING VALUE FOR $\alpha \times 10^6$ m^2/s	6. STARTING VALUE FOR λ W/mK	7. OPTIMISED VALUE FOR $\alpha \times 10^6$ m^2/s	8. OPTIMISED VALUE FOR λ W/mK	9. INITIAL INNER CYLINDER TEMPERATURE °C	10. INITIAL OUTER CYLINDER TEMPERATURE °C	11. OPTIMISED INNER CYLINDER TEMPERATURE °C	12. OPTIMISED OUTER CYLINDER TEMPERATURE °C
A	41.9	1.7285	0.1	0.0001	0.6	0.6	0.04	0.11	18.4	18.4	42.6	34.0
B	"	1.7296	1.0	0.01	0.3	0.3	"	"	"	"	42.7	"
C	"	1.7287	"	0.001	"	"	"	"	"	"	42.6	"
D	"	1.7293	0.1	0.0001	0.6	0.6	"	"	"	"	"	"
E	"	0.9570	"	"	1.0	10.0	0.09	"	70.5	62.6	82.4	73.9
F	"	1.0195	"	"	0.6	0.6	"	0.12	"		82.3	74.0
G	"	10.5539	"	"	0.003	0.003	0.04	0.09	20.0	20.0	46.9	36.4
H	"	"	"	"	0.6	0.6	"	"	"	"	"	"
I	93.9	17.6496	"	"	0.3	0.3	"	0.4	20.6	20.6	70.3	54.9
J	23.6	3.4976	"	"	0.6	0.6	0.06	0.09	20.0	20.0	36.0	30.0

α = THERMAL DIFFUSIVITY

λ = THERMAL CONDUCTIVITY

OPTIMISED TEMPERATURES = VALUES AFTER 4 MINUTES

LITERATURE VALUES FOR: $\alpha = 0.07 - 0.3 \times 10^{-6}\ m^2/s$

$\lambda = 0.20 - 0.44$ W/mK

For line (I) Table 9

$$\text{average deviation} = \frac{\sqrt{17.6496}}{8} = \frac{4.24}{8}$$

$$= \underline{\underline{0.53^{\circ}C}}$$

The computer programme and flow diagram used for these calculations are shown in Appendix (2).

It can be seen that a number of parameters have to be fed to the computer, in order to initiate the calculations, these are also listed in Appendix (2).

4.10. RESULTS FROM THE THERMAL CONDUCTION EXPERIMENTS

These results were obtained using the apparatus (Figure (26)) in the static state.

The results for thermal conductivity (λ) and thermal diffusivity (α) are plotted in Figures (34) and (35). The results are tabulated in Table (10).

It can be seen that 'α' and 'λ' change very little over the temperature range investigated.

The results for 'λ' agree with Lohe (6) as shown in Figure (34).

THERMAL CONDUCTIVITY — DEPENDENCE ON TEMPERATURE

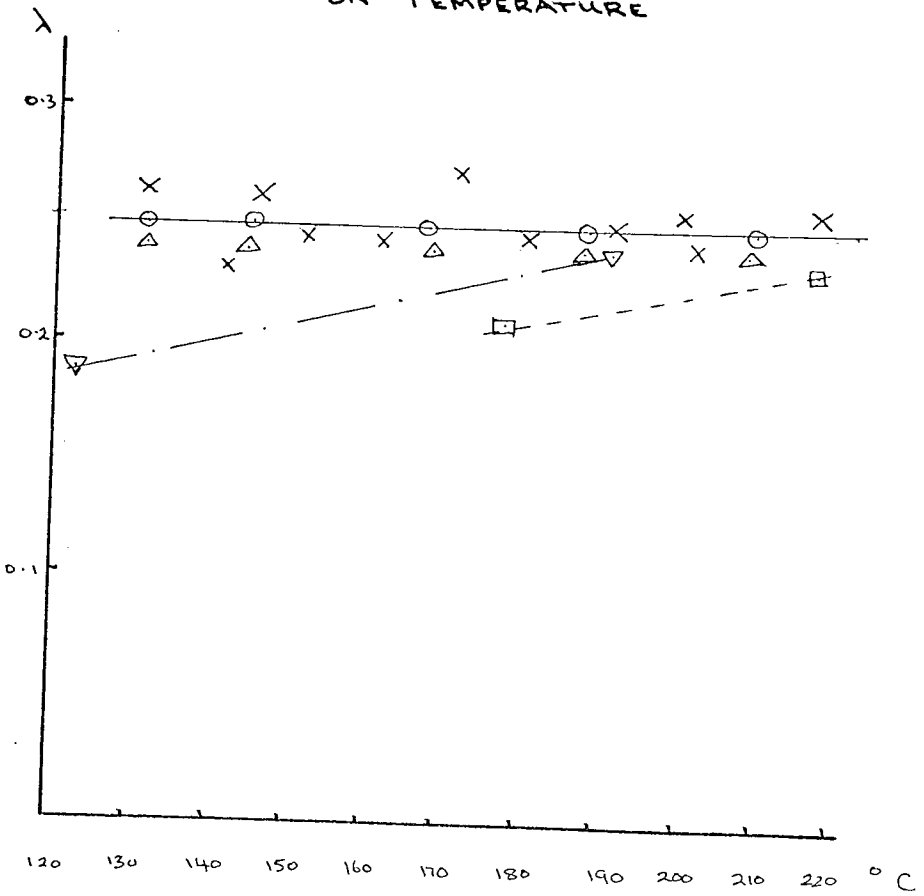

X = EXPERIMENTAL RESULTS
⊙ = LOHE (300 Kp/cm²)
△ = LOHE (1 Kp/cm²)
⊡ = FULLER AND FRICKE
▽ = UNDERWOOD ET AL

FIG. 34.

THERMAL DIFFUSIVITY – DEPENDENCE ON TEMPERATURE

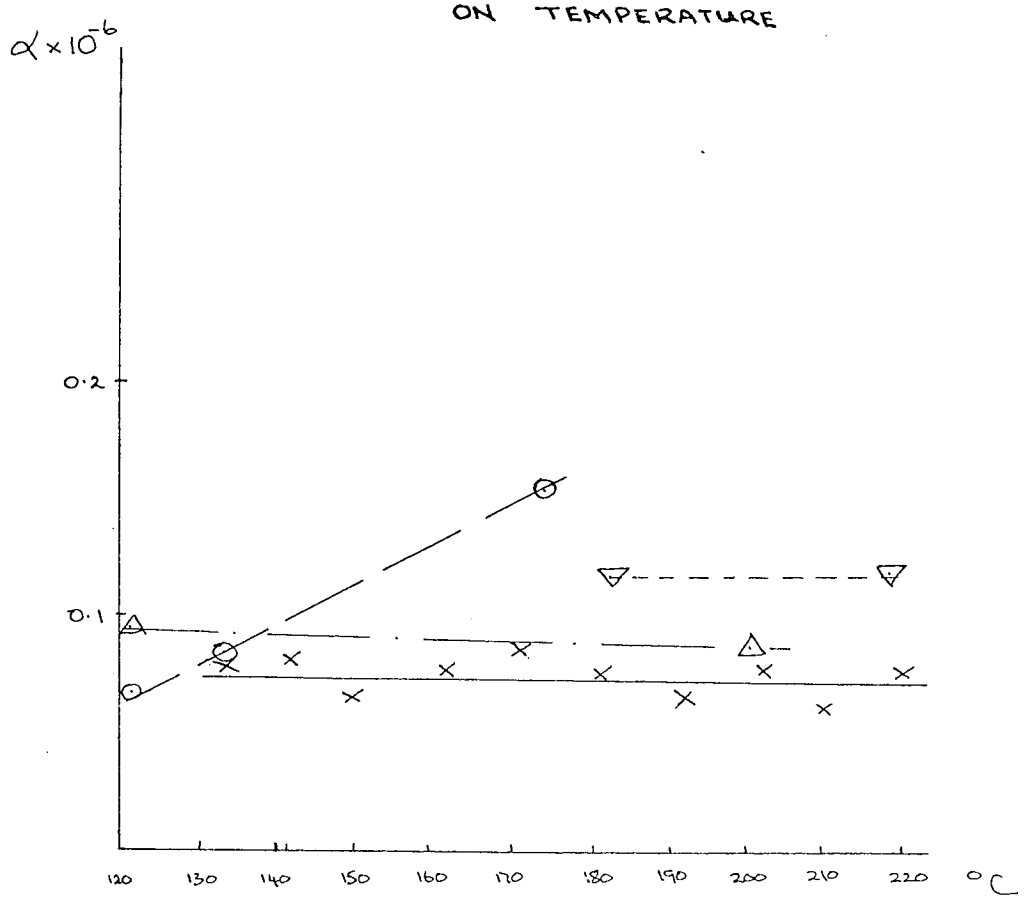

× = EXPERIMENTAL RESULTS
⊙ = GUILLERM
△ = FRIELINGSDORF
▽ = SHOULDBERG

FIG. 35.

TABLE 10 RESULTS FROM HEAT CONDUCTION EXPERIMENTS

Initial Temperature °C	Heat Flow Rate W/m	Temperature Rises Inner Cylinder	Outer Cylinder	Thermal Conductivity W/mK	Thermal Diffusivity $m^2/s \times 10^{-6}$
219.0	47.6	4.5	0.8	0.26	0.080
198.0	31.6	2.9	0.4	0.24	0.080
197.0	43.1	4.0	0.6	0.26	0.080
190.5	36.0	3.3	0.5	0.25	0.070
180.0	23.4	2.2	0.3	0.24	0.080
172.9	48.4	4.5	1.4	0.28	0.090
162.2	61.9	5.8	0.9	0.24	0.075
151.8	59.0	6.5	0.8	0.24	0.070
145.2	49.9	4.4	0.7	0.26	0.070
140.2	31.6	2.9	0.6	0.23	0.075
130.6	43.1	4.1	0.6	0.27	0.080

The results for 'α' agree with those of Frielingsdorf (21) as shown in Figure (35).

These results were calculated using the Simplex programme, as in the previous section (4.9).

The only changes in the parameters fed to the programme were :-

1. CA = C_a = heat capacity of inner cylinder
   = 189.9 J/K

2. CB = C_b = heat capacity of outer cylinder
   = 240.2 J/K

4.11. RESULTS FROM THE ROTATING APPARATUS

These experiments were performed with thermal energy inputs to the sample from the inner cylinder resistance heater and from viscous heating from the shearing of the melt.

The situation would have been simpler if viscous heating alone had been imposed on the sample. However, in extrusion both types of heating are present, therefore, for a closer approach to reality it was considered desirable to use both forms for this work. The two effects were separated by determining the relationship between heat flow rate from the inner cylinder heater, and the resultant temperature

EXPERIMENTAL AND PREDICTED TEMPERATURE RISES DUE TO VISCOUS HEATING AT 80 RPM (MEAN SHEAR RATE = 23·6 s^{-1})

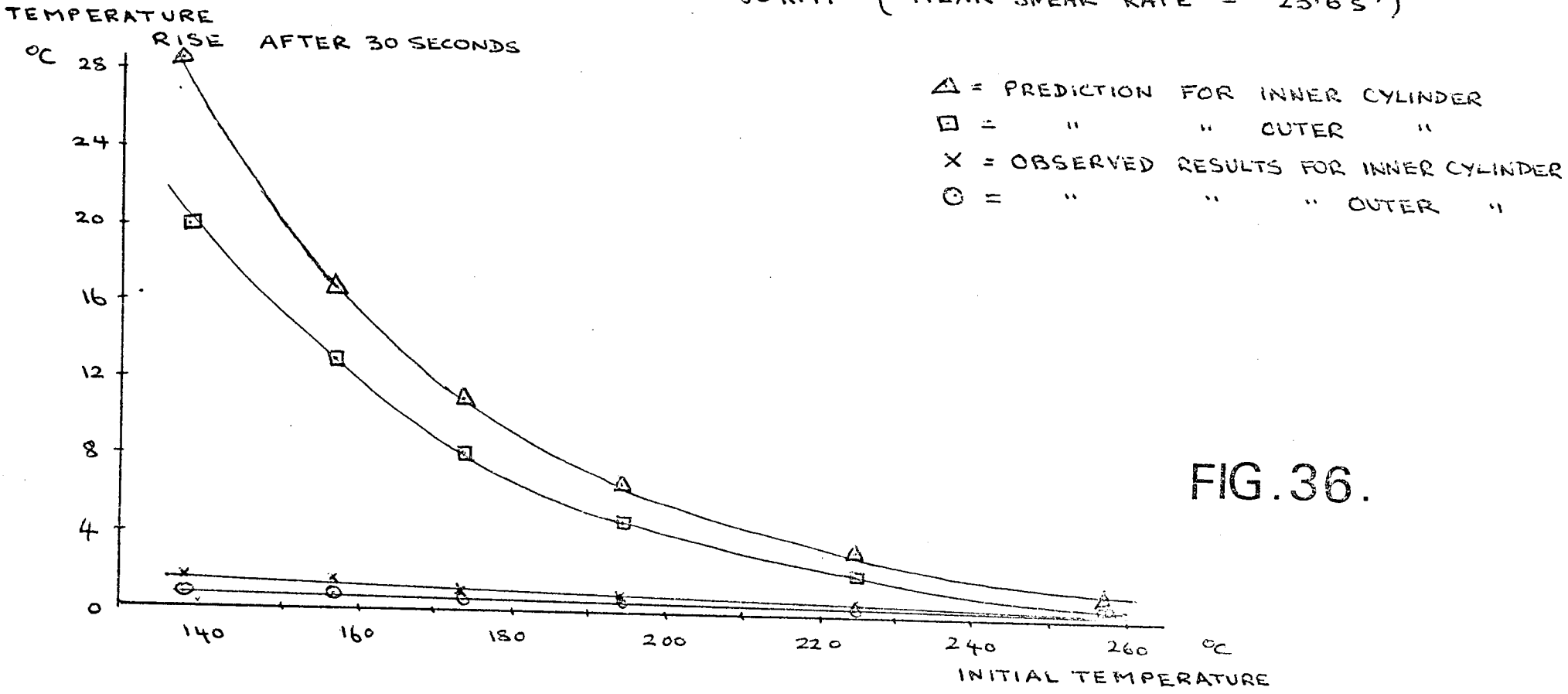

FIG. 36.

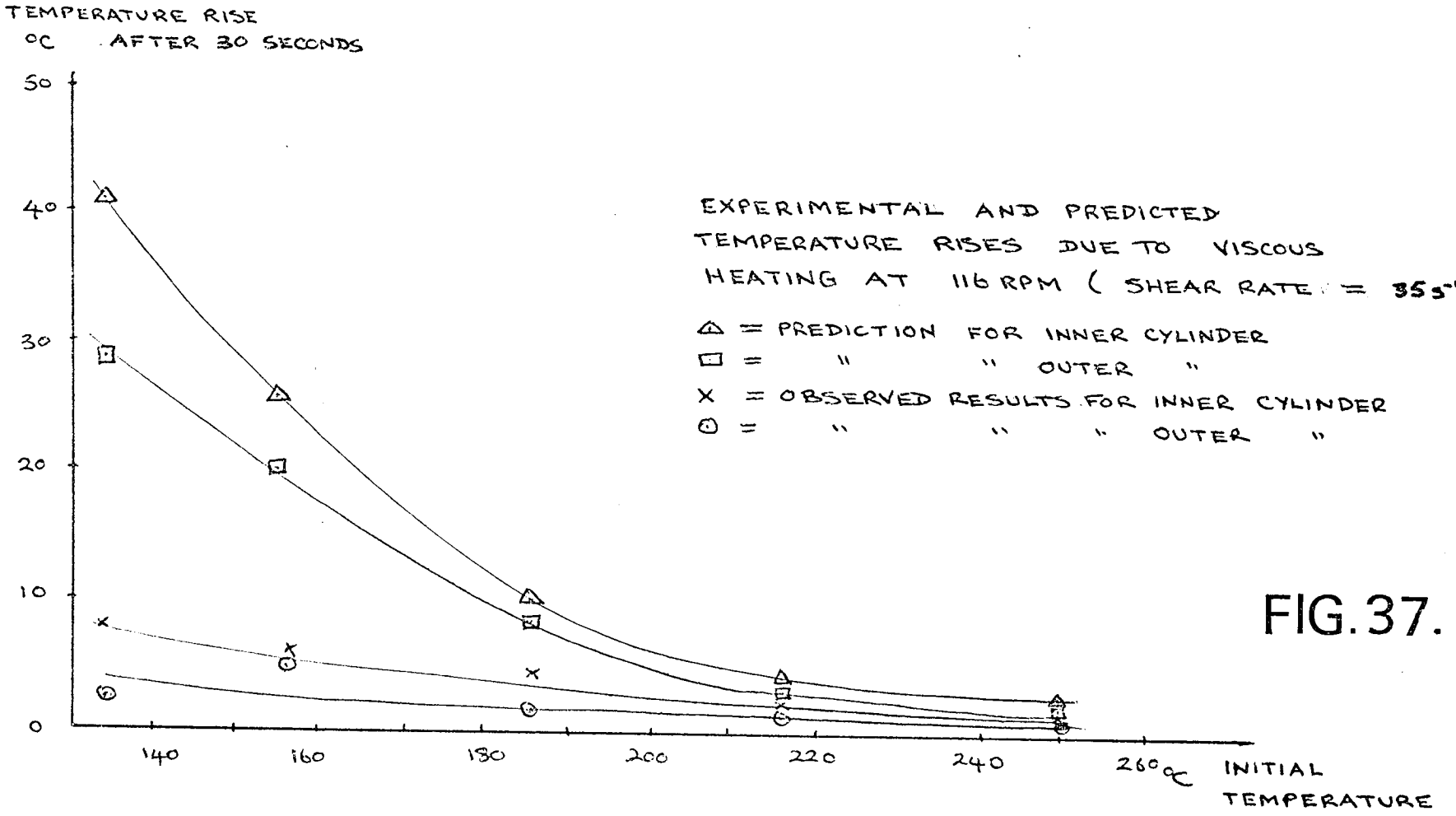

EXPERIMENTAL AND PREDICTED TEMPERATURE RISES DUE TO VISCOUS HEATING AT 116 RPM (SHEAR RATE = 35 s^{-1})

△ = PREDICTION FOR INNER CYLINDER
□ = " " OUTER "
X = OBSERVED RESULTS FOR INNER CYLINDER
⊙ = " " " OUTER "

FIG. 37.

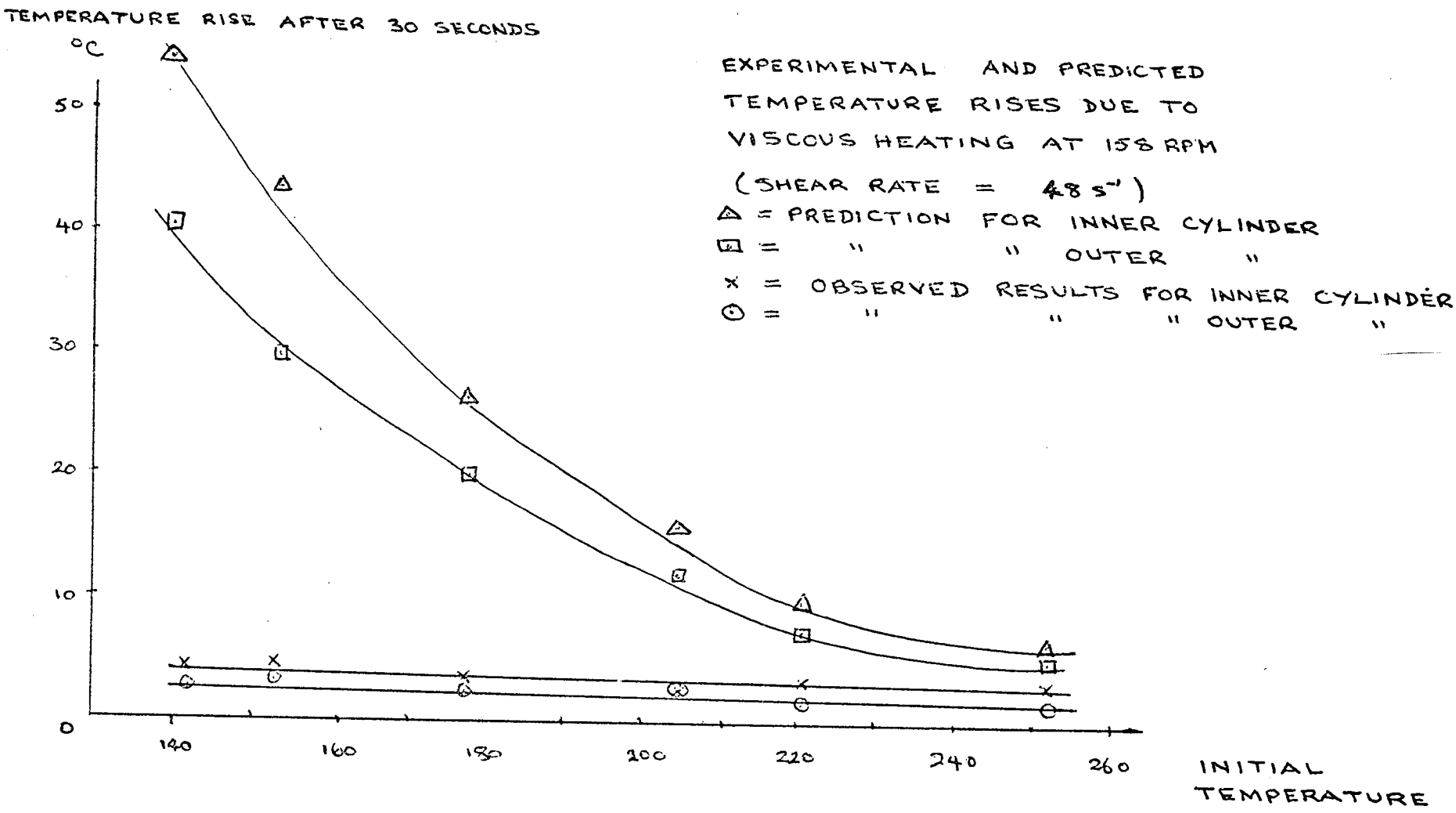
TEMPERATURE RISE AFTER 30 SECONDS
°C
50
40
30
20
10
0
140
160
180
200
220
240
260
INITIAL TEMPERATURE
EXPERIMENTAL AND PREDICTED TEMPERATURE RISES DUE TO VISCOUS HEATING AT 158 RPM
(SHEAR RATE = 48 s⁻¹)
△ = PREDICTION FOR INNER CYLINDER
□ = " " OUTER "
× = OBSERVED RESULTS FOR INNER CYLINDER
⊙ = " " " OUTER "

FIG. 38.

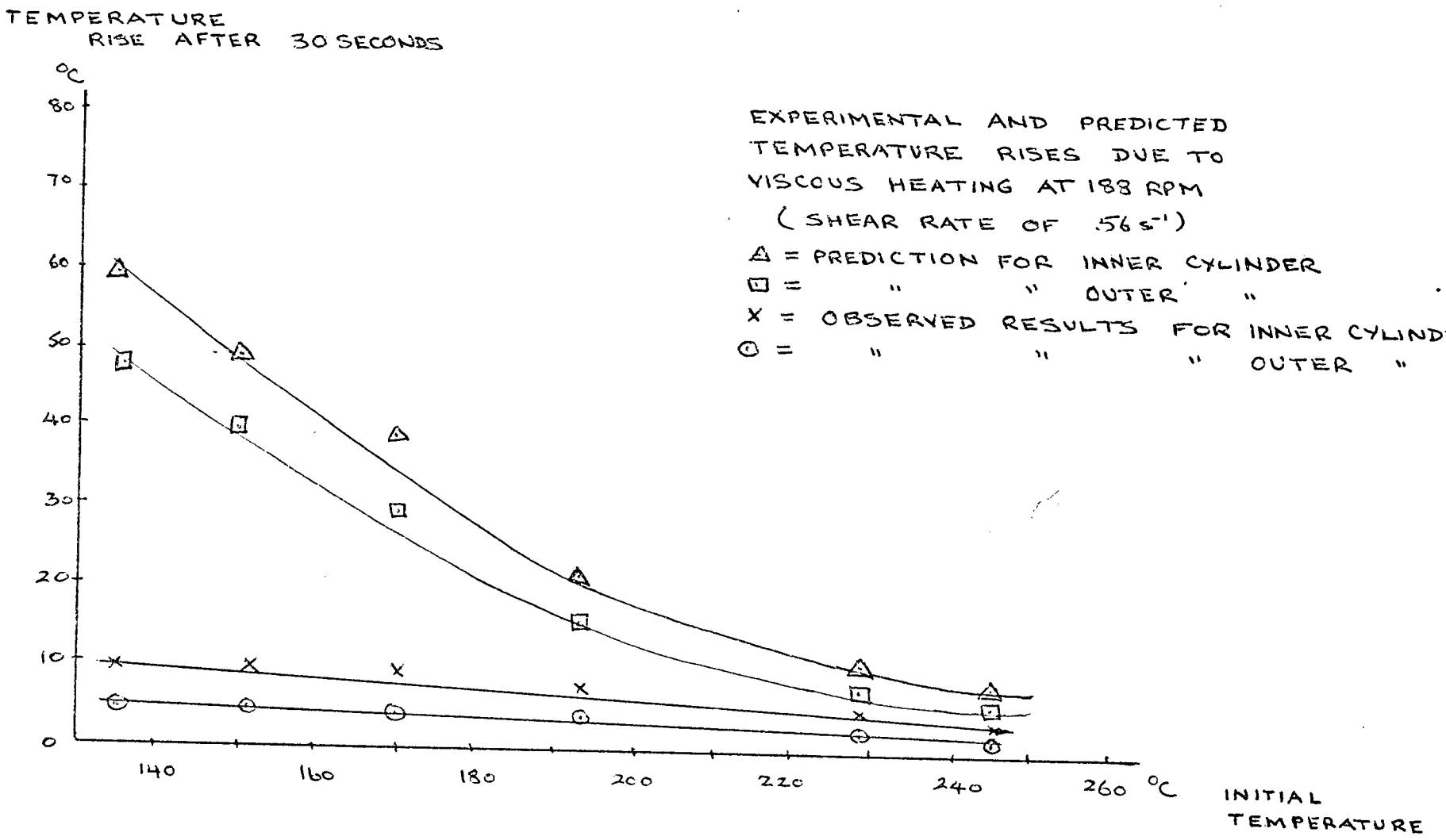
TEMPERATURE
RISE AFTER 30 SECONDS
°C
80
70
60
50
40
30
20
10
0
140
160
180
200
220
240
260 °C
INITIAL
TEMPERATURE
EXPERIMENTAL AND PREDICTED
TEMPERATURE RISES DUE TO
VISCOUS HEATING AT 188 RPM
(SHEAR RATE OF .56 s⁻¹)
△ = PREDICTION FOR INNER CYLINDER
□ = " " OUTER "
X = OBSERVED RESULTS FOR INNER CYLINDER
⊙ = " " " OUTER "

FIG. 39.

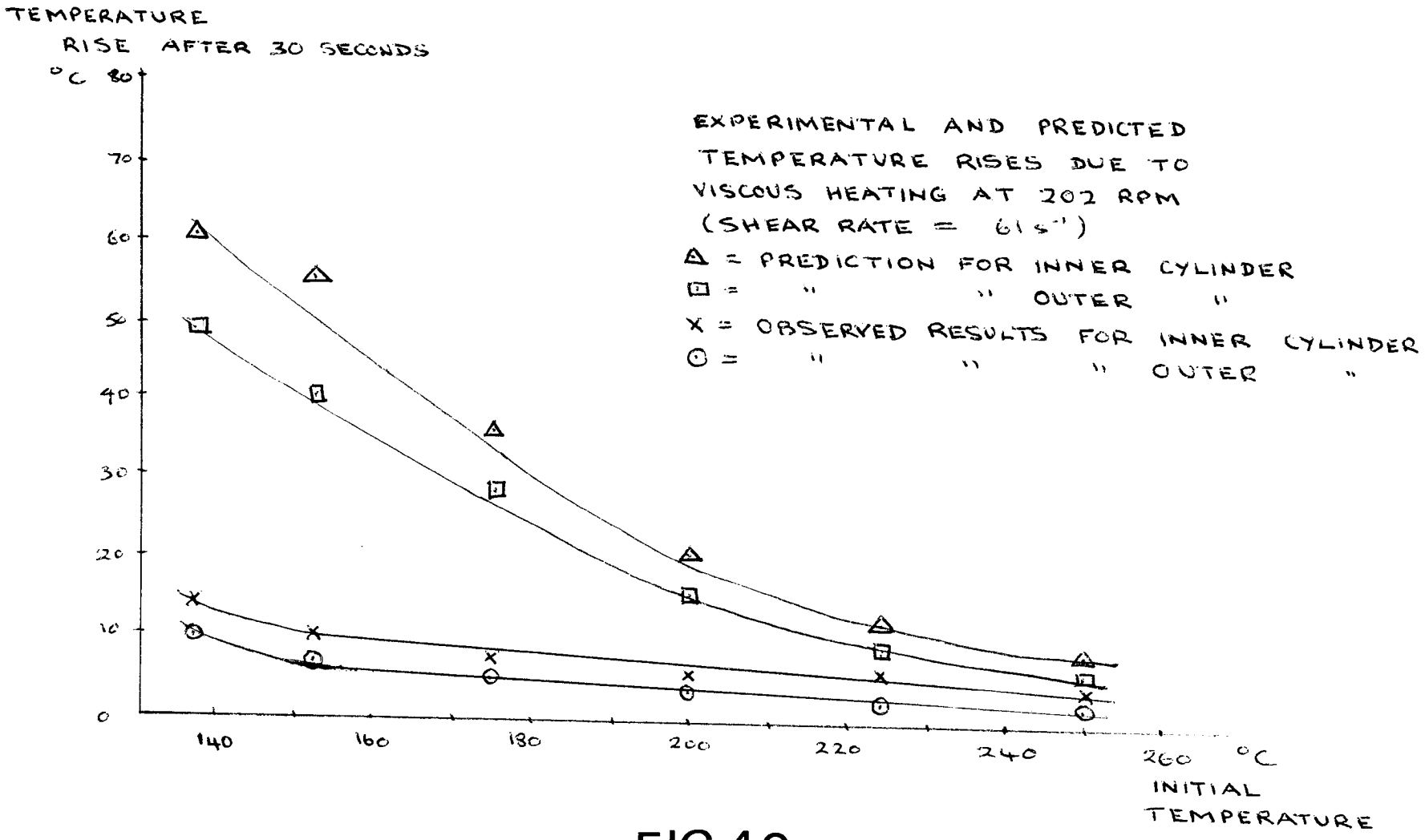
TEMPERATURE
RISE AFTER 30 SECONDS
°C
80
70
60
50
40
30
20
10
0
140
160
180
200
220
240
260
°C
INITIAL
TEMPERATURE
EXPERIMENTAL AND PREDICTED
TEMPERATURE RISES DUE TO
VISCOUS HEATING AT 202 RPM
(SHEAR RATE = 61 s⁻¹)
△ = PREDICTION FOR INNER CYLINDER
□ = " " OUTER "
X = OBSERVED RESULTS FOR INNER CYLINDER
⊙ = " " " OUTER "

FIG.40.

TABLE II.

R.P.M.	APPROXIMATE MEAN SHEAR RATE (s^{-1})	INITIAL TEMPERATURE °C	HEAT FLOW RATE (W/m)	THEORETICAL TEMPERATURE RISE AFTER 30 SECONDS		THEORETICAL TEMPERATURE RISE DUE TO CONDUCTIVE HEATING AFTER 30 SECONDS	
				INNER CYLINDER	OUTER CYLINDER	INNER CYLINDER	OUTER CYLINDER
80	24	257.0	34.6	4.8	1.7	3.2	0.5
"	"	224.0	77.1	10.4	3.5	7.2	1.1
"	"	194.0	47.6	11.0	5.3	4.4	0.7
"	"	174.0	61.9	16.3	9.1	5.8	0.9
"	"	156.0	44.1	20.7	13.5	4.1	0.6
"	"	138.0	49.9	30.0	20.7	4.6	0.7
116	35	249.5	40.0	6.9	2.9	3.7	0.5
"	"	224.0	67.8	11.6	5.0	6.3	0.3
"	"	155.0	27.0	27.9	20.3	2.5	0.4
"	"	133.0	31.6	43.8	33.2	2.9	0.4
158	48	253.0	37.6	8.1	4.0	3.5	0.5
"	"	222.0	63.9	14.5	7.5	5.9	0.9
"	"	206.7	46.4	16.8	9.8	4.3	0.7
"	"	179.4	42.2	25.3	17.3	3.9	0.6
"	"	153.0	23.4	39.3	29.8	2.2	0.3
"	"	141.7	31.6	49.5	37.9	2.9	0.4
188	56	244.0	54.8	12.0	6.1	5.1	0.8
"	"	229.0	65.4	15.4	8.1	6.0	0.9
"	"	196.0	48.4	23.0	15.0	4.5	0.7
"	"	169.5	43.1	35.6	25.5	4.0	0.6
"	"	152.2	23.3	46.9	35.9	2.2	0.3
"	"	135.5	38.8	66.3	51.5	2.6	0.5
202	61	250.5	69.4	12.2	5.9	5.5	0.9
"	"	225.7	75.6	17.8	9.4	8.1	0.7
"	"	200.6	59.0	23.5	14.8	7.5	0.8
"	"	174.5	36.0	34.0	24.6	3.3	0.5
"	"	154.0	45.4	49.7	37.2	4.2	0.6
"	"	139.6	37.0	64.5	50.3	3.4	0.5

TABLE 12

R.P.M.	APPROXIMATE MEAN SHEAR RATE (s^{-1})	INITIAL TEMPERATURE °C	HEAT FLOW RATE (W/m)	EXPERIMENTAL TEMPERATURE RISE AFTER 30 SECONDS		EXPERIMENTAL TEMPERATURE RISE DUE TO CONDUCTIVE HEATING AFTER 30 SECONDS	
				INNER CYLINDER	OUTER CYLINDER	INNER CYLINDER	OUTER CYLINDER
80	24	257.0	34.6	3.0	0.5	3.2	0.5
"	"	224.0	77.1	7.9	1.4	7.2	1.1
"	"	194.0	47.6	5.5	1.3	4.4	0.7
"	"	174.0	61.9	7.0	1.5	5.8	0.9
"	"	156.0	44.1	5.5	1.2	4.1	0.6
"	"	138.0	49.9	6.2	1.5	4.6	0.7
116	35	249.5	40.0	5.7	2.0	3.7	0.5
"	"	224.0	67.8	8.8	1.8	6.3	0.3
"	"	155.0	27.0	7.5	6.0	2.5	0.4
"	"	133.0	31.6	8.9	2.7	2.9	0.4
158	48	253.0	37.6	7.0	3.5	3.5	0.5
"	"	222.0	63.9	11.5	3.5	5.9	0.9
"	"	206.7	46.4	6.3	2.7	4.3	0.7
"	"	179.4	42.2	7.1	2.8	3.9	0.6
"	"	153.0	23.4	5.0	2.5	2.2	0.3
"	"	141.7	31.6	6.3	2.8	2.9	0.4
188	56	244.0	54.8	10.5	3.8	5.1	0.8
"	"	229.0	65.4	12.0	3.9	6.0	0.9
"	"	196.0	48.4	8.0	4.2	4.5	0.7
"	"	169.5	43.1	10.5	3.5	4.0	0.6
"	"	152.2	23.3	11.0	4.3	2.2	0.3
"	"	135.5	38.8	12.0	5.0	2.6	0.5
202	61	250.5	59.4	10.0	3.4	5.5	0.9
"	"	225.7	75.6	14.4	4.3	8.1	0.7
"	"	200.6	59.0	12.0	4.3	7.5	0.8
"	"	174.5	36.0	9.3	5.0	3.3	0.5
"	"	154.0	45.4	10.2	9.5	4.2	0.6
"	"	139.6	37.0	13.9	13.4	3.4	0.5

rise of the cylinders. The temperature rise due to conducted heat could then be subtracted and the temperature rise due to viscous heating determined.

From section 3.4, equation (48) states :

$$\frac{\partial T}{\partial t} = \alpha \frac{\partial}{\partial r}\left[\frac{1}{r}\frac{\partial}{\partial r}\left(r\frac{\partial T}{\partial r}\right)\right] + \frac{K_0 B e^{A/(T+273.2)}}{\rho C_p} \cdot 4\left(\frac{b}{r}\right)^4 \left(\frac{aV_a}{b^2-a^2}\right)^{n+1}\left(\frac{(r^2+b^2)}{r^2}\right)^{n-1} \quad \ldots.(48)$$

The first term, on the right hand side, is the thermal conduction through the sample, and the second term is the viscous heating. The above equation contains parameters which are constant throughout the experiments and these together with the data necessary for the programme are listed in Appendix (3).

Figures (36) to (40) show the theoretical and experimental temperature rises after 30 seconds heating, for each shear rate and each starting temperature which was used. It is obvious there is a wide difference between the two figures especially near the "melting point" of the polymer (130°C). Figures are listed in Tables (11) and (12).

Figures (41) to (44) show the temperature profiles predicted by the theory.

Figures (41 and (42) show the profiles at the lowest shear rate (80 r.p.m. - 24 s^{-1}) and at low (138.0°C) and high (257.0°C) temperatures. There is very little difference between the theoretical viscous heating profile and the combined profile

for thermal conduction and viscous heating (Figure (42)). At the higher temperature (257.0°C) the viscous heating is predicted to fall to such a low level that only the combined temperature profile for viscous and thermal conductive heating is shown. The profiles for viscous heating only and for thermal conductive heating are not shown because the temperatures are very close to the combined profile. The figures are given in Tables(16), (17)and (18).

Figures (43) and (44) show the predicted temperature profiles for the highest shear rate (202 r.p.m. - 61 s^{-1}) at low (139.6°C) and high (250.5°C) temperatures. It can be seen from Figures (41) and (43) that at the lower temperatures the theory predicts large fluctuations in temperature for viscous heating only. These effects, if real, perhaps indicate that there is a "mixing action" within the polymer that is, there is turbulence. Alternatively, they may simply be a reflection of the low conductivitity of the polymer. The heat generated by viscous heating being unable to dissipate quickly because of the poor thermal conductivity of the melt.

At high melt temperatures the temperature profiles are much smoother, presumably because the effect of viscous heating is considerably reduced.

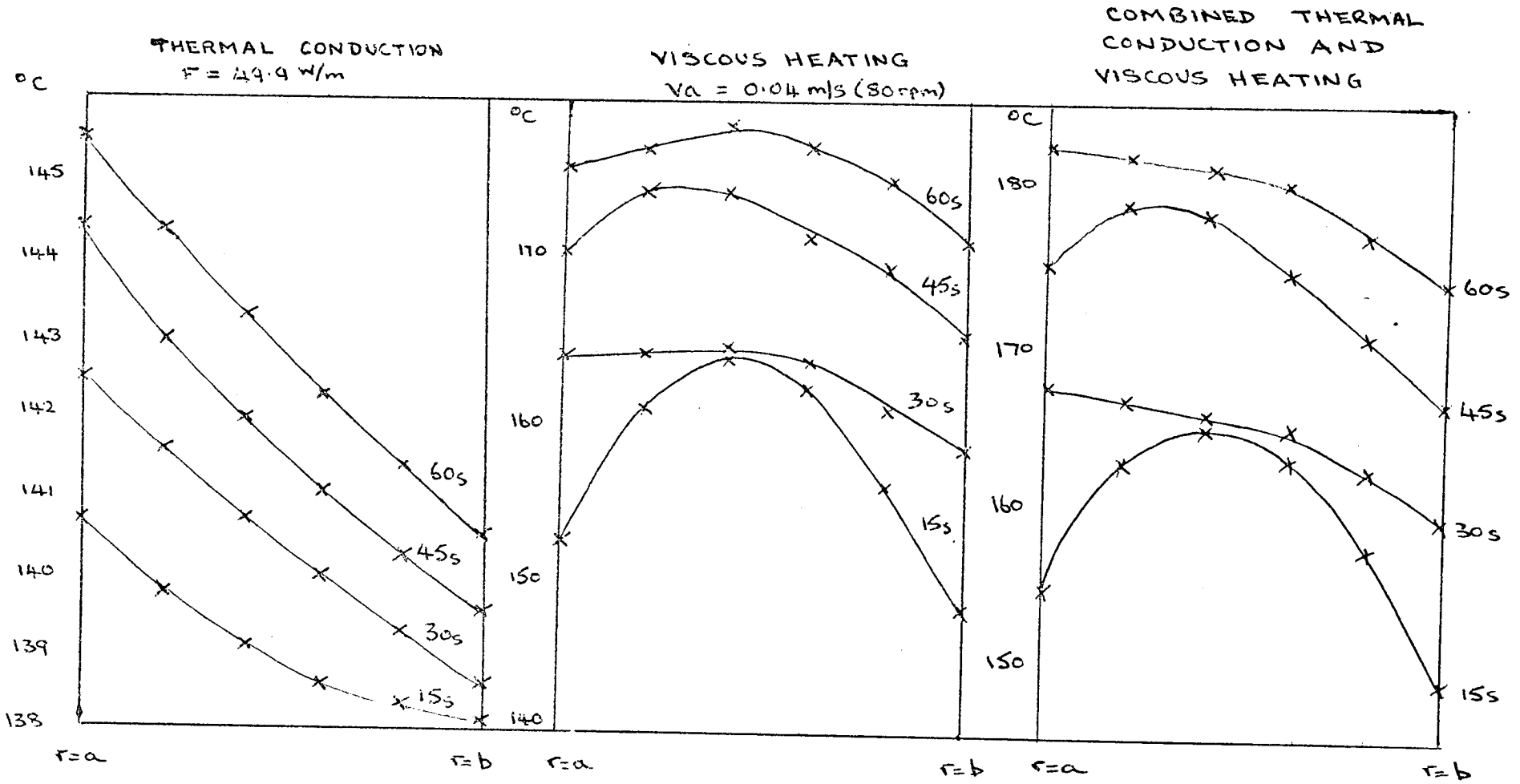

PREDICTED TEMPERATURE PROFILES WITHIN THE SAMPLE AFTER SET TIME INTERVALS

INITIAL TEMPERATURE = 138·0°C

F = HEAT FLOW RATE FROM HEATER

Va = VELOCITY OF ROTATION OF THE INNER CYLINDER

FIG.41.

TABLE (13) PREDICTED TEMPERATURES DUE TO THERMAL CONDUCTION

$F = 49.9\ W/_m$ $V_a = 0$

Radius $\times 10^{-2}$(m)	Initial Temperature (^oC)	Time Interval(s)			
		15	30	45	60
0.47 *	138.0	140.8	142.6	144.3	145.6
0.504	"	139.8	141.7	143.0	144.4
0.538	"	139.1	140.8	142.0	143.3
0.572	"	138.7	140.0	141.1	142.3
0.606	"	138.4	139.3	140.3	141.4
0.64 **	"	138.2	138.7	139.6	140.6

TABLE (14) PREDICTED TEMPERATURES DUE TO VISCOUS HEATING ONLY

$V_a = 0.04\ m/s$ (80 r.p.m.)

Radius $\times 10^{-2}$(m)	Initial Temperature (^oC)	Time Interval(s)			
		15	30	45	60
0.47 *	138.0	152.2	164.1	170.4	176.8
0.504	"	161.1	163.8	174.4	177.8
0.538	"	163.7	164.2	174.4	178.0
0.572	"	161.9	163.2	172.6	177.2
0.606	"	156.6	161.1	169.8	174.9
0.64 **	"	147.6	158.3	165.2	172.0

TABLE (15) PREDICTED TEMPERATURES DUE TO BOTH THERMAL CONDUCTIVE AND VISCOUS HEATING

V_a = 0.04 m/s (80 r.p.m.) F = 49.9 w/m

Radius $\times 10^{-2}$(m)	Initial Temperature (°C)	Time Interval(s)			
		15	30	45	60
0.47 *	138.0	154.7	168.0	175.3	182.6
0.504	"	162.6	166.7	178.0	181.8
0.538	"	164.6	166.1	177.0	181.4
0.572	"	162.4	164.7	174.5	179.8
0.606	"	156.9	161.9	171.2	176.9
0.64 **	"	147.7	158.7	166.2	173.5

N.B. Experimental Temperatures

After 30 seconds 144.2 */ 139.5 **

After 60 seconds 152.5 */ 142.5 **

* Inner cylinder

** Outer cylinder

FIG. 42.

PREDICTED TEMPERATURE PROFILE
IN SAMPLE (POWER LAW)
VISCOUS HEATING AND CONDUCTION
INITIAL TEMPERATURE - 257.0°C
SHEAR RATE - 33.5 SEC.$^{-1}$ (80 RPM)
HEAT FLOW RATE = 34.6 W/m

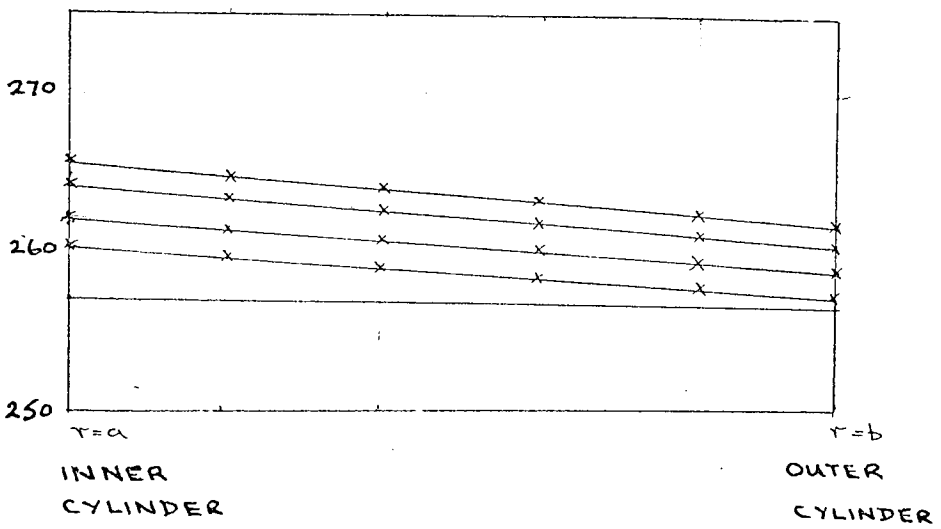

TABLE (16) PREDICTED TEMPERATURES FOR THERMAL CONDUCTION

F = 34.6 w/m

Radius $\times 10^{-2}$(m)	Initial Temperature (°C)	Temperature after time interval(s)			
		15	30	45	60
0.47 *	257.0	258.9	260.2	261.3	262.3
0.504	"	258.2	259.6	260.5	261.5
0.538	"	257.8	258.9	259.8	260.7
0.572	"	257.5	258.4	259.1	259.9
0.606	"	257.3	257.9	258.6	259.3
0.64 **	"	257.1	257.5	258.1	258.8

TABLE (17) PREDICTED TEMPERATURES FOR VISCOUS HEATING

V_a = 0.04 m/s (80 r.p.m)

Radius $\times 10^{-2}$(m)	Initial Temperature (°C)	Temperature after time interval(s)			
		15	30	45	60
0.47 *	257.0	257.8	258.7	259.4	260.2
0.504	"	258.2	258.8	259.7	260.4
0.538	"	258.4	258.9	259.8	260.4
0.572	"	258.3	258.8	259.6	260.3
0.606	"	258.0	258.6	259.3	260.0
0.64 **	"	257.5	258.2	258.9	259.6

TABLE (18) PREDICTED TEMPERATURES FROM BOTH THERMAL CONDUCTION AND VISCOUS HEATING

$F = 34.6\ W/_m$ $V_a = 0.04$ m/s (80 r.p.m.)

Radius $\times 10^{-2}$(m)	Initial Temperature (°C)	Temperature after time interval(s)			
		15	30	45	60
0.47 *	257.0	259.7	261.8	263.7	265.7
0.504	"	259.5	261.4	263.1	264.7
0.538	"	259.2	260.8	262.4	264.0
0.572	"	258.7	260.1	261.7	263.1
0.606	"	258.2	259.4	260.9	262.3
0.64 **	"	257.6	258.7	260.0	261.4

Experimental Temperatures

After 30 seconds 260.0*/257.5 **

After 60 seconds 264.5*/259.2 **

* Inner Cylinder

** Outer Cylinder

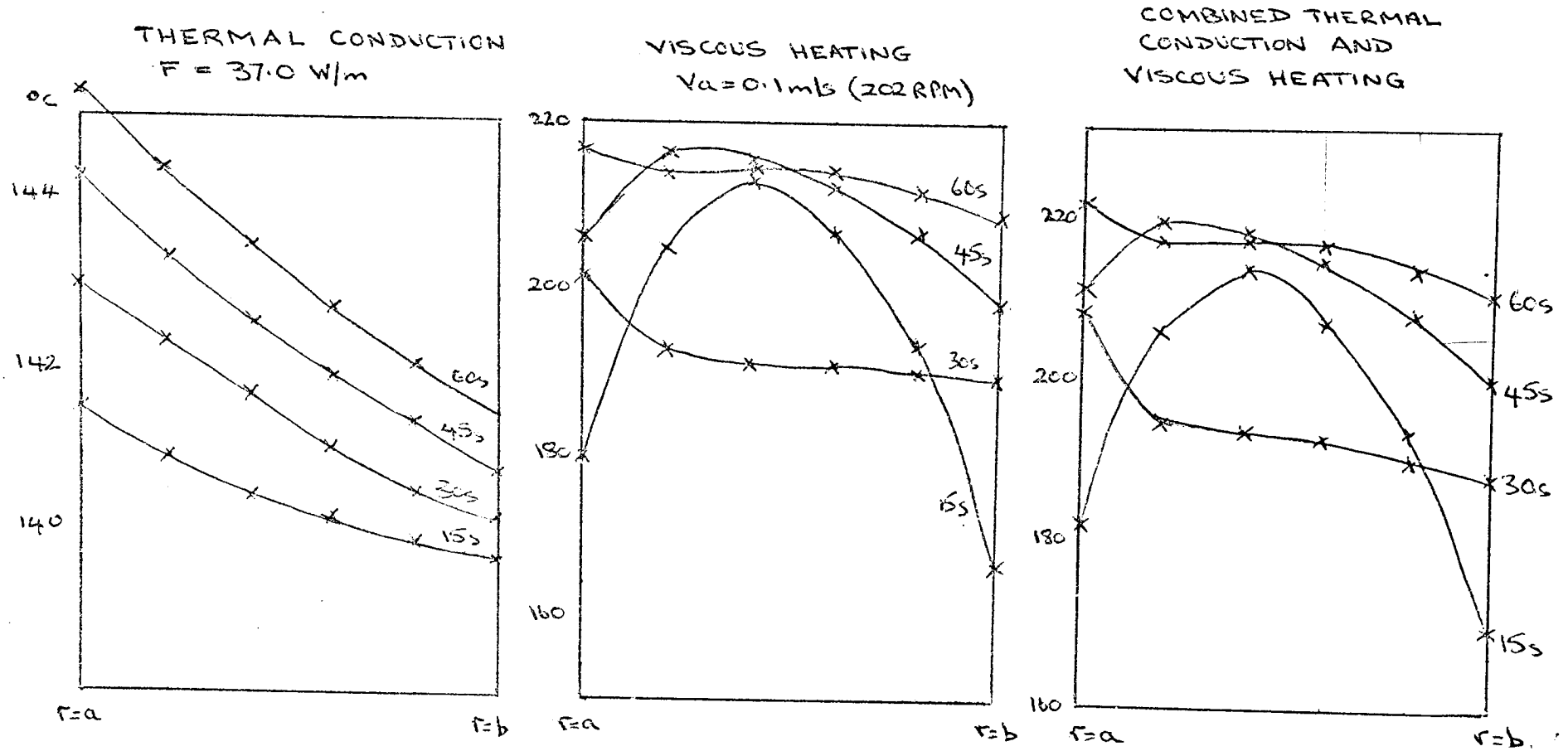

PREDICTED TEMPERATURE PROFILES WITHIN THE SAMPLE AFTER SET TIME INTERVALS.

F = HEAT FLOW RATE FROM HEATER

Va = VELOCITY OF ROTATION OF THE INNER CYLINDER

INITIAL TEMPERATURE = 139.6°C

FIG.43.

TABLE (19) PREDICTED TEMPERATURES FOR THERMAL CONDUCTION

$F = 37.0\ W/_m$

Radius $\times 10^{-2}$(m)	Initial Temperature (°C)	Temperature after time interval(s)			
		15	30	45	60
0.47 *	139.6	141.6	143.0	144.2	145.3
0.504	"	140.9	142.3	143.3	144.4
0.538	"	140.4	141.7	142.6	143.5
0.572	"	140.1	141.0	141.9	142.8
0.606	"	139.9	140.5	141.3	142.1
0.64 **	"	139.7	140.1	140.8	141.5

TABLE (20) PREDICTED TEMPERATURES FOR VISCOUS HEATING

$V_a = 0.1$ m/s (202 r.p.m.)

Radius $\times 10^{-2}$(m)	Initial Temperature (°C)	Temperature after time interval(s)			
		15	30	45	60
0.47 *	139.6	179.9	201.3	206.8	216.8
0.504	"	205.3	192.8	217.1	213.9
0.538	"	212.5	191.5	216.5	215.7
0.572	"	207.5	191.0	212.6	215.5
0.606	"	192.6	189.4	207.6	212.2
0.64 **	"	167.0	189.4	198.4	209.1

TABLE (21) PREDICTED TEMPERATURES FOR BOTH THERMAL CONDUCTION AND VISCOUS HEATING

F = 37.0 W/m Va = 0.1 m/s (202 R.P.M.)

Radius $\times 10^{-2}$(m)	Initial Temperature (°C)	Temperature after time interval(s)			
		15	30	45	60
0.47 *	139.6	181.7	204.1	210.3	220.9
0.504	"	206.4	194.7	219.6	217.0
0.538	"	213.2	192.8	218.3	218.0
0.572	"	207.8	191.9	213.9	217.3
0.606	"	192.8	189.9	208.5	213.5
0.64 **	"	167.1	189.7	199.1	210.1

Experimental Temperatures :

After 30 seconds 153.5*/153.0 **

After 60 seconds 167.2*/166.0 **

* Inner cylinder

** Outer cylinder

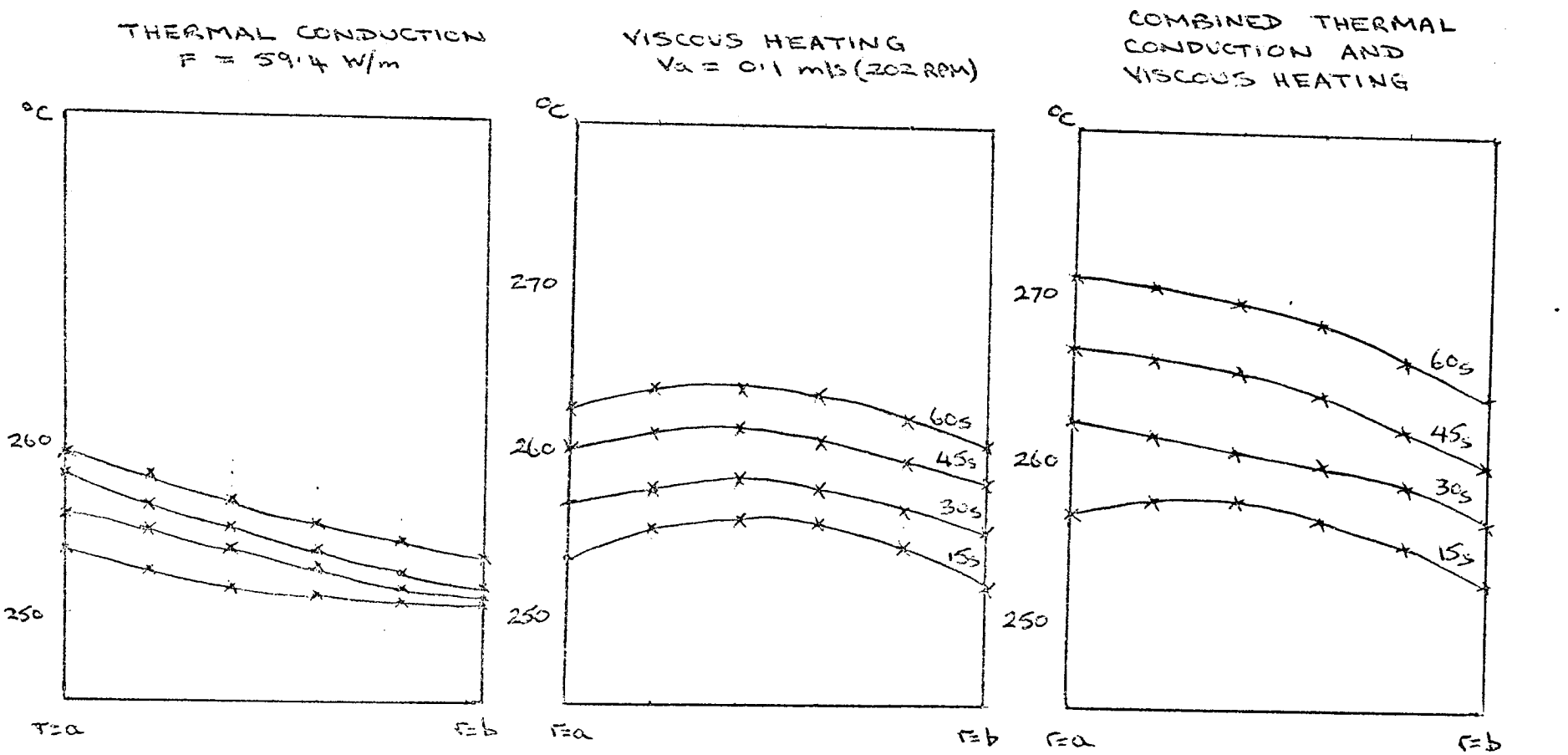

PREDICTED TEMPERATURE PROFILES WITHIN THE SAMPLE AFTER SET TIME INTERVALS

F = HEAT FLOW RATE FROM HEATER
INITIAL TEMPERATURE = 250·5°C

Va = VELOCITY OF ROTATION OF THE INNER CYLINDER

FIG. 44.

TABLE (22) PREDICTED TEMPERATURES DUE TO THERMAL CONDUCTION

$F = 59.4\ W/_m$

Radius $\times 10^{-2}$(m)	Initial Temperature (^oC)	Temperature after time interval(s)			
		15	30	45	60
0.47 *	250.5	253.8	256.0	258.0	259.6
0.504	"	252.6	254.9	256.5	258.2
0.538	"	257.8	253.8	255.2	256.8
0.572	"	251.3	252.8	254.2	255.6
0.606	"	250.9	252.0	253.2	254.5
0.64 **	"	250.7	251.3	252.4	253.6

TABLE (23) PREDICTED TEMPERATURES DUE TO VISCOUS HEATING

$V_a = 0.1$ m/s (202 r.p.m.)

Radius $\times 10^{-2}$(m)	Initial Temperature (^oC)	Temperature after time interval(s)			
		15	30	45	60
0.47 *	250.5	253.7	257.4	260.2	263.0
0.504	"	255.8	258.0	261.4	263.7
0.538	"	256.4	258.2	261.5	263.9
0.572	"	256.0	257.9	261.0	263.5
0.606	"	254.7	257.0	259.9	262.4
0.64 **	"	252.6	255.6	258.3	261.0

TABLE (24) PREDICTED TEMPERATURES DUE TO BOTH THERMAL CONDUCTION AND VISCOUS HEATING

F = 59.4 W/m Va = 0.1 m/s (202 R.P.M.)

Radius $\times 10^{-2}$(m)	Initial Temperature (^{o}C)	Temperature after time interval(s)			
		15	30	45	60
0.47 *	250.5	256.9	262.7	267.8	271.4
0.504	"	257.8	262.1	266.9	270.5
0.538	"	257.7	261.3	265.8	269.4
0.572	"	256.7	260.0	264.2	267.9
0.606	"	255.1	258.3	262.3	265.9
0.64 **	"	252.8	256.4	260.0	263.7

Experimental Temperatures

After 30 seconds 260.5 */253.5 **

After 60 seconds 268.5 */258.4 **

* Inner cylinder

** Outer cylinder

5.0 DISCUSSION

5.1. RESULTS FROM THE STATIC APPARATUS

Typical results are shown in Table 9, section 4.9, and the results will be discussed in order of the column numbers in the table.

1. The heat flow rate from the inner cylinder heater, measured in watts per metre (W/m). The power in watts was measured with an ammeter and voltmeter and converted to W/m by dividing by the length of the specimen.

2. The final value of the objective function of the "Simplex" programme indicates the accuracy of the calculated temperatures compared to the experimental temperatures, i.e. it is a measure of the average deviation of the calculated temperatures from the measured temperatures.

In Table 9 the largest final value (i.e. the least accurate result) for the objective function was 17.6496, and this was after eight time steps of 30 seconds. This gives a value for the average deviation of 0.53°C (from section 4.9). Therefore, the experimental and calculated temperatures would agree, in this case, to within about 0.5°C.

This degree of accuracy from the programme was acceptable since it was the same as the reproducibility of the experiments. The potentiometric recorder

was capable of measuring to 0.1°C. Above the poorest result was chosen, but more representative data in Table 9 gives agreement between experimental and calculated temperatures of the order of 0.1 - 0.2°C.

3. The initial size of the "Simplex" determines the size of step which the programme will use in the initial stages of optimisation. The size of this step could influence the efficiency of the programme. For example, it could cause the running time of the programme to be longer than necessary and computer time is expensive. However, when the quantity was changed from 0.1 to 1.0 no effect was observed on the computer time.

4. The final size of the "Simplex" determines the smallest steps which would be allowed during optimisation. Once this step size has been reached the "Simplex" could not reduce further, therefore, this quantity would be expected to influence the accuracy of the calculations. Values ranging from 0.01 to 0.0001 were tried with no significant changes in "α" or "λ" or the computed temperature profiles.

5. The initial (guessed) value of thermal diffusivity (α) given to the programme, so that the optimisation could begin, could affect the results. If a constant minimum was not found for each initial value used, then the optimised values for "α" would change.

Initial values from 0.003 - 1.0 x 10^{-6} m^2/s were used and no influence on the final optimised value of "α" was observed.

The computed values of "α" were in the range 0.04 - 0.09 x 10^{-6} m^2/s, whereas literature values varied from 0.07 - 0.3 x 10^{-6} m^2/s. The results were therefore low but stable enough to show that the programme was determining the true minimum points in the optimisation. Improvements in design of the rotating apparatus were expected to improve the value of "α" (e.g. smaller bore outer cylinder to improve thermal contact between sample and cylinder.)

6. As discussed in (5) above for "α" it was necessary to supply a guessed value to initiate the optimisation. In this case, a value for thermal conductivity (λ) was required. Chosen values ranged from 0.003 - 10.0 W/mK and these produced no changes in the final calculated results for "λ". The results were again low ranging from 0.11 - 0.14 W/mK, whereas literature values varied from 0.20 - 0.44 W/mK.

However, agreement was considered good enough to proceed with this approach for the reasons given in (5).

7. The optimised value for "α" was the calculated value best suited to the experimental conditions of energy input and temperatures.

8. The optimised value of " λ" was the calculated value best suited to the experimental conditions of energy input and temperatures.

9. The initial temperatures of the inner cylinder of the apparatus.

10. The initial temperature of the outer cylinder of the apparatus.

11. The temperature of the inner cylinder after 4 minutes heating as calculated by the programme. This should be the same or very close to the experimental temperatures. These can be compared directly or an average deviation can be obtained from column 2 in Table (9) as previously explained.

12. The temperature of the outer cylinder after 4 minutes heating as calculated by the programme. Comparison with experimental temperatures can be made as in (11).

5.2. THERMAL CONDUCTION EXPERIMENTS

The overall results were satisfactory when compared to published results (see section (4.10).

The temperature dependence of both thermal conductivity (λ) and thermal diffusivity (α) were found to be insignificant.

From Figures (12) and (13) some authors found an increase in "α" and "λ"

with increasing temperature. Polyethylene is commonly referred to as a crystalline polymer. This means that a high percentage (>50%) of the material does crystallise on cooling from the melt.

In the solid state, the crystalline regions have a higher thermal conductivity than the amorphous regions. The dominant effect observed, when the temperature is raised, is the destruction of the crystalline areas. This leads to a fall in thermal conductivity since the amorphous content of the polymer is increasing and the crystalline content decreasing.

In the melt state, there are no crystalline areas, the material is totally amorphous.

Increasing the temperature with the material in this state increase the molecular vibrations and should lead to an increase in thermal conductivity. Opposing the above effect is the thermal expansion which occurs. This causes an increase in volume and a reduction in density. The result is that the thermal conductivity should decrease.

Most literature values report an increase or constant values for conductivity and diffusivity. Presumably the trend which is observed depends on the material used and the conditions under which the measurements are taken. If the material is confined in an enclosed space as it has to be in measurements on the melt, the thermal expansion cannot occur freely and the volume increase (density reduction) cannot

occur to the maximum extent.

The molecular mobility of the melt will be very dependent upon the molecular weight of the polymer and therefore will vary from one author's results to another . The higher the molecular weight the less mobility the melt will have, at any given temperature, when compared to a polymer of lower molecular weight.

5.3. VISCOUS HEATING EXPERIMENTS

5.3.1. Introduction to Discussion

It can be seen from Figures(36) - (40) that the theoretical predictions do not agree with the experimental results. The latter suggest that viscous heating is virtually independent of temperature and much lower than would be predicted under the experimental conditions.

There would appear to be two possible reasons for this :-

(a) The apparatus did not produce the required shear rates in the sample and/or temperature measurements were inaccurate.

(b) The theory overestimated the viscous heating because of the assumptions which were used in its derivation.

In the following section the malfunction of the apparatus as defined by (a) above is discussed.

5.3.2. Discussion of Apparatus

The apparatus consisted of two cylinders, one stationary, and one which could be rotated at any speed between 10 - 220 r.p.m. The space between the cylinders was filled with the polymer sample. The object was to induce inter-laminar shearing in the sample and thus produce a high level of viscous heating. To do so there must be good adhesion at the metal-polymer interfaces (i.e. slippage must not occur.) The material was melted and in doing so it expanded. The expansion should have produced pressure on the cylinders, since the only means of escape for the polymer, was to extrude itself between the inner cylinder and the PTFE bearing. The gap was of the order of 0.005" (0.127 mm) and thus significant pressure would be required to push the material through this space.

The adhesion between the molten polymer and the metal cylinders was found to be very good. It was observed, that samples could not be removed from the apparatus after each experiment, unless the viscosity of the polymer was low enough (at a temperature of 180 - 200°C) to enable the cylinders to be slid apart. Allowing the material to resolidify was not helpful, in fact, it appeared to increase the adhesion between the cylinders and the sample. The shrinkage which occurred on cooling was therefore not sufficient to overcome the adhesion between the material and the outer cylinder.

These observations suggest that slippage between the metal and polymer was unlikely.

Results from the use of coloured tracers in the sample (see section 4.8) appear to support the above conclusions. However, the use of a Keyed outer cylinder produced significant percentage increases in the temperature rises. This suggests that the adhesion between polymer and metal was not as good as it appeared and even 0.005" (0.127 mm) deep keys will significantly affect the viscous heating.

Work by Galt and Maxwell indicates that some "slippage" is an inherent part of the polymer flow process in dies. The shear forces build up until the stored elastic energy overcomes the adhesive forces between the polymer and the die wall resulting in slippage leading to flow of the material through the die at the interface. This slip-stick mechanism is continually repeated during the flow process.

However, the question arises as to whether die flow is comparable to the experimental situation. Presumably, although the shearing process is different, the fundamental properties of the material do not change and shear rates in die flow are comparable or in excess of those in the experimental work in this project. The flow behaviour must be assumed to be independent of the applied shear forces and therefore if slippage occurs in die flow it will probably occur in the experiments because it is a basic property of the material to behave in that way.

The conclusion which could be drawn from the above discussion is that the

apparatus was not capable of performing the function required of it because of the properties of the polymer.

The material possibly cannot undergo the continuous deformation assumed under the conditions used. However, only indirect evidence can be offerred in support of this conclusion (i.e. the work of Galt and Maxwell (**37**)) and evidence from work on cone and plate viscometers such as the Weissenberg Rheogonimeter. The maximum shear rate permissable in a cone and plate viscometer depends on the geometry of the platens but is typically of the order of 10 - 20 sec^{-1}. (These experiments were performed at 24 - 61 sec^{-1}.) Above the critical shear rate the material is ejected from between the platens. This effect is known to be due to the elastic nature of the polymer and may be analogous to the effects postulated in the experimental apparatus.

It seems probable, that the sample is not undergoing interlaminar shearing but a type of "plug flow". If plug flow is occurring, then the whole mass of the sample will be moving and a slip-stick mechanism would be operating at the interfaces.

The apparatus would not allow investigation of the flow of the polymer since it was totally enclosed. The techniques attempted failed because they required visual examination of the sample and this was not possible.

Modifications to the apparatus would have been necessary. For

example, use of a split outer cylinder would possibly have enabled the specimen to be removed intact. Results from experiments on the flow behaviour of polymers under the experimental conditions would probably help in the design of future equipment.

Another experimental error which could occur is that of temperature measurements.

Were the temperatures which were measured :-

(a) reliable ?

(b) accurate ?

Reliability, in terms of reproducibility was tested by repeating some experimental runs several times. The temperatures agreed to within $0.5^{\circ}C$.

In addition, thermocouples were always calibrated before use by comparison with a mercury-in-glass thermometer at several temperatures (both being immersed in a constant temperature medium).

The temperatures should be accurate, since the experiments used to measure thermal conductivity and thermal diffusivity (using the rotating apparatus in the static state) were satisfactory, when compared to literature values. The viscous heating experiments were performed on the same apparatus with the same thermocouple locations.

If the temperatures measured in the static state were accurate then it must be assumed that the temperatures measured in the viscous heating experiments were also accurate. The rate of temperature rise in the viscous heating experiments was slightly higher but not so much greater that the response time of the thermocouples would have been different from the static experiments.

5.3.3. Discussion of Assumptions in the Theory

After discussing the apparatus it is now necessary to consider the theory used and the assumptions made in the development.

The first assumption occurs in Equations (35), (36) and (37). (Section 3.4.)

i.e. $$\rho \frac{\partial V_\theta}{\partial t} = \frac{1}{r} \cdot \frac{\partial}{\partial r} (r T_{r\theta}) \qquad \ldots\ldots\ldots (35)$$

$$T_{r\theta} = \eta \left(\frac{\partial V_\theta}{\partial r} \right) \qquad \ldots\ldots\ldots (36)$$

Combining (35) and (36)

$$\rho \frac{\partial V_\theta}{\partial t} = \eta \frac{\partial}{\partial r} \left(\frac{1}{r} \cdot \frac{\partial}{\partial r} (r V_\theta) \right) \qquad \ldots\ldots\ldots (37)$$

The step from (35) to (37) via (36) involves an important assumption which is that apparent viscosity "η" is independent of the radial position "r" in the sample. If the assumption had not been made the results would have been as follows.

$$\rho \frac{\partial V_\theta}{\partial t} = -\frac{1}{r} \cdot \frac{\partial}{\partial r}(r \tau_{r\theta}) \qquad \ldots\ldots\ldots (35)$$

$$= -\frac{1}{r} \cdot \frac{\partial}{\partial r}\left(r \cdot \eta\left(\frac{\partial V_\theta}{\partial r}\right)\right)$$

$$= -\frac{1}{r}\left(r \frac{\partial}{\partial r}\left(\eta \frac{\partial V_\theta}{\partial r}\right) + \eta\left(\frac{\partial V_\theta}{\partial r}\right)\right)$$

$$= -\frac{1}{r}\left(r\left(\eta \frac{\partial^2 V_\theta}{\partial r^2} + \frac{\partial \eta}{\partial r} \cdot \frac{\partial V_\theta}{\partial r}\right) + \eta\left(\frac{\partial V_\theta}{\partial r}\right)\right)$$

$$= -\eta \frac{\partial^2 V_\theta}{\partial r^2} - \frac{\partial \eta}{\partial r} \cdot \frac{\partial V_\theta}{\partial r} - \frac{\eta}{r} \cdot \frac{\partial V_\theta}{\partial r} \qquad \ldots\ldots (35A)$$

The above equation is exactly the same as that obtained by assuming "η" and "r" are independent except for the term $(\partial\eta/\partial r \cdot \partial V_\theta/\partial r)$

The effect of omitting this term can be assessed by considering its magnitude in relation to that of the other terms of the equation in which it appears.

For the first term on the right hand side of the equation :

i.e. $\eta \frac{\partial^2 V_\theta}{\partial r^2}$

it is necessary to know the rate of change of shear rate ($\partial V_\theta/\partial r$) with "r". This can be found by plotting the shear rate profile through the sample.

The shear rate at any point is given by :-

$$\frac{\partial V_\theta}{\partial r} = \frac{a V_a}{b^2 - a^2}\left(\frac{b^2 + r^2}{r^2}\right) \qquad \ldots\ldots\ldots (44)$$

(Section 3.4)

THEORETICAL SHEAR RATE PROFILE IN THE SAMPLE
AT 80 RPM (24 s^{-1}), INITIAL TEMPERATURE = 138.0°C

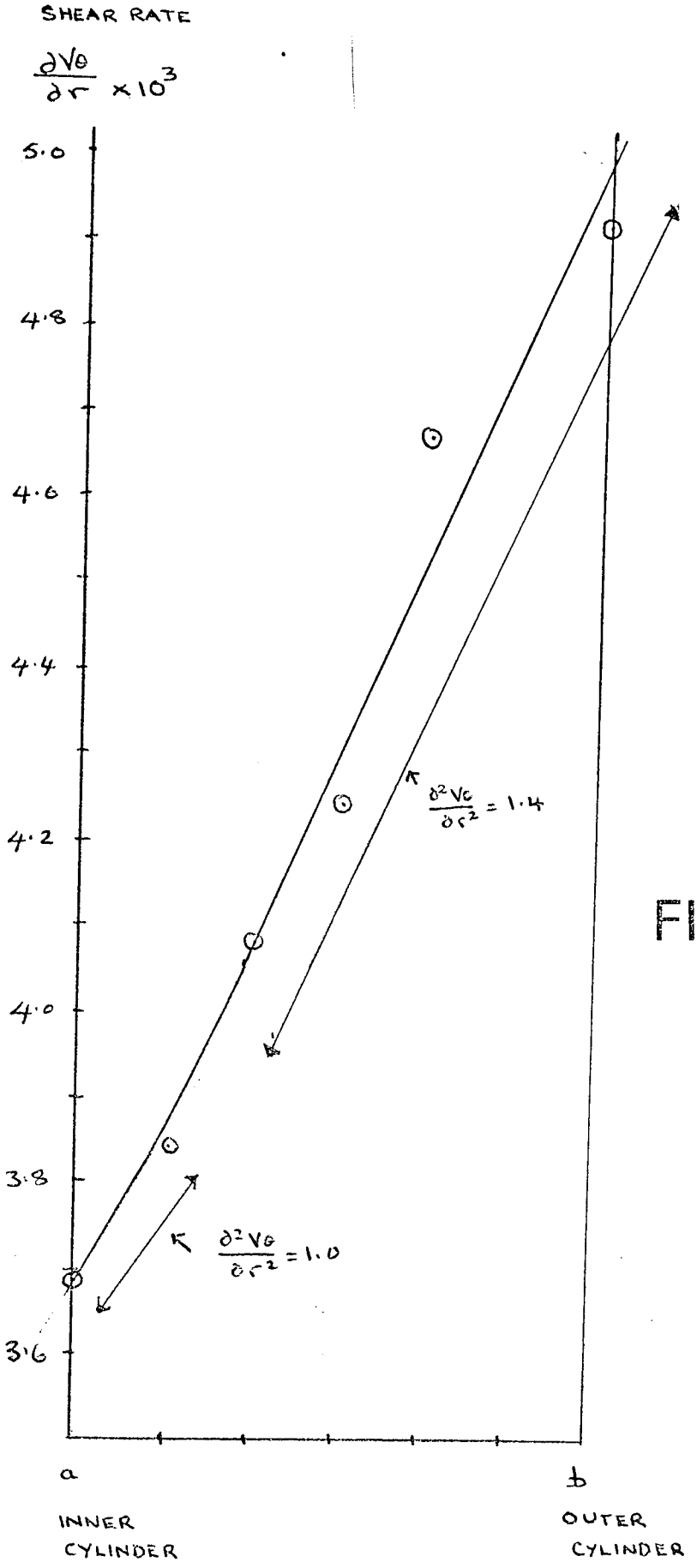

FIG.45.

THEORETICAL VISCOSITY PROFILE IN SAMPLE

AFTER 30 SECONDS

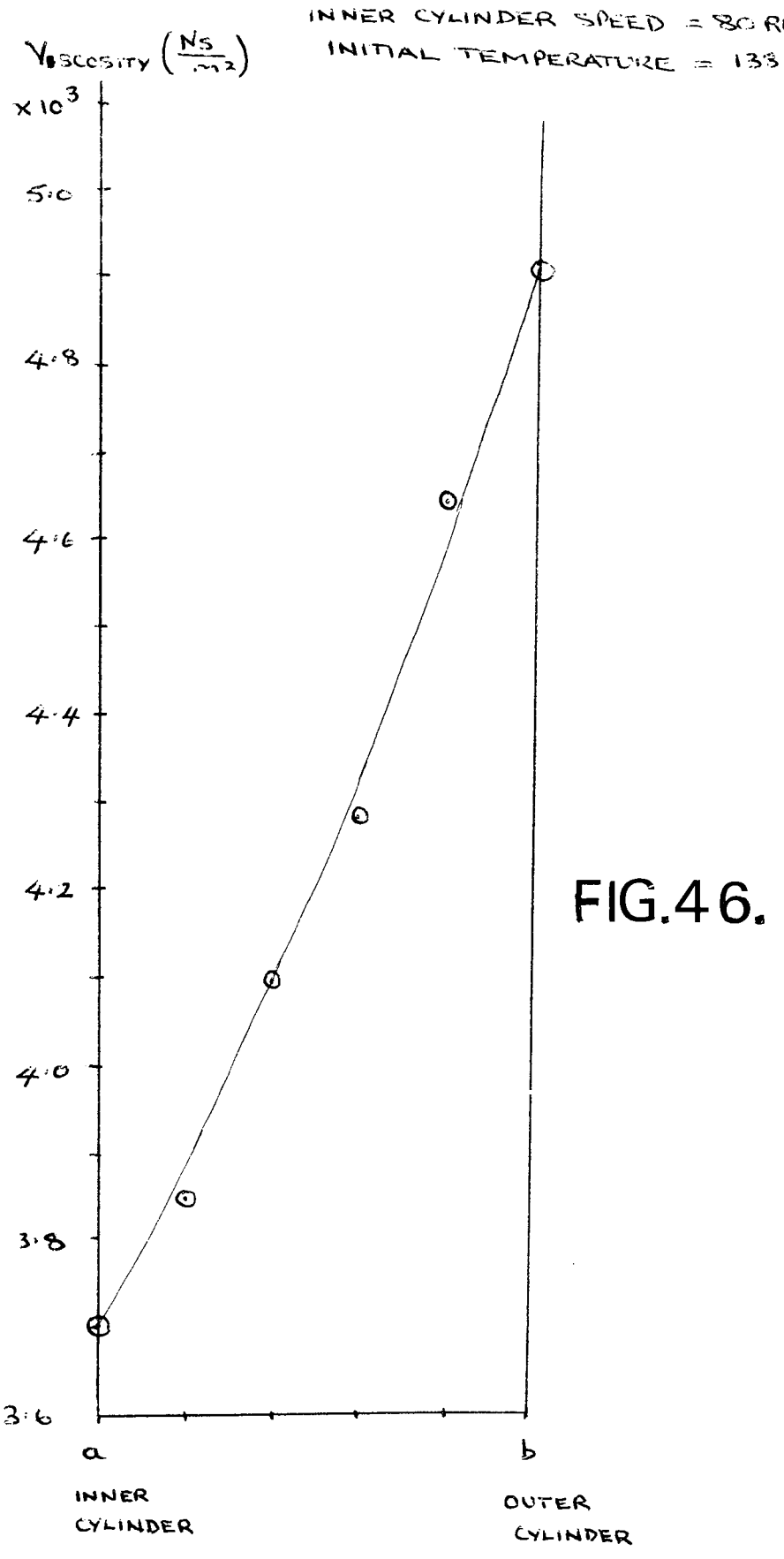

FIG.46.

The above equation was used to obtain the figure in Table (25). The values quoted are for 80 r.p.m. cylinder speed since this was the only speed where reliable torque measurements were taken.

From the slope of the graph shown in Figure (45) the value of $\left(\frac{\partial^2 V_\theta}{\partial r^2}\right)$ can be obtained. The values used are shown in Figure (45).

The value of viscosity at any point is also required and this can be calculated from :-

$$\eta = K_o \left(\frac{\partial V_\theta}{\partial r}\right)^{n-1} B.e^{A/(T+273.2)} \qquad \ldots\ldots\ldots(40)$$

(Section 3.4)

K_o = 1.7×10^4 $N/_m 2$

B = 3.85×10^{-4}

A = 2550

n = 0.469

The values of "T" were obtained from Figure (41). Table (25) shows the values obtained for viscosity and for the whole term under consideration.

For the second term of equation (35A) it is necessary to plot the viscosity profile in the sample to obtain $\left(\frac{\partial \eta}{\partial r}\right)$. The temperature profile used was that in Figure (41).

The viscosity values have already been calculated above. The resultant graph is shown in Figure (46). Table (27) shows the results.

TABLE (25)

Radial Distance (m) $\times 10^{-2}$	Shear Rate $\left(\frac{\partial V_\theta}{\partial r}\right)$ (s^{-1})	$\left(\frac{\partial^2 V_\theta}{\partial r^2}\right)$ * $\times 10^3$	Viscosity(η) $N_s/m^2 \times 10^3$	$\eta\left(\frac{\partial^2 V_\theta}{\partial r^2}\right)$ $\times 10^6$
0.47	28.4	1.4	3.7	5.18
0.504	26.2	1.4	3.85	5.39
0.538	23.8	1.4	4.10	5.74
0.572	22.4	1.4	4.29	6.00
0.606	20.8	1.0	4.65	4.24
0.64	19.8	1.0	4.92	4.5

* From slope of graph in Figure (4-5) assuming sample thickness to be unit length.

TABLE (26)

Radial Distance (m) $\times 10^{-2}$	$\eta\left(\frac{\partial V_\theta}{\partial r}\right)$ $\times 10^{7}$
0.470	2.24
0.504	2.00
0.538	1.82
0.572	1.68
0.606	1.59
0.640	1.52

TABLE (27)

Radial Distance (m) $\times 10^{-2}$	Shear Rate $\left(\frac{\partial V_\theta}{\partial r}\right)$ (s^{-1})	Viscosity(η) $N_{s/m^2} \times 10^{3}$	$\left(\frac{\partial \eta}{\partial r}\right)$ $\times 10^{2}$	$\left(\frac{\partial \eta}{\partial r} \cdot \frac{\partial V_\theta}{\partial r}\right)$ $\times 10^{4}$
0.47	28.4	3.7	5.17	1.47
0.504	26.2	3.85	"	1.36
0.538	23.8	4.10	6.80	1.62
0.572	22.4	4.29	8.44	1.89
0.606	20.8	4.65	"	1.75
0.64	19.8	4.92	"	1.67

Finally, the last term

$$\frac{\eta}{r}\left(\frac{\partial V_\theta}{\partial r}\right)$$

is relatively easy to calculate since all the necessary values have already been calculated.

Comparing the magnitudes of the three terms in equation (35A) it can be seen that the omission of ($\partial\eta/\partial r \cdot \partial V_\theta/\partial r$) is of little consequence.

Range of values for	$\eta\left(\frac{\partial^2 V_\theta}{\partial r^2}\right)$	$4.4 - 6.0 \times 10^6$
" " " "	$\left(\frac{\partial \eta}{\partial r} \cdot \frac{\partial V_\theta}{\partial r}\right)$	$1.5 - 1.7 \times 10^4$
" " " "	$\left(\eta/r \cdot \frac{\partial V_\theta}{\partial r}\right)$	$1.5 - 2.2 \times 10^7$

(See Table (26))

Expressed as a percentage the term ($\partial\eta/\partial r \cdot \partial V_\theta/\partial r$) is only about 1% of the next smallest term.

i.e. $10^4/10^6 \cdot 100 = 1\%$

It appears, therefore, that the original assumption of " η " independent of " r " was not serious in that its affect on the velocity profile would be small.

The second assumption in the theory involves the separation effects of the temperature and radial position on the velocity profile. The decoupling of these effects was produced by assuming :-

a) $\frac{\partial V_\theta}{\partial t} = 0$ b) K = constant

The first assumption states there is no change in velocity with time at any point in the sample. This is perfectly reasonable at the boundary surfaces. At the inner cylinder surface the velocity is equal to that of the rotating cylinder and at the outer cylinder it is zero.

During the experiment the polymer temperature is rising and therefore the viscosity must be falling. From the power law equation :

$$\tau = \eta_a \dot{\gamma}$$

τ = shear stress

η_a = apparent viscosity

$\dot{\gamma}$ = shear rate

if "η_a" falls either, or both, "τ" and "$\dot{\gamma}$" must also change.

Torque measurements at 80 r.p.m. indicated no reduction in torque in the duration of the experiments. It can, therefore, be assumed that shear stress (τ) does not change consequently "$\dot{\gamma}$" must increase to balance the effects of the viscosity reduction. In order to increase the shear rate the velocity of the melt must increase in the areas away from the boundary surfaces, Figure (47) illustrates how this could occur. These conditions would lead to the theory underestimating the actual viscous heating effect.

This assumption ($\partial V_0/\partial t = 0$) therefore, has no bearing on the difference

POSSIBLE EFFECT OF A CHANGE IN SHEAR RATE WITH A CONSTANT INNER CYLINDER SPEED

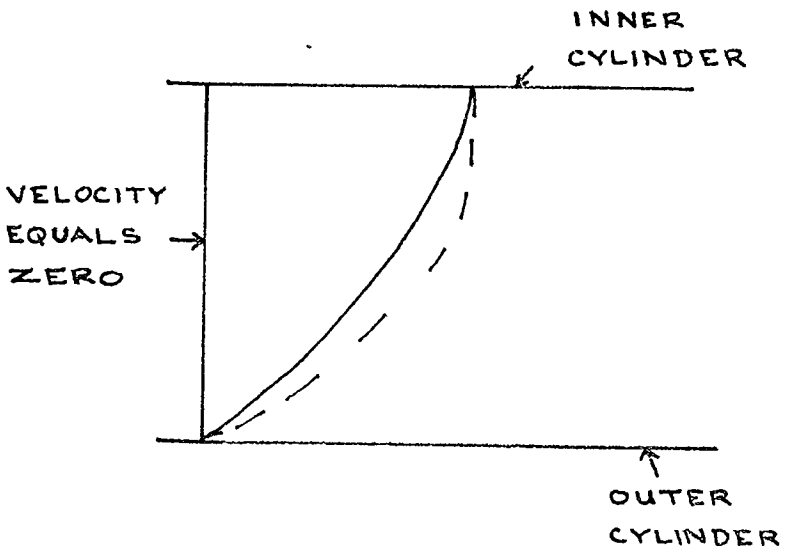

INITIAL VELOCITY PROFILE IS SHOWN AS FULL LINE
NEW PROFILE SHOWN AS DOTTED LINE

FIG.47.

between experimental and theoretical results observed in this project. Assumptions in the theory need to overestimate the heating effect if they are to explain the observed differences.

Mathematically, if it had not been assumed that :

$$\partial V_\theta / \partial t = 0$$

but that $\partial V_\theta / \partial t$ = constant.

Then : equation (41) would have been :-

$$\left(\frac{\partial V_\theta}{\partial r}\right)^{n-1} \frac{\partial}{\partial r}\left(\frac{1}{r} \cdot \frac{\partial}{\partial r}\left(r . V_\theta\right)\right) = C_o$$

or $$\left(\frac{\partial V_\theta}{\partial r}\right)^{n-1} \frac{\partial}{\partial r}\left(\frac{1}{r} \frac{\partial}{\partial r}\left(r . V_\theta\right)\right) - C_o = 0$$

Then $\left(\frac{\partial V_\theta}{\partial r}\right)^{n-1} \neq 0$ for r = a to r = b.

Therefore :

$$\frac{1}{r} \frac{\partial}{\partial r}(r V_\theta) = C_o r$$

$$r V_\theta = \frac{C_o r^3}{3} + C_1$$

Now at r = a $V_\theta = V_a$

$$a V_a = \frac{C_o a^3}{3} . C_1$$

at $r = b \quad V_\theta = o$

$$0 = \frac{C_o b^3}{3} + C_1$$

$$\therefore \quad C_1 = - C_o \frac{b^3}{3}$$

$$a\, Va = \frac{C_o}{3} (b^3 - a^3)$$

$$r\, V_\theta = \frac{C_o}{3} (b^3 - r^3)$$

$$\therefore \quad \frac{V_\theta}{Va} = \frac{a(b^3 - r^3)}{r(b^3 - a^3)}$$

Comparing the velocity profiles from equation (43) and from the above equation :

TABLE (28)

Radial Distance (m) x 10^{-2}	Velocity (m/s) Equation(43)	Velocity m/s Equation above
0.47	0.040	0.040
0.504	0.030	0.032
0.538	0.022	0.023
0.572	0.015	0.015
0.606	0.007	0.008
0.64	0.00	0.00

It can be seen that the assumption leads to a slightly lower result for the velocity. This as previously deduced would lead to an underestimation of viscous heating. However, the difference between the two can be seen to be small.

The second assumption was that "K" = constant. This can be seen to be false by considering Figure (31) where "K" is given by the intercept on the log axis. From the graph in Figure (31) it is obvious that "K" is sensitive to temperature. If it were constant then it follows that the temperature of the melt must not rise which is again untrue.

However, the assumption was of no significance in affecting the compuied velocity profile.

Equation (37) states :-

$$\rho \frac{\partial V_\theta}{\partial t} = \eta \frac{\partial}{\partial r}\left(\frac{1}{r}\frac{\partial}{\partial r}(rV_\theta)\right)$$

$$= K\left(\frac{\partial V_\theta}{\partial r}\right)^{n-1} \cdot \frac{\partial}{\partial r}\left(\frac{1}{r}\frac{\partial}{\partial r}(rV_\theta)\right)$$

Assuming only $\frac{\partial V_\theta}{\partial t} = 0$

Then $K\left(\frac{\partial V_\theta}{\partial r}\right)^{n-1} \frac{\partial}{\partial r}\left(\frac{1}{r}\cdot\frac{\partial}{\partial r}(rV_\theta)\right) = 0$

Now $K\left(\frac{\partial V_\theta}{\partial r}\right)^{n-1} \neq 0$ since it is apparent viscosity.

$\therefore$ $\frac{1}{r}\cdot\frac{\partial}{\partial r}(rV_\theta) = 2C_1$

Therefore the derived equation for velocity profile is unchanged (i.e. equation(43).)

During the course of deriving equation (43), it was assumed that the boundary velocities at the inner and outer cylinders were "Va" (i.e. the velocity of the inner cylinder) and zero at the stationary outer cylinder. These assumptions would not be true if any slippage occurred between metal and polymer at either surface. As already mentioned, no experimental evidence could be obtained to determine if such motion occurred. Die flow experiments by Galt and Maxwell (37) did show that non-zero velocities could be observed in polymers very close to the die wall where the material would be expected to be static. It was concluded that this motion was due to slippage at the boundary surface in the die and was an inherent part of the flow process of the polymer. This being so, the process would occur in die flow and in the shearing experiments.

The precise nature of the correction required to describe the polymer exactly is not known since rheological theory for polymers is not yet sufficiently advanced (38).

If the boundary velocities were not as assumed, then how would this affect the theory? At the inner cylinder surface the velocity is "Va" and presumably it is safe to assume the melt does not exceed the velocity of that surface.

There could, however, be a slip-stick mechanism operating, which would mean the melt was sometimes at rest and sometimes moving at the same speed as the inner cylinder, or at some slower speed. This would result in an oscillating shear stress and not a continuous shear stress as assumed in the theory. The average shear

rate would therefore be lower than anticipated. An error such as this could contribute to an overestimation of viscous heating by the theory.

Considering the outer cylinder boundary surface the object of the experiments was to produce interlaminar shear within the polymer and not "plug type flow" of the whole mass.

If a slip-stick mechanism were predominant at this boundary then this would almost certainly lead to a plug flow effect with the whole mass of polymer shifting relative to the stationary cylinder.

The result of course would be very little interlaminar shear and presumably very small temperature rise such as those observed.

Viscous heating in sample at 80 r.p.m. and an initial temperature of 138°C

(viscous heating calculated from equation (4.7) section 3.4.)

TABLE 29

Radial Distance (m)	Viscous Heating			
	$w/m^3 (\times 10^5)$	$w/m (\times 10^3)$	$J/s (\times 10^3)$	$J (\times 10^3)$
0.47×10^{-2}	4.04	2.91	0.59	17.7
$0.504 \times$ "	3.22	2.32	0.47	14.1
$0.538 \times$ "	2.66	1.92	0.39	11.7
$0.572 \times$ "	2.11	1.52	0.31	9.3
$0.606 \times$ "	1.75	1.26	0.256	7.7
$0.64 \times$ "	1.44	1.04	0.211	6.3

Specific heat of polymer = 0.7 cal/g°C. (I.C.I. monograph. "properties of alkathene")

Volume of sample = $1.7 \times 10^{-5}\ m^3$

Density of sample = $0.77\ g/cm^3$ at $140^{\circ}C$

(I.C.I. monograph "properties of alkathene")

$\therefore$ Weight of sample = $1.7 \times 10^{-5} \cdot 0.77\ g/cm^3 \cdot \frac{10^6\ cm^3}{m^3}$

$$= 13.1\ g$$

$\therefore$ Thermal capacity of sample = $13.1\ g \cdot 0.70 \frac{cal}{g.^{\circ}C} \cdot \frac{J}{0.24\ cal}$

$$= 38.2\ J/K$$

Thermal capacity of cylinders = $190 + 240\ J/K$

$$= 410\ J/K$$

Total thermal capacity = $410 + 38.2$

$$= 448\ J/K$$

TABLE (16) TEMPERATURE RISES DUE TO VISCOUS HEATING

Theoretical Temperature * Rise °C	Experimental Temperature ** Rise °C
~ 26	2
~ 26	-) Experimental
~ 26	-) Temperatures
~ 25	-) could only be
~ 23	-) measured at the
~ 20	0.8 boundaries

* Results obtained from Table (14).

** Results obtained from Table (12).

$2^{\circ}C$ rise at the inner cylinder boundary requires :-

$$2 \times 448 \text{ J} = \underline{\underline{896 \text{ J}}}$$

i.e. $\underline{0.896 \times 10^3 \text{ J}}$

Therefore, we can determine the degree of slip at this boundary which would result in the above viscous heating.

No slip	17.7×10^3 J	(TABLE. 29)
50% slip	8.85×10^3 J	
75% slip	4.42×10^3 J	
90% slip	1.77×10^3 J	
95% slip	0.88×10^3 J	(c.f. 0.896×10^3 J)

Therefore, on this basis there could be only 5% of the theoretically available mechanical energy actually transformed into heat.

At the outer cylinder the energy required to raise the temperature by the experimentally observed amount is :-

$$0.5 \times 448 \text{ J} = 224 \text{ J}$$

i.e. 0.224×10^3 J

No slip	6.34×10^3 J	(TABLE 29)
50% slip	3.17×10^3 J	
75% slip	1.58×10^3 J	
90% slip	0.634×10^3 J	
95% slip	0.317×10^3 J	
96% slip	0.254×10^3 J	(c.f. 0.224×10^3 J)
97% slip	0.19×10^3 J	

Therefore, at this surface approximately 4% of the available energy is transformed to heat.

If the theory is correct then it would appear that there is almost total slippage at both surfaces.

The rheological theory used in this project to describe the viscous heating and flow behaviour of the polymer was based on the power law. This is probably the most usual rheological equation for plastics technologists to use. However, an inherent assumption of the power law is that the melt is purely viscous. This means

the polymer should exhibit no elasticity and all the energy of deformation supplied to the material would be converted to heat. The assumption is in error since all polymers exhibit some degree of elasticity except at high temperatures (region of liquid flow, see section 2,5).

The consequence of using the power law will therefore be to over estimate the viscous heating effect. However, this could not be the explanation of the difference between the results and theory in this case. The difference is much too large as can be seen from the following argument.

Temperature rise of inner cylinder = 27°C

Temperature rise of outer cylinder = 20°C

(From Figure (36))

Energy input from viscous heating to inner cylinder = (thermal capacity of inner cylinder + polymer sample) x (temperature rise of inner cylinder)

$= 27\ (190 + 38)\ J$

$= 27 \times 228\ J$

$= 6.15 \times 10^3\ J$

Similarly for the outer cylinder :-

Energy input $= 20\ (240 + 38)$

$= 20 \times 278$

$= 5.56 \times 10^3\ J$

The difference between the theoretical and experimental temperature rise for the inner and outer cylinders multiplied by the thermal capacities as above gives the energy stored.

Energy stored at inner cylinder surface = (27 - 2) . 228

$= 5.7 \times 10^3$ J

Energy stored at outer cylinder surface = (20 - 0.5) . 278

$= 5.42 \times 10^3$ J

If it is assumed that the polymer used in the experiments was a rubber then from the following equation the resilience of the material can be found.

$$H = (100 - r)\, E/100$$

where H = heat generated

r = resilience (%) (a measure of the ratio of elastic to viscous nature of the material)

E = energy input

The above equation really applies to a single blow or bounce of a rubbery material and not to the continuous deformation which the experiments produce. The experiments are therefore an extreme case but the equation should be sufficiently valid to indicate if the energies involved are realistic.

In this case : $H = 6.15 \times 10^3 - 5.7 \times 10^3$

(for the inner cylinder)

$= 0.45 \times 10^3$ J

$E = 6.15 \times 10^3$ J

$\therefore \quad 0.45 \times 10^3 = (100 - r) \frac{6.15 \times 10^3}{10^2}$

$= (100 - r)\, 6.15 \times 10$

$r = 100 - \frac{46.0}{61.5}$

$= 100 - 7.5$

$r = 92.5\ \%$

At the outer cylinder surface :-

$H = 5.56 \times 10^3 - 5.42 \times 10^3$

$= 0.14 \times 10^3$ J

$E = 5.56 \times 10^3$ J

$0.14 \times 10^3 = (100 - r) \frac{5.56 \times 10^3}{10^2}$

$r = 100 - \frac{140}{55.6}$

$= 100 - 2.52$

$r = 97.5\%$

The material, would therefore need to have a resilience of about 95% to satisfy the energy conditions given above. This represents an extremely high level of elasticity, even for a rubber, and is certainly impossible to achieve with a non-elastomeric polymer. The use of the power law, as the rheological model, does ignore the elasticity of the material and will contribute to some extent to the difference in the results, but it cannot be the total explanation, or indeed, the most important one.

Summarising, the evidence for slippage is :-

1. Calculations show about 95% slippage, at both surfaces, would account for the difference between the experimental and theoretical temperature rises.

2. A keyed outer cylinder shows a significant increase in temperature rise based on the original temperature rise. However, the magnitude is still small compared to theory.

3. Galt and Maxwell (37) showed that a slip stick mechanism was the normal mechanism of flow through a die for polymers. A similar mechanism should operate under the experimental conditions, since the flow is not dependent on the method of application of the deformational force. The polymer, in both cases, is being induced to flow in contact with a metallic surface.

4. Low torque values are obtained from experiments. The theoretical torque required to shear the polymer at a given shear rate can be calculated from its reheological properties as was shown in section 4.5., page 71.

The evidence against : -

1. The very good adhesion which was observed when the apparatus was dismantled.

Overall the weight of evidence suggests that slippage is occurring and with the experimental apparatus is was not possible to prevent it. Further experimental work would be necessary and apparatus suitable for such work would need to be designed.

6.0 CONCLUSIONS

1. The temperature rise due to viscous heating was very much lower than anticipated.

   The evidence obtained suggests that the polymer sample is not being subjected to the required shear rate. This is thought to be due to slippage at the boundary surfaces of the specimen. This type of behaviour may be typical of polymers (and viscoelastic materials in general) and could be related to the elastic characteristics of the material.

2. The theory which was developed appears to be satisfactory. The approximations made were shown not to contribute significantly to the difference between the predicted and observed results.

3. The theory predicts that internal heating (viscous heating) is a better method of raising the temperature of the sample than is external heating (from band heaters, etc.).

   The prediction is also made that the temperature rise produced by viscous heating becomes extremely high at moderate shear rates (202 r.p.m. - 61 s^{-1}). There is also evidence of an unsteady temperature profile, at least, for the initial 15 - 30 seconds which may be a reflection of the low conductivity of the polymer melt.

Viscous heating is, nevertheless, a desirable form of heating since it will lead to much more rapid heating and melting of low density polyethylene and presumably other polymers too. The disadvantage appears to be the control of the temperature rise.

4. More work is required to investigate the flow behaviour of polymers being sheared in the same way as in the experiments described in this thesis. When the flow behaviour is understood then subsequent investigation of viscous heating effects would be made very much easier and would be very helpful in the design of any future model apparatus.

APPENDIX 1.

FRINGED MICELLE CONCEPT OF POLYMER CRYSTALLISATION

X-ray studies of crystalline polymers show broad and diffuse reflections compared to those from well developed simple crystals. Diffraction theory indicates that this broadening can arise from either small crystallite size or the presence of lattice defects but the patterns from polymers are usually too weak to permit discrimination between these possibilities. Historically, the hypothesis of small crystallite size was thought to be most probable.

Rough estimates based on this assumption indicated that crystalline size was usually only a few hundred angstroms. Diffuse background scatter suggested the co-existence of an appreciable amorphous fraction. It was suggested that polymer chains were aligned over distances corresponding to the crystallite dimensions at various points along the molecule. Since the molecules are long the remaining maligned material constitutes the amorphous regions. Figure (48) shows the sort of arrangement which the concept requires. It will be noticed that one molecular chain can form several crystallites.

This theory was popular for many years but with the discovery of polymer single crystals and spherulites it was gradually superceeded and today spherulitic theory is more popular. Further discussion of these theories is beyond the scope of this work.

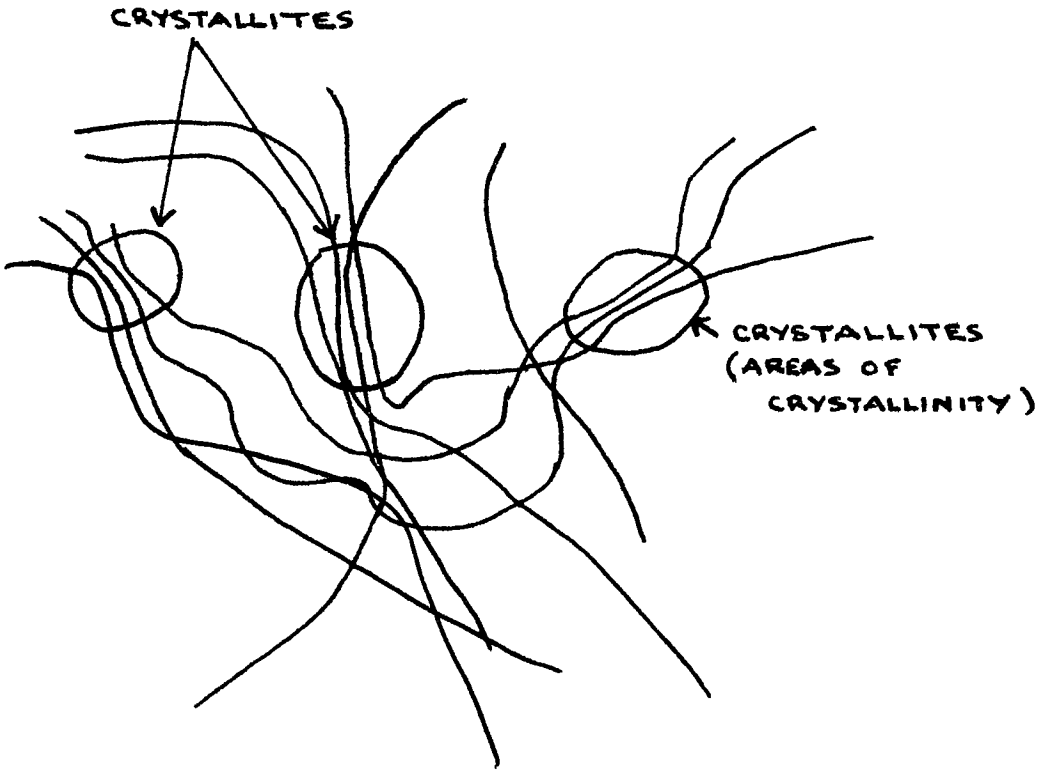

FIGURE (48) FRINGED MICELLE THEORY OF POLYMER CRYSTALLISATION

APPENDIX 2.

SIMPLIFIED FLOW DIAGRAM FOR SIMPLEX OPTIMISATION PROGRAM

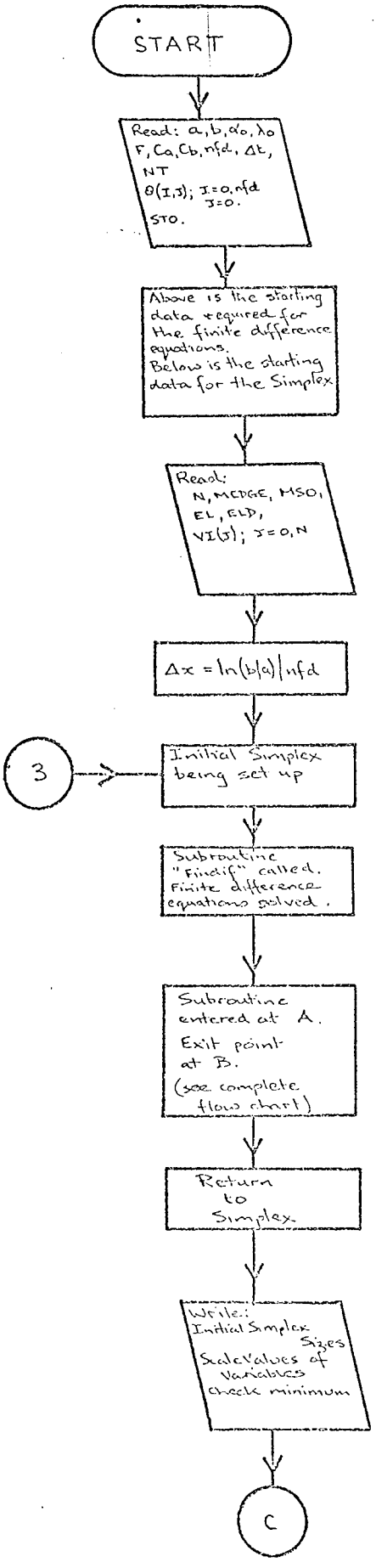

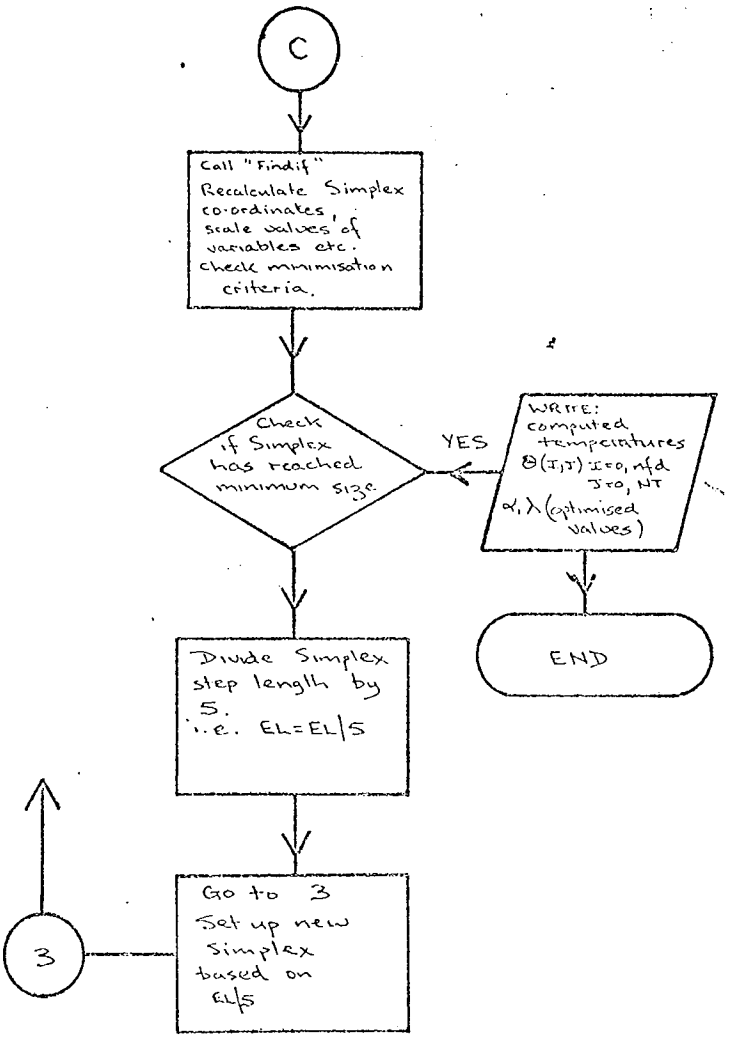
C
Call "Findif"
Recalculate Simplex co-ordinates, scale values of variables etc.
Check minimisation criteria.
Check if Simplex has reached minimum size
YES
WRITE: computed temperatures
Θ(I,J) I=0, nfd
J=0, NT
α, λ (optimised values)
END
Divide Simplex step length by 5.
i.e. EL=EL/5
Go to 3
Set up new Simplex based on EL/5
3

COMPLETE FLOW DIAGRAM FOR SIMPLEX OPTIMISATION AND FINITE DIFFERENCE SOLUTION TO HEAT CONDUCTION SITUATION

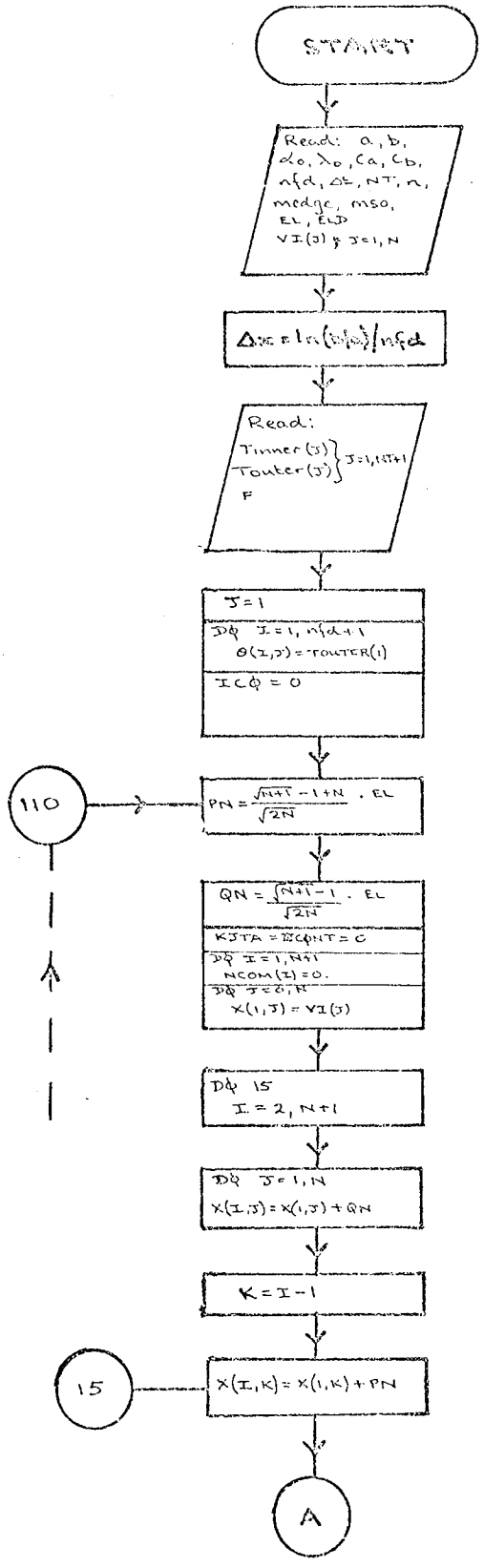

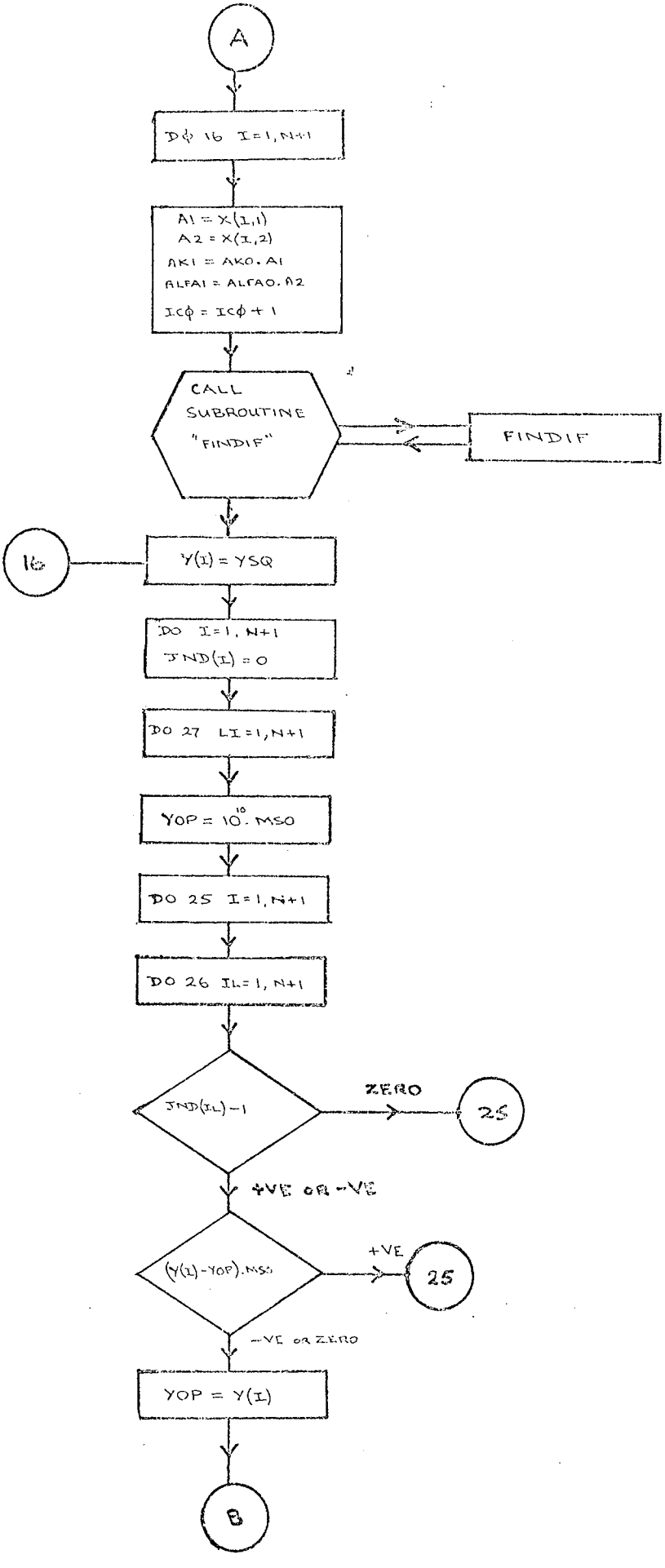
A
DO 16 I=1,N+1
A1 = X(I,1)
A2 = X(I,2)
AK1 = AK0. A1
ALFA1 = ALFA0. A2
IC0 = IC0 + 1
CALL SUBROUTINE "FINDIF"
FINDIF
16
Y(I) = YSQ
DO I=1, N+1
JND(I) = 0
DO 27 LI=1,N+1
YOP = 10^10. MS0
DO 25 I=1,N+1
DO 26 IL=1, N+1
JND(IL)-1
ZERO
25
+VE OR -VE
(Y(I)-YOP).MS0
+VE
25
-VE OR ZERO
YOP = Y(I)
B

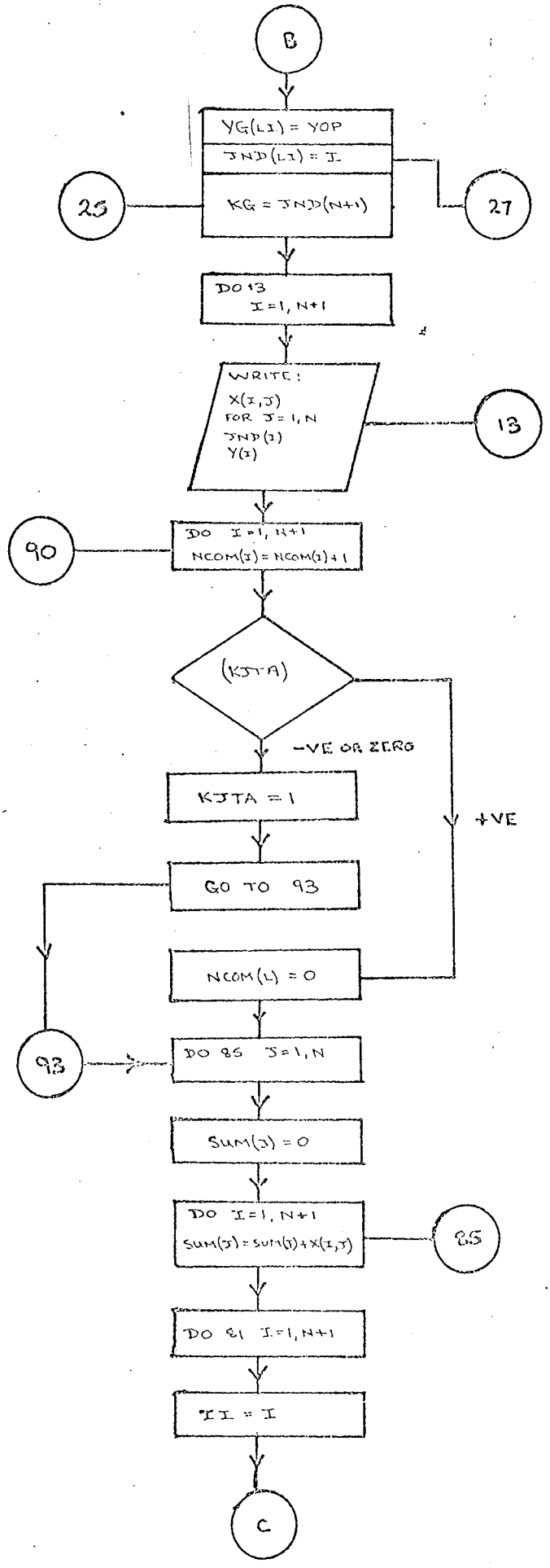
B
YG(LI) = YOP
JND(LI) = I
25
KG = JND(N+1)
27
DO 13
I=1, N+1
WRITE:
X(I,J)
FOR J = 1, N
JND(J)
Y(J)
13
90
DO I=1, N+1
NCOM(I) = NCOM(I)+1
(KJTA)
-VE OR ZERO
+VE
KJTA = 1
GO TO 93
NCOM(L) = 0
93
DO 85 J=1, N
SUM(J) = 0
DO I=1, N+1
SUM(J) = SUM(J)+X(I,J)
85
DO 81 I=1, N+1
II = I
C

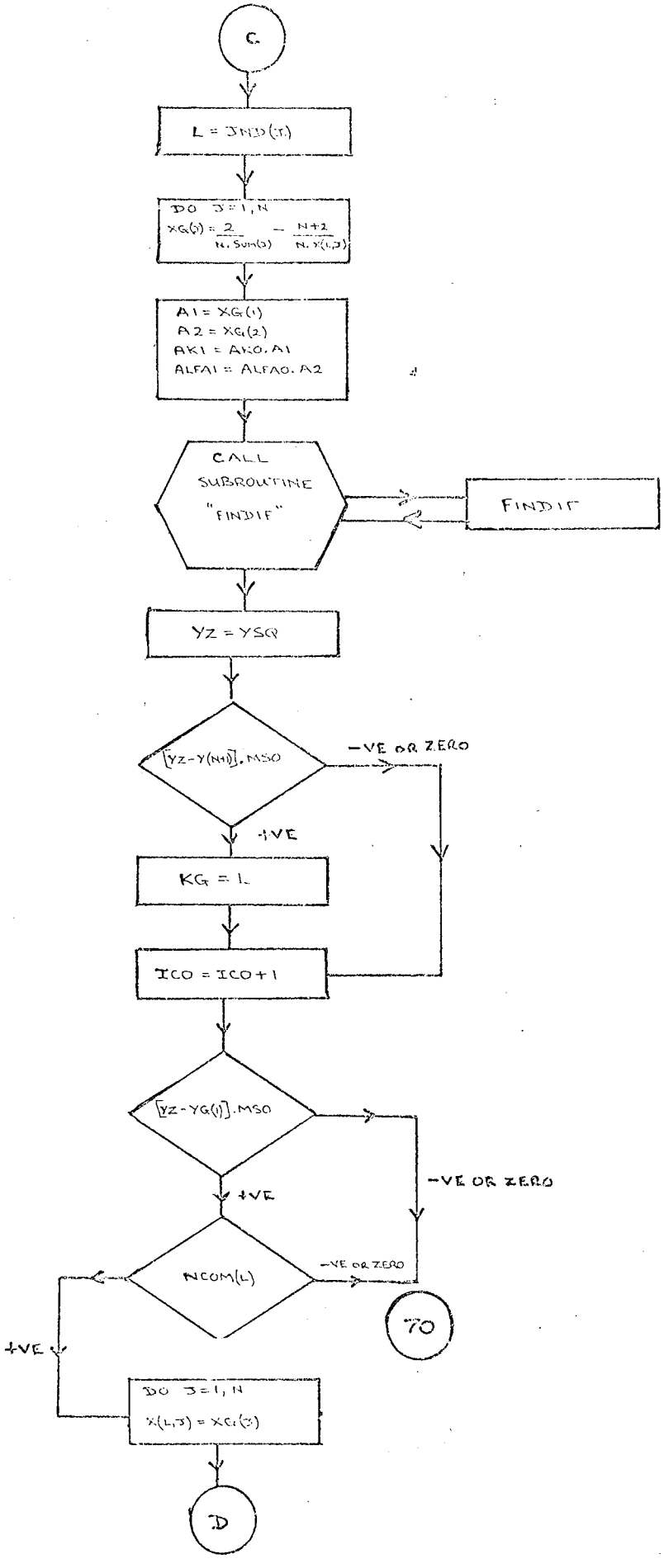
C
L = JND(I)
DO J=1,N
XG(J) = 2 / N.Sum(J) - N+2 / N.X(L,J)
A1 = XG(1)
A2 = XG(2)
AK1 = AK0.A1
ALFA1 = ALFA0.A2
CALL SUBROUTINE "FINDIF"
FINDIF
YZ = YSQ
[YZ-Y(NH)].MSO
-VE OR ZERO
+VE
KG = L
ICO = ICO+1
[YZ-YG(1)].MSO
-VE OR ZERO
+VE
NCOM(L)
-VE OR ZERO
70
+VE
DO J=1,N
X(L,J) = XG(J)
D

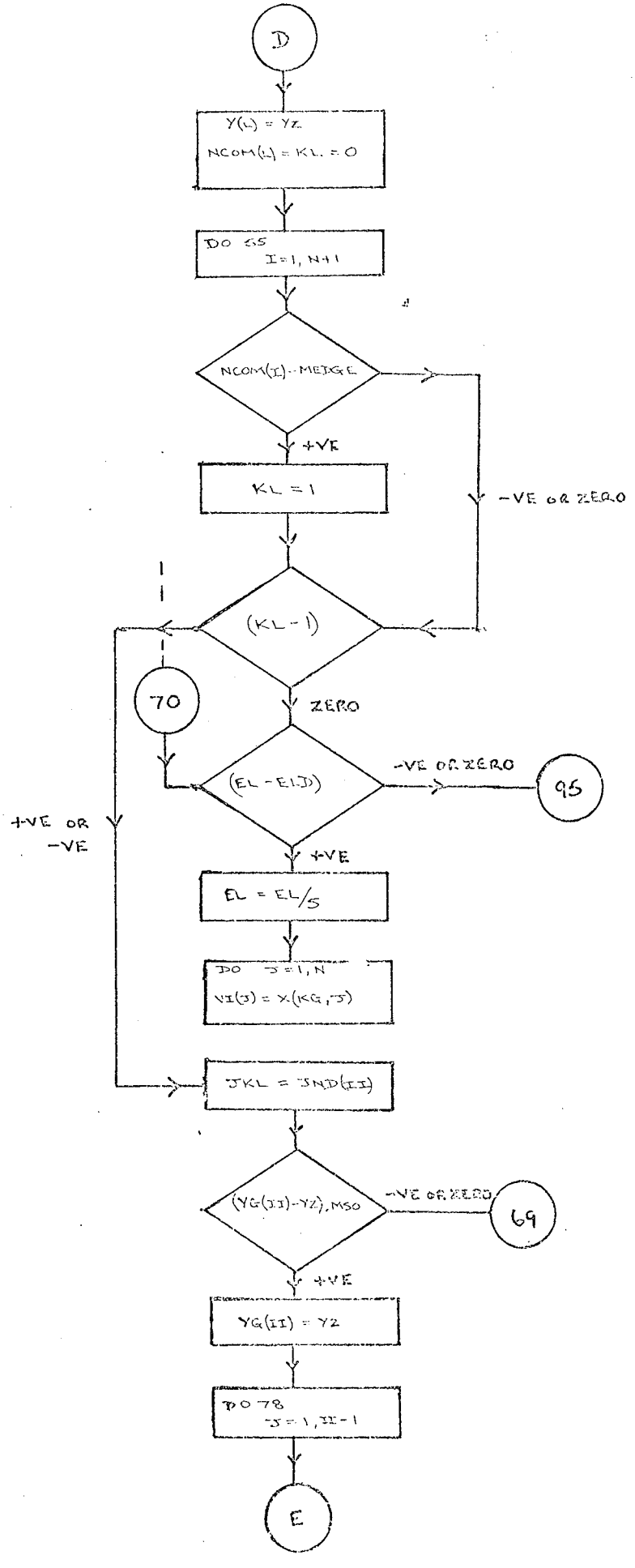
D
Y(L) = YZ
NCOM(L) = KL. = 0
DO 65
I=1, N+1
NCOM(I)-MERGE
+VE
-VE OR ZERO
KL = 1
(KL-1)
70
ZERO
(EL-ELJ)
-VE OR ZERO
95
+VE OR
-VE
+VE
EL = EL/5
DO J=1, N
VI(J) = X(KG, J)
JKL = JND(II)
(YG(II)-YZ), MSO
-VE OR ZERO
69
+VE
YG(II) = YZ
DO 78
J=1, II-1
E

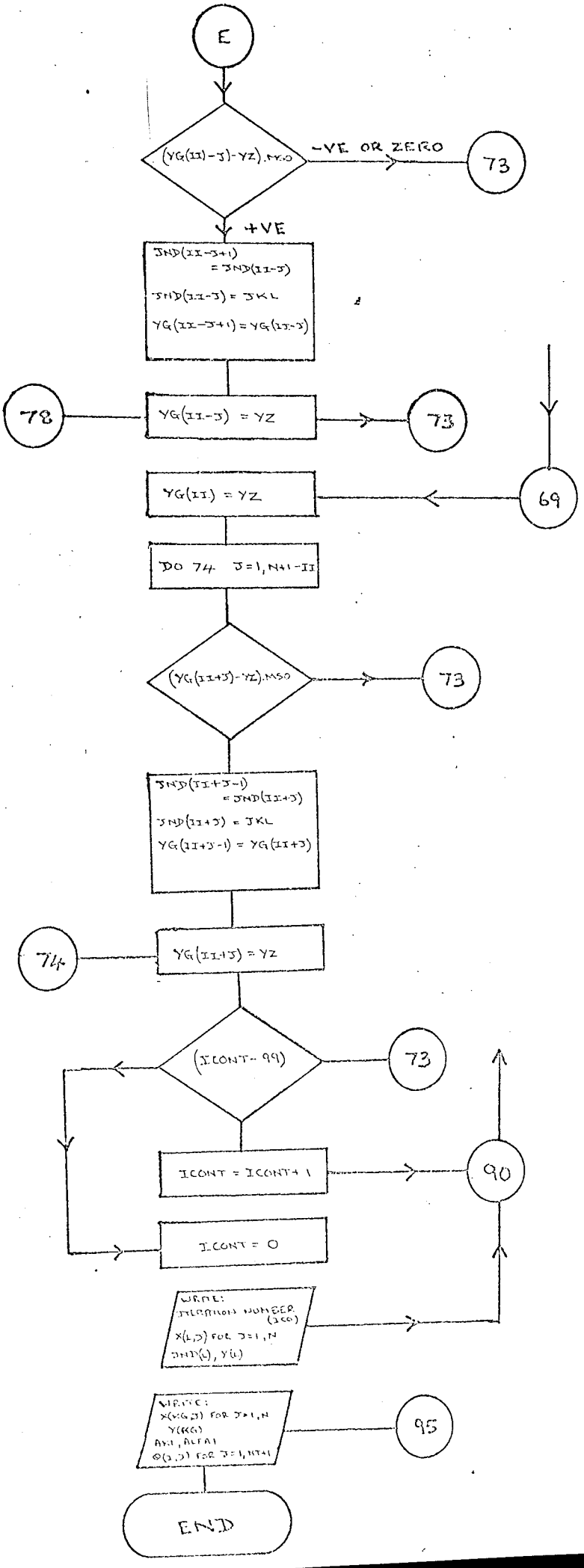
E
(YG(II)-J)-YZ).MI
-VE OR ZERO
73
+VE
JND(II-J+1) = JND(II-J)
JND(II-J) = JKL
YG(II-J+1) = YG(II-J)
78
YG(II-J) = YZ
73
69
YG(II) = YZ
DO 74 J=1,N+1-II
(YG(II+J)-YZ).MI
73
JND(II+J-1) = JND(II+J)
JND(II+J) = JKL
YG(II+J-1) = YG(II+J)
74
YG(II+J) = YZ
(ICONT-99)
73
ICONT = ICONT+1
90
ICONT = 0
WRITE:
ITERATION NUMBER (ICO)
X(L,J) FOR J=1,N
JND(L), Y(L)
WRITE:
X(NG,J) FOR J=1,N
Y(NG)
AXI, ALFAI
O(J,J) FOR J=1,NT+1
95
END

FLOW DIAGRAM FOR GAUSSIAN ELIMINATION

(SUBROUTINE "FINDIT" FOR SIMPLEX PROGRAM)

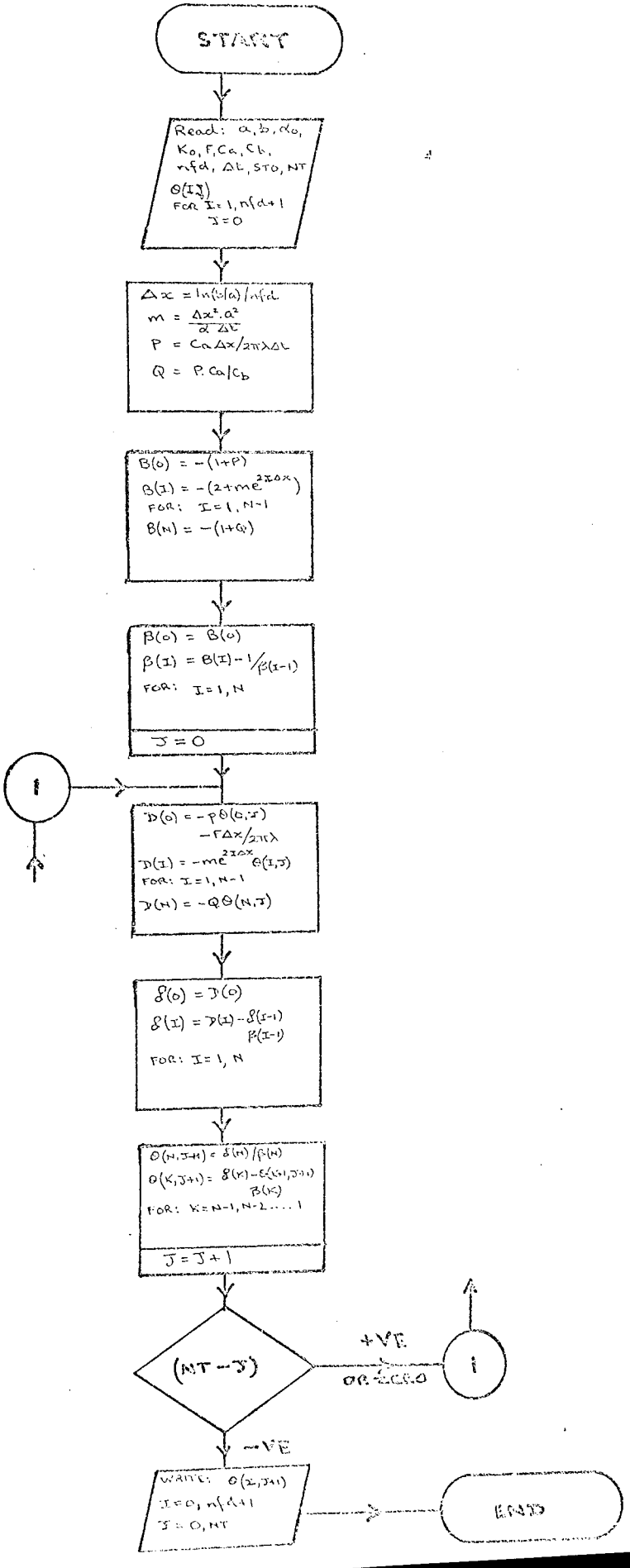

COMPUTER PROGRAM
(HEAT CONDUCTION)

```
      MASTER SIMPLEX
      INTEGER DT
      DIMENSION X(10,11),V1(10),Y(11),NCOM(11),JND(11),SUM(10),
                                                    XG(10),
     1 YG(11)
      COMMON THETA(30,45),TINNER(45),TOUTER(45),DX,DT,AR,CA,
                                                    CB,F,NFD,NT,
     1SLOPE(10),FI(10)
 1000 FORMAT(7F0.0)
      READ(1,1000)  AR,BR,ALFAO,AKO,F,CA,CB
 1001 FORMAT(310)
      READ(1,1001) NFD,DT,NT
      DX=ALOG(BR/AR)/NFD
      READ(1,250)N,MEDGE,MSO,EL,ELD
  250 FORMAT(315,2F10.5)
      READ(1,300)(VI(J),J=1,N)
  300 FORMAT(2F0.0)
      JCO=0
  109 CONTINUE
 1002 FORMAT(6F0.0)
      READ(1,1002)(TINNER(J),J=1,NT+1)(TOUTER(J),J=1,NT+1)
      J=1
      DO 12 I=1,NFD+1
   12 THETA(I,1)=TOUTER(J)+(TINNER(J)-(TOUTER(J))*(NFD-(I-1))/NFD
```

```
      ICO=0
110   PN=((N+1,)**,5-1,+N)/(N*2,**,5)*EL
      QN=((N+1,)**,5-1,)/(N*2,**,5)*EL
      KJTA=0
      ICONT=0
      DO 5 I=1,N+1
 5    NCOM(I)=0
      DO 7 J=1,N
 7    X(1,J)=VI(J)
      DO 15 1=2,N+1
      DO 10 J=1,N
10    X(I,J)=X(1,J)+QN
      K=I-1
15    X(I,K)=X(1,K)+PN
      DO 16 I=1,N+1
      A1=X(I,1)
      A2=X(I,2)
      AK1=A1*AKO
      ALFA1=A2*ALFAO
      ICO=ICO+1
      GALL FINDIF(AK1,ALFA1,YSQ)
16    Y(I)=YSQ
      DO 29 I=1,N+1
29    JND(I)=0
```

```
      DO 27 LI=1,N+1.
      YOP =10**10,*MSO
      DO 25 I=1,N+1
      DO 26 IL=1,N+1
      IF(JND(IL)-I) 26,25,26
   26 CONTINUE
      IF((Y(I)-YOP)*MSO) 20,20,25
   20 YOP=Y(I)
      YG(LI)=YOP
      JND(LI)=I
   25 CONTINUE
   27 CONTINUE
      KG=JND(N+1)
      WRITE(2,375)
  375 FORMAT(1H1,30X,16H INITIAL SIMPLEX ///15X,22H+INDEPENDANT
                                                        VARIABL
     1ES,68X,9H+FUNCTION)
      DO 13 I=1,N+1
      WRITE(2,400) (X(I,J),J=1,N)
  400 FORMAT(1HO,12X,6F10,3)
   13 WRITE(2,450) JND(I),Y(I)
  450 FORMAT(1H+,BOX,12,20X,F10,3)
   90 DO 50 I=1,N+1
   50 NCOM(I)=NCOM(I)+1
```

```
      IF(KJTA) 91,91,92
   91 KJTA=1
      GO TO 93
   92 NCOM(L)=0
   93 DO 85 J=1,N
      SUM(J)=0
      DO 80 I=1,N+1
   80 SUM(J)=SUM(J)+X(I,J)
   85 CONTINUE
      DO 81 I=1,N+1
      II=I
      L=JND(I)
      DO 82 J=1,N
   82 XG(J)=2./N*SUM(j)-(N+2)/N*X(L,J)
      A1=XG(1)
      A2=XG(2)
      AK1=A1*AKO
      ALFA1=A2*ALFAO
      CALL FINDIF(AK1,ALFA1,YSQ)
      YZ=YSG
      IF((YZ-Y(N+1))*MSO) 180,180,181
  181 KG=L
  180 ICO=ICO+1
      IF((YZ-YG(1))*MSO) 81,81,84
```

```
 84  IF(NCOM(L)) 81,81,88
 81  CONTINUE
     GO TO 70
 88  DO 86 J=1,N
 86  X(L,J)=XG(J)
     Y(L)=YZ
     NCOM(L)=0
     KL=0
     DO 55 I=1,N+1
     IF(NCOM(I)-MEDGE)55,55,60
 60  KL=1
 55  CONTINUE
     IF(KL-1) 65,70,65
 70  IF(EL-ELD) 95,95,100
100  EL=EL/5
     DO 105 J=1,N
105  VI(J)=X(KG,J)
     GO TO 110
 65  JKL=JND(11)
     IF((YG(II)-YZ)*MSO) 69,69,71
 71  YG(II)=YZ
     DO 78 J=1,II-1
     IF((YG(II-J)-YZ)*MSO)73,73,77
 77  JND(II-J+1)=JND(II-J)
```

```
      JND(II-J)=JKL
      YG(II-J+1)=YG(II-J)
   78 YG(II-J)=YZ
      GO TO 73
   69 YG(II)=YZ
      DO 74 J=1,N+1-II
      IF((YG(II+J)-YZ)*MSO) 76,76,73
   76 JND(II+J-1)=JND(II+J)
      JND(II+J)=JKL
      YG(II+J-1)=YG(II+J)
   74 YG(II+J)=YZ
   73 IF(ICONT-99)173,174,174
  173 ICONT=ICONT+1
      GO TO 90
  174 ICONT=0
      WRITE(2,425) ICO
  425 FORMAT(1HO,10X,17H ITERATION: NUMBER,2X,I7)
      WRITE(2,400) (X(L,J),J=1,N)
      WRITE(2,450) JND(L),Y(L)
      IF(Y(L)/4,GE,0,5)GO TO 94
C                 PROGRESS SLOW PROGRAM TERMINATED
      GO TO 70
   94 CONTINUE
      TO TO 90
```

```
 95  WRITE(2,350)(X(KG,J),J=1,N),Y(KG)
350  FORMAT(1H1,10X,41H FINAL OPTIMUS VALUE USING SIMPLEX
                                                  METHOD ///
     1 5X,2F10,4,5X,F10,4)
      WRITE(2,370) AK1,ALFA1
370  FORMAT(/ 20X,4H AK1,10X,6H ALFA1 /// 15X,F10,4,10X,F11,10)
      WRITE(2,17)
 17   FORMAT(/ 30X,14H THETA VALUES ///)
      DO 14 I=1,NFD+1
140   FORMAT(5X,18F8,1)
 14   WRITE(2,140)(THETA(I,KK),KK=1,NT+1)
      JCO=JCO+1
      IF(JCO,LE,2)GO TO 109
      STOP
      END

      SUBROUTINE FINDIF(AK,ALFA,SUMSQ)
      INTEGER DT
      DIMENSION BETA(30),DELTA(30),TO(30)
      COMMON THETA(30,45),TINNER(45),TOUTER(45),DX,DT,AR,CA,
                                                  CB,F,NFD,NT,
     1 SLOPE(10),FI(10)
      AM=(DX*DX*AR*AR)/(ALFA*DT)
      P=(CA*DX)/(2,*3,14159**AK*DT)
```

```
      Q=(CB*DX)/(2*3,14159*AK*DT)
      BETA(1)=-(1+P)
      DO 3 I=2,NFD
    3 BETA(I)=-(2,+AM*(EXP(2,*(I-1)*DX)))-1/BETA(I-1)
      BETA(NFD+1)=-(1+Q)-1/BETA(NFD)
      J=1
    9 DELTA(1)=-P*THETA(1,J)-F*DX/(2,*3,14159*AK)
      DO 4 I=2,NFD
    4 DELTA(I)=-AM*(EXP(2,*(I-1)*DX))*THETA(I,J)-DELTA(I-1)/BETA(I-1)
      DELTA(NFD+1)=-Q*THETA(NFD+1,J)-DELTA(NFD)/BETA(NFD)
      THETA(NFD+1,J+1)=DELTA(NFD+1)/BETA(NFD+1)
      DO 6 I=1,NFD
      K=NFD+1-I
    6 THETA(K,J+1)=(DELTA(K)-THETA(K+1,J+1))/BETA(K)
      J+J+1
      IF(NT-J)8,9,9
    8 SUMSQ=0
      DO 11 KK=1,NT+1
   11 SUMSQ=(TINNER(KK)-THETA(1,KK))*(TINNER(KK)-THETA(1,KK))+
                                                    (TOUTER(KK
     1)-THETA(NFD+1,KK))*(TOUTER(KK)-THETA(NFD+1,KK))+SUMSQ
      RETURN
      END
```

LIST OF SYMBOLS

N	=	number of variables in the objective function
MEDGE	=	N + 1
MSO	=	minimisation factor (= -1)
EL	=	starting size for simplex
ELD	=	final size for simplex
VI(J)	=	array for scale factors (scale factors used to change values of variable to be optimised)
TOUTER(J)	=	array of outer cylinder starting temperatures
TINNER(J)	=	array of inner cylinder starting temperatures
ICO	=	count for number of iterations
PN,QN	=	factors determining points of simplex
KJTA	=	count
ICONT	=	count determines number of intermediate print out statements
X(I,J)	=	variables to be optimised
A1,A2	=	scale factors for variables to be optimised
AKI	=	new value of λ
ALFAI	=	new value of α
AKO	=	starting guess for λ
ALFA0	=	starting guess for α
Y(I)	=	objective function (= YSQ = YOP)

AR = a = radius of inner cylinder = 3/16" = 0.0047 m

BR = b = radius of outer cylinder bore = $\frac{1}{4}$" = 0.0064 m

ALFAO = α_o = starting guess for thermal diffusivity, normally this was 0.3×10^{-6} m^2/s, but other values were used to check the convergence of the programme (as Table (9))

AKO = λ_o = starting guess for thermal conductivity, normally 0.3 W/mK but changed as Table (9).

F = heat flow rate per unit length (W/m) this was usually different for each run. Table (9) shows values ranging from 23.6 - 93.9 W/m.

CA = C_a = heat capacity of inner cylinder measured as described in section In this case its value was 164.3.

CB = C_b = heat capacity of outer cylinder measured as in section In this case its value was 197.5.

NFD = n = space step in finite difference analysis, usually its value was 5 or 6.

DT = T = time step in finite difference analysis, most often a time interval of 30 seconds was used, but in some cases 15 seconds or 60 seconds was used.

NT = number of time steps of T required in the calculation, in Table (9) eight steps of 30 seconds were taken to give an experimental time of 4 minutes.

N = number of variables to be optimised by the Simplex programme. In this case N = 2 since thermal conductivity and thermal diffusivity were being calculated.

MEDGE = N + 1, i.e. the number of variables in the Simplex plus one, this term is used as a count for the termination of a loop in the programme.

MSO = a term which is given the value of either $\pm$ 1 and indicates whether the Simplex optimisation routine is to maximise (+ 1) or minimise (- 1) the objective function.

EL = initial size of Simplex as in Table (9) usually 0.1.

ELD = final size of Simplex as in Table (9) usually 0.001.

VI(J) = 1.0

INDEX TO SYMBOLS IN SUBROUTINE

a	=	inner cylinder diameter (m)
b	=	outer cylinder diameter (m)
α_o	=	starting guess for α (m^2/s)
λ_o	=	starting guess for λ (W/mK)
F	=	heat flow rate (W/m)
C_a	=	inner cylinder thermal capacity $(\frac{J}{mK})$
C_b	=	outer cylinder thermal capacity $(\frac{J}{mK})$
nfd	=	number of space steps in finite difference equations
t	=	time step in finite difference (sec.)
(I,J)	=	array of temperatures: when i = o
		values = starting temperatures (^oC)
STO	=	starting temperatures (^oC)
NT	=	number of time steps in finite difference equations
Δx	=	space step in finite difference (m)
B(I) β(I) D(I) δ(I)	=	variables used in gaussian elimination
I	=	algebraic symbol used for space step
J	=	algebraic symbol used for time step

APPENDIX 3

FLOW DIAGRAM FOR NEWTON - RAPHSON SOLUTION TO CONDUCTION AND VISCOUS HEATING SITUATION

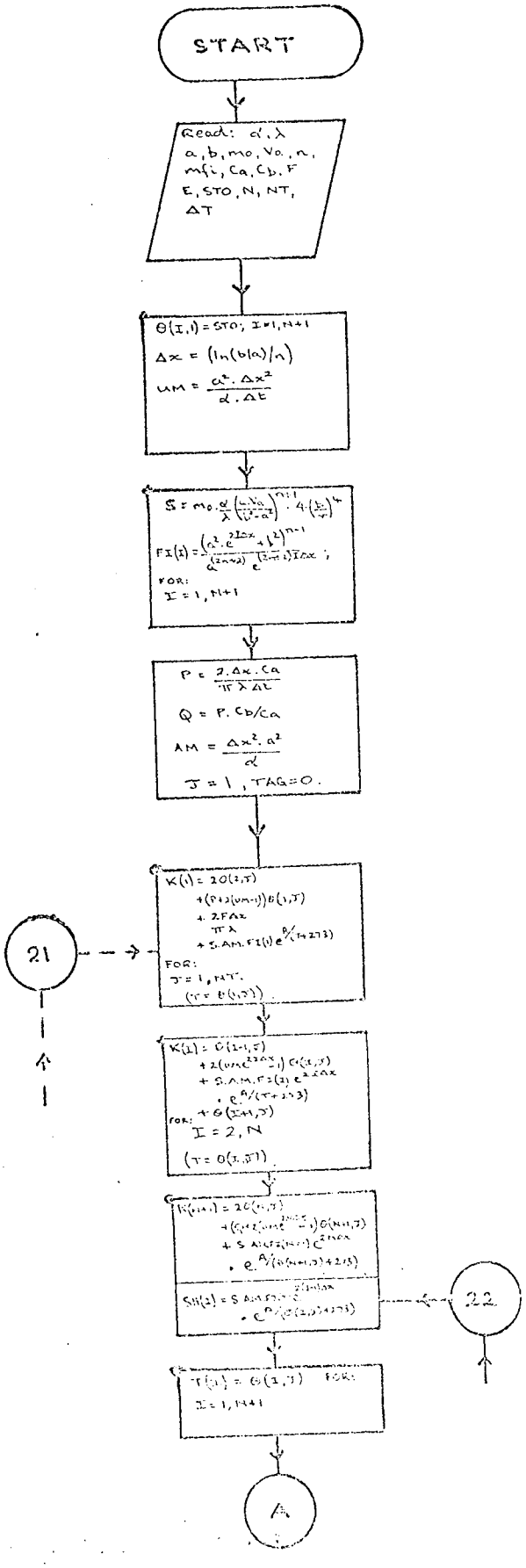

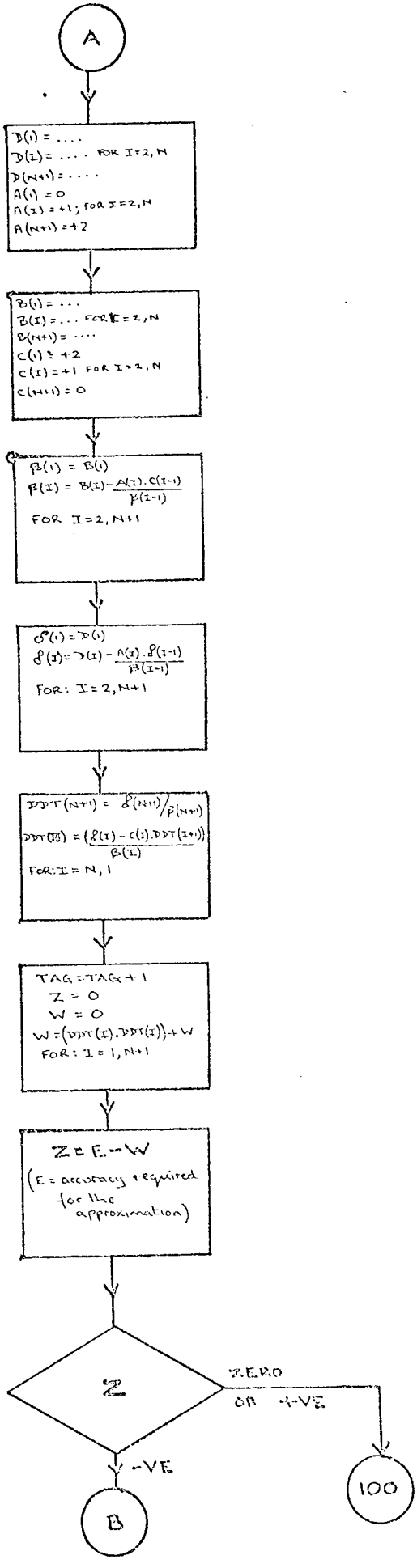
A
D(1) = ...
D(I) = ... FOR I=2, N
D(N+1) = ...
A(1) = 0
A(I) = +1; FOR I=2, N
A(N+1) = +2
B(1) = ...
B(I) = ... FOR I=2, N
B(N+1) = ...
C(1) = +2
C(I) = +1 FOR I=2, N
C(N+1) = 0
P(1) = B(1)
P(I) = B(I) - A(I).C(I-1) / P(I-1)
FOR I=2, N+1
S(1) = D(1)
S(I) = D(I) - A(I).S(I-1) / P(I-1)
FOR: I = 2, N+1
DDT(N+1) = S(N+1) / P(N+1)
DDT(II) = (S(I) - C(I).DDT(I+1)) / P(I)
FOR: I = N, 1
TAG = TAG + 1
Z = 0
W = 0
W = (DDT(I).DDT(I)) + W
FOR: I = 1, N+1
Z E.-W
(E = accuracy required for the approximation)
Z
ZERO OR +VE
-VE
B
100

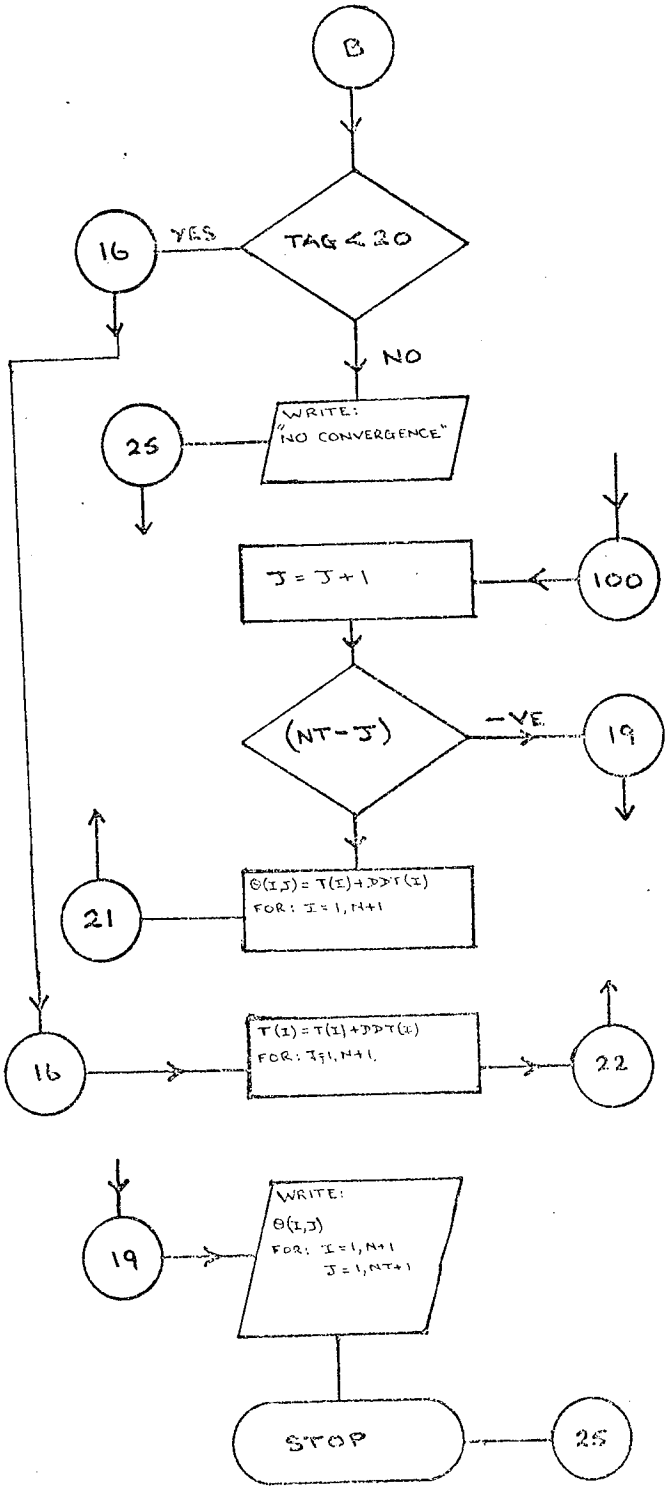
B
TAG < 20
YES
16
NO
WRITE:
"NO CONVERGENCE"
25
J = J + 1
100
(NT - J)
-VE
19
Θ(I,J) = T(I) + DDT(I)
FOR: I = 1, N+1
21
T(I) = T(I) + DDT(I)
FOR: I=1, N+1,
16
22
WRITE:
Θ(I,J)
FOR: I = 1, N+1
J = 1, NT+1
19
STOP
25

COMPUTER PROGRAM (VISCOUS HEATING)

```
      MASTER SHEAR
      INTEGER TAG
      INTEGER DT
      REAL K(9),MFI,MO
      DIMENSION T(10),THETA(9,9),A(10),B(10),C(10),BETA(10),DELTA(10),
     1DDT(10),SH(9),FI(9),D(10),TINNER(9),TOUTER(9)
    3 FORMAT (9FO=O)
      READ(1,3)ALFA,AK,AR,BR,MD, MFI,CA,CB,E
      READ(1,30)N,NT,DT
   30 FORMAT(3I0)
      DX=ALOG(BR/AR)/N
      UM=(AR*AR*DX*DX)/(ALFA*DT)
      P=(2*DX*CA)/(3.14159*AK*DT)
      Q=P*CB/CA
      JCO=0
  103 CONTINUE
      J=1
      TAG=0
      READ(1,250)VA
      READ(1,250)STO
      READ(1,250)F
  250 FORMAT(IFO=0)
      DO 31 I=1,N+1
   31 THETA(I,1)=STO
```

```
      S=MO* ALFA/AK* (CAR* VA/(BR* BR-AR* AR))** (NFI+1))* 4* BR** 4
      DO 40 I=1,M+1
   40 FI(I)=(CAR* AR* EXP(2* (I-1)* DX)+BR* BR)** (MFI-1))
      /(AR** (2* MFI+2)* EXPC
     1(2* MFI+2)* (I-1)*DX))
      AM=(DX* DX* AR* AR)/ALFA
   21 DO 6 I-1,N+1
    6 T(I)=THETA(I,J)
      K(1)=-2* THETA(2,J)-(P+2* (UM-1))* THETA(1,J)-(2* F* DX)/(3.14159* AL)-S
     1* AM* FI(1)* EXP(5873/(THETA(1,J)+273.2))
      DO 4 I-2,N
    4 K(I)=(THETA(I-1,J)+2* (UM* EXP(2* (I-1)* DX)-1)* THETA(I,J)+S* FI(I)* AM
     1* EXP(2* (I-1)*DX)* EXP(5873/(THETA(I,J)+273.2))+THETA(I+1,J))
      K(N+1)=-2* THETA(N,J)-(Q+2* (UM* EXP(2* N* DX)-1))* THETA(N+1,J)-
                                                          S* FI(N+
     II)* AM* EXP(2* N* DX)*EXP(5873/(THETA(N+1,J)+273.2))
   22 DO 100 I=1,N+1
      SH(I)=S* AM* FI(I)* EXP(2* (I-1)* DX)* EXP(5873./(T(I)+273.2))
  100 CONTINUE
      D(*1)=.K(1)+(2* T(2)-(P+2*)(UMH))* T(1)+S* FI(1)* AM* EXP(5873/(T(1)+273)
     1.2)))
      DO 7 I=2,N
    7 D(I)=-K(I)+(+T(I-1)-2* (UM* EXP(2* (I-1)* DX)+1)* T(I)+S* FI(I)* AM* EXP(2
     1* (I-1)* DX)* EXP(5873/(T(I)+273.2))+T(I+1))
      D(N+1)=-K(N+1)+(2* T(N)-(Q+2* (UM* EXP(2* N* DX)+1))* T(N+1)+S* AM*
                                                          FI(N+1
```

```
1* EXP(2* N* DX)* EXP(5873/(T(N+1)+273 .2)))
  A(I)=0
  DO 8 I=2,N
8 A(I)=-1
  A(N+1)=-2
  B(I)=+(P+2*(UM+1))+EXP(5873/(T(I)+273 .2))* 5873/(CTCI)+273 .2)(T(I)
 1+273 .2))* S* AM* FI(I)
  DO 8 I=2,N
 9B(I)=+2*(UM* EXP(2*(I-1)* DX)+1)+5* AM* FI(I)*EXP(2*(I-1)*DX)* EXP(5873
 1/(T(I)+273 .2))* 5873/((T(I)+273 .2)*(T(I)+273 .2))
  B(N+1)=+(Q+2*(UM* EXP(2* N* DX)+1))+S* AM* FI(NH)* EXP(2* N* DX)* EXP(5873
 1/(T(N+1)+273 .2))* 5873/((T(N+1)+273 .2)*(T(N+1)+273 .2))
  C(I)-=2
  DO 10 I=2,N
10 C(I)=-1
  C(N+1)=0
  BETA(I)=B(I)
  DO 11 I=2,N+1
11 BETA(I)=B(I)-A(I)* C(I-1)/BETA(I-1)
  DELTA(I)=D(I)
  DO 12 I=2,N+1
12 DELTA(I)=D(I)-A(I)*DELTA(I-1)/BETA(I-1)
  DDT(N+1)=DELTA(N+1)/BETA(N+1)
  DO 13 I=1,N
```

```
      II=N+1-I
   13 DDT(II)=(DELTA(II)-C(II)*DDT(JJ+1))/BETA(II)
      WRITE(2,28)(DDT(I),I=1,N+1)
   28 FORMAT(2X,6E16.81)
      TAG=TAG+1
      Z=O
      W=O
      DO 14 II=1,N+1
   14 W=(DDT(II)*DDT(II))+W
      Z=(W-E)
      DO 34 I=1,N+1
   34 T(I)=T(I)+DDT(I)
      IF(Z.LT.O) GO TO 15
      IF(TAG .LT.20) GO TO 22
      WRITE(2,18)
   18 FORMAT(15X,15H NO CONVERGENCE)
      GO TO 25
   15 J=J+1
      DO 33 I=1, N+1
   33 THETA(I,J)=T(I)+DDT(I)
      IF(NT-J)19,21,21
   19 WRITE (2,23)
   23 FORMAT(/,30X,13H THETA VALUES/)
      DO 29 I=1,N+1
```

```
 29 WRITE(2,32) (THETA(I,J),J=1,NT+1)
 32 FORMAT(20X,24F10.1)
    WRITE(2,1100)
1100 FORMAT(//17H VISCOUS HEATING //)
    WRITE(2,1200)(SH(I),I=1,N)
1200 FORMAT(/8E12.4/)
 25 CONTINUE
    JCO=JCO+1
    IF(JCO.LT.19) GO TO 109
    STOP
    END
    FINISH
```

REFERENCES

1. Anderson, D.R., Chem. Rev.
   66, (6), 677, (1964)

2. Hansen, D. and Ho, C.C.
   J. Poly.Sci. A3, 659, (1965)

3. Eiermann, K
   Rubb.Chem.Tech. 39, 841, (1969)

4. Peierls, R.E.
   "Quantum Theory of Solids" Oxford (1965)

5. Lohe, P. Koll. Z. 203, (1/2), 115, (1965)
   204, (1/2), 7, (1965)
   205, (1), 1, (1965)

6. Knappe, W.
   Kunst. 51, 707, (1961)

7. Sheldon, R.P. and Lane, K.
   Polymer, 6, 77, (1965)
   " 6, 205, (1965)

8. Cherkosova, L.N.
Russ. J. Phys. Chem. 33, 224, (1959)

9. ASTM Std. C177-63, Pt. 14, 17, (1967)

10. Kline, D.E.
J. Poly.Sci. 50, 441, (1961)

11. Eiermann, K. and Knappe, W.
Ange. Phys. 14, (8), 484, (1962)

12. Fuller, T. and Fricke, A.
J. Appl. Poly. Sci. 15, 1729 (1971)

13. Underwood, W. and McTaggart, R.
Chem. Eng.Symp. (Storrs).

14. Vos, B.
Appl. Sci. Res. A5, 425, (1955)

15. Beatty, K., Armstrong, A. and Schoenborn, E.
Ind. Eng. Chem. 42, (8), 1527 (1950)

16 Gast, T. Hellwege, K. and Kolheppe, E.
Koll. Zeits. 152, 24, (1957)

17. Mischenko, M., Samilov, A. and Buchatokii, V
Soviet Plastics, No. 3, 64, (1967)

18. Braden, M.
Trans. P.I., 103, 17, (1965)

19. Frielingsdorf, H.
Chem. Ing. Tech. 32, 291, (1960)

20. Guillem, S.
Plast. Mod. Elast. 20 116, (1968)

21. Hattori, M.
Koll. Zeits 202, (1), 11, (1965)

22. Kirchenko, Y. Olenik, B. and Chadovich, T.
Inz. Fiz. Zhurn. 7 (5), 70 (1964)

23. Shouldberg, R.H.
J. Appl. Poly. Sci. 7 1597, (1963)

24. Tobolsky, A.V.
"Properties and Structure of Polymers" Publ. Wiley and Sons (1960)

25. Street, L.

Int. Plast. Eng., 1, 289 (1961)

26. Menges, G and Klenk, P.

Kunst. 57, 598, (1967)

27. Gale, G.M.

RAPRA Technical Review No. 46

28. Tadmor, Z.

Poly. Eng. Sci. 6, (3), 185 (1966)

29. Tanner, K,

Kunst, 47, 440 (1957)

30. Janeschitz-Kriegel, H and Schijf, J

Plast. and Polym. 37 (132) 523 (1969)

31. Jepson, C.

Ind. Eng. Chem. 45 992 (1953)

32. Griskey, R. and Wiehe, I.

AICHE, J. 12 (2) 308 (1966)

33. Crank, J.

"Mathematics of Diffusion" Oxford Univ. Press

34. ICI Monograph

"Non Linear Optimisation Techniques"

35 Bird, R.B., Stewart, W. and Lightfoot, E.N.

"Transport Phenomena", McGraw Hill Press

36. Mendleson, R.A.

SPE, Tech. Papers Conf. Sept. 19th - 20th (1968) p. 7 - 18

37. Galt, J. and Maxwell, B.

Mod. Plast. Dec. 1964, 115

38. Cogswell, F and Lamb, P.

Trans. Journ. P.I. 35 (120) Dec. 1967, 809